Evaluation of protective immune responses against *Litomosoides sigmodontis* and analysis of *L. sigmodontis* extract on T cell modulation and glucose tolerance in diet-induced obese mice

Dissertation

zur

Erlangung des Doktorgrades (Dr. rer. nat.)

der

Mathematisch-Naturwissenschaftlichen Fakultät

der

Rheinischen Friedrich-Wilhelms-Universität Bonn

vorgelegt von

Stefan-Julian Frohberger

aus

São Paulo/Brasilien

Bonn 2019

Angefertigt mit Genehmigung der Mathematisch-Naturwissenschaftlichen Fakultät
der Rheinischen Friedrich-Wilhelms-Universität Bonn

1. Gutachter: Prof. Dr. Achim Hörauf

2. Gutachter: Prof. Dr. Irmgard Förster

Tag der Promotion: 11.10.2019

Erscheinungsjahr: 2019

Erklärung

Die hier vorgelegte Dissertation habe ich eigenständig und ohne unerlaubte Hilfsmittel angefertigt. Die Dissertation wurde in der vorgelegten oder in ähnlicher Form noch bei keiner anderen Institution eingereicht. Es wurden keine vorherigen oder erfolglosen Promotionsversuche unternommen.

Bonn, 18.04.2019

Teile dieser Arbeit wurden vorab veröffentlicht in folgenden Publikationen:

"Susceptibility to *L. sigmodontis* infection is highest in animals lacking IL-4R/IL-5 compared to single knockouts of IL-4R, IL-5 or eosinophils"

Stefan J. Frohberger, Jesuthas Ajendra, Jayagopi Surendar, Wiebke Stamminger, Alexandra Ehrens, Benedikt C. Buerfent, Katrin Gentil, Achim Hoerauf, Marc P. Hübner. **Accepted**. **Parasit Vectors**. 2019.

"S100A8/A9 deficiency increases neutrophil activation and protective immune responses within the lung against invading infective L3 larvae of the filarial nematode *Litomosoides sigmodontis*"

Stefan J. Frohberger, Frederic Fercoq, Anna-Lena Neumann, Jayagopi Surendar, Wiebke Stamminger, Alexandra Ehrens, Estelle Remion, Thomas Vogl, Achim Hoerauf, Coralie Martin, Marc P. Hübner. **Submitted.**

Des Weiteren wurden Auszüge auf verschiedenen Konferenzen als Vortrag oder Poster präsentiert

Table of Contents

Summary

Parasitic helminths are responsible for numerous tropical diseases which represent a major health problem in tropical and subtropical regions such as lymphatic filariasis (elephantiasis), causing lymphedema in limbs and scrotum in lymphatic filariasis patients and onchocerciasis (river blindness) leading to blindness and severe dermatitis in onchocerciasis patients. Helminths modulate the immune system of their hosts to their benefit, enabling and prolonging parasite survival in the host. On the other hand, several human and animal studies confirmed a protective effect of helminth infections and worm extracts on allergic and autoimmune diseases and more recently on metabolic diseases such as diet-induced insulin resistance. In order to obtain a better understanding of filarial immunomodulation and protective immune responses against filariae, the *Litomosoides sigmodontis* model was used. As type 2 immune responses are in general associated with protective immune responses against filariae, the present thesis directly assessed the role of eosinophils, IL-5 and IL-4R on *L. sigmodontis* infection. Therefore, wild-type (WT) BALB/c mice and mice deficient for eosinophils (dblGATA), IL-5, IL-4R and both IL-5/IL-4R were used. Analyses were performed at the peak of microfilaremia (71 days post infection (dpi)) and during a late time point of infection (119dpi). Following necropsy parasitological (worm and microfilaria load) as well as immunological parameters (cytokine levels, major immune cell types) within the thoracic cavity (the site of adult worm residence) and the spleen were analysed. A negative correlation between thoracic cavity eosinophil numbers and the adult worm burden as well as microfilaremia was observed. Alternatively activated macrophages (AAMs) correlated negatively with microfilaremia and positively with the adult worm load, which was associated with an extended adult worm survival in dblGATA, IL-$5^{-/-}$ and IL-$4R^{-/-}$/IL-$5^{-/-}$ mice. Mice deficient for IL-4R/IL-5 had the highest susceptibility for *L. sigmodontis* infection, an earlier

onset of microfilaremia, highest microfilariae (MF) loads and an extended adult worm survival. Another focus of this dissertation was the role of the damage-associated proteins S100A8/A9 during *L. sigmodontis* infection. S100A8/A9 was shown to provide an anti-inflammatory effect within the lung during the migratory phase of infective L3 larvae. Therefore, S100A8/A9$^{-/-}$ mice exhibited a decreased worm burden, which was associated with an increased inflammatory immune response within the lung compared to WT controls. The reduced worm burden in S100A8/A9$^{-/-}$ mice was also given following subcutaneous (s.c.) infection and the immune response within the skin was not altered in comparison to WT controls. The S100A8/A9-mediated protective mechanisms occurred in the lung via neutrophils, but not in the skin. Furthermore, the impact of the aryl hydrocarbon receptor, belonging to the family of Pattern Recognition Receptors (PRRs), during *L. sigmodontis* infection was analyzed. AhR$^{-/-}$ mice exhibited an increased worm burden, which was presumably based on limited protective immune responses within the skin and increased vascular permeability, facilitating larval migration and parasite survival.

The next part of this thesis studied the beneficial immunomodulatory effect of *L. sigmodontis* adult worm extract (LsAg) during diet-induced glucose intolerance and T cell inflammation. Repeated intraperitoneal (i.p.) injections of LsAg improved glucose tolerance, but not insulin sensitivity in obese mice. The protective effect was associated with a decreased type 1 inflammation in adipocytes, which represent a main cause of insulin resistance. IFN-γ, TNF and IL-17 were decreased in CD4+ T cells in LsAg treated mice. Furthermore TNF and IL-17 were significantly lower in CD8+ T cells in LsAg-treated animals compared to corresponding controls. Our study revealed that filarial extracts present potential candidates to treat diet-induced insulin resistance. Finally, I contributed to the identification of novel macrofilaricidal compounds by *in vivo* testing in the *L. sigmodontis* rodent model with several industry partners.

Zusammenfassung

Parasitäre Helminthen sind für eine Vielzahl von tropischen Krankheiten verantwortlich, die ein großes Gesundheitsproblem in den Tropen und Subtropen darstellen. Bei der lymphatischen Filariose (Elephantiasis) leiden Patienten unter Lymphödemen in den Gliedmaßen und bei der Onchozerkose (Flussblindheit) unter schwerwiegender Dermatitis sowie Blindheit. Helminthen modulieren das Immunsystem ihres Wirtes zu ihrem Vorteil, welches das langfristige Überleben des Parasiten im Wirt ermöglicht. Zudem belegen humane und tierexperimentelle Studien, dass Helmintheninfektionen und -extrakte Allergien, Autoimmunerkrankungen sowie metabolische Krankheiten lindern und sogar verhindern können. Neue Therapieansätze gegen Filarieninfektionen, Allergien und Autoimmunerkrankungen werden mittels des Models *L. sigmodontis* untersucht und identifiziert. In der vorliegenden Arbeit wurde der direkte Einfluss von Eosinophilen, IL-5 und IL-4R auf die *L. sigmodontis* Infektion in WT BALB/c Mäusen und Mauslinien, welche defizient für Eosinophile (dblGATA), IL-5, IL-4R und IL-5/IL-4R sind, untersucht. Parasitologische sowie immunologische Parameter wurden während des Mikrofilarienpeaks (71dpi) und zu einem späten Zeitpunkt der Infektion (119dpi) analysiert. In der Pleuralhöhle befindliche Eosinophile korrelierten negativ mit der adulten Wurm- und Mikrofilarienlast. Alternativ aktivierte Makrophagen korrelierten ebenfalls negativ mit der Mikrofilarämie, jedoch positiv mit der adulten Wurmlast, die mit einer erhöhten Lebenserwartung der adulten Würmer in den Eosinophil-defizienten Mauslinien assoziiert war. Dabei konnte festgestellt werden, dass die IL-4R/IL5 defizienten Tiere alle MF positiv waren. Zusätzlich wiesen diese Tiere die höchste Mikrofilarienlast auf, die zusätzlich mit einer frühzeitigen Mikrofilarienfreisetzung assoziert war.

Des Weiteren wurde im Rahmen dieser Dissertation eine anti-inflammatorische Rolle für S100A8/A9 in der Lunge während der *L. sigmodontis* Infektion nachgewiesen.

S100A8/A9$^{-/-}$ Mäuse waren durch eine geringere Adultwurmlast charakterisiert, die zusätzlich mit einer verstärkten inflammatorischen Immunantwort in der Lunge im Vergleich zu den WT Kontrollen assoziiert war. Subkutane und intradermale Injektionen von infektiösen L3 Larven in S100A8/A9$^{-/-}$ Mäusen hatten keinen Einfluss auf die Infektionslast. Dies zeigt, dass S100A8/A9-assozierte Immunantworten in der Haut nicht die Wurmlast beeinflussen. Zudem konnte gezeigt werden, dass ein durch Neutrophile initiierter protektiver Mechanismus in der Lunge stattfindet, da die Depletion von Neutrophilen in der Lunge in einer erhöhten Wurmlast in S100A8/A9$^{-/-}$ Tieren resultierte.

Ein weiterer Teil der Dissertation beschäftigte sich mit dem Einfluss des Aryl Hydrocarbon Rezeptors (AhR) auf die *L. sigmodontis* Infektion. AhR$^{-/-}$ Mäuse waren durch eine erhöhte Wurmlast charakterisiert, die vermutlich auf eingeschränkte Immunantworten innerhalb der Haut, der Pleuralhöhle sowie einer erhöhten vaskulären Permeabilität zurückzuführen ist.

Zusätzlich wurde in dieser Thesis der Effekt von adultem *L. sigmodontis* Wurmextrakt während einer Diät-induzierten Glukoseintoleranz auf die Zytokinproduktion von T Zellen untersucht. Intraperitoneale Injektionen von LsAg verbesserten die Glukosetoleranz, jedoch hatten keinen Einfluss auf die Insulintoleranz in adipösen Mäusen. Dieser protektive Effekt war mit einer verminderten Typ 1 Inflammation in den Adipozyten assoziiert. Darüber hinaus resultierte die Behandlung mit LsAg in einer verringerten pro-inflammatorischen Zytokinproduktion in CD4+ (IFNγ, TNF, IL-17) und CD8+ T Zellen (TNF, IL-17) im Vergleich zu PBS behandelten adipösen Kontrolltieren. Zusammengefasst stellen Filarienextrakte vielversprechende neue Therapieansätze für die Diät-induzierte Insulinresistenz dar. Letztendlich unterstütze ich die Identifizierung neuer makrofilarizider Substanzen im *L. sigmodontis* Nagetiermodell, die in enger Zusammenarbeit mit diversen Industriepartnern durchgeführt wurden.

1. Introduction

1.1 Great diversity of parasitism

Parasitism represents a type of symbiotic relationship between two species, whereupon one member, the parasite, benefits at the expense of the host [1]. The word parasite is derived from the Latin form of the Greek word “parasites”, implying “one who eats at the table of another”. Parasites are found in every taxon, belonging to the most successful and adaptable life forms [2]. More than half of all living organisms undergo a parasitic phase at some point in their life cycle.

Many studies in the past have already confirmed that parasites can cause major adverse health consequences on their hosts [1, 3], inducing immune or stress responses, or direct deprivation of resources [4, 5]. These detriments are usually sub-lethal, but can still influence the fitness-related properties of the host negatively [6], impairing movement, behaviour and foraging [7]. More than one hundred different types of organisms exist, which exhibit a parasitic phase in/on humans, including lice, ticks, mites, fungi, protozoa and helminths. Two major groups of parasites exist: (i) The protozoa and (ii) helminths which are further divided into cestodes, trematodes and nematodes. Infection with helminths produces debilitating and chronic diseases [8, 9] and among the helminths, the nematodes are the most abundant groups of invertebrates on earth and therefore, the nematode infections are one of the most prevalent infections world-wide.

1.2 Biology of Nematodes

Nematodes, also known as roundworms, belong to the phylum *Nematoda*. They represent a manifold group of metazoa and are among the most abundant multicellular animals on earth. It is estimated that more than 40.000 species exist, although just half of them have been identified and classified. Nematodes account for 80% [10] of all individual animals and occur

as parasites in animals, plants or as free living forms in almost every ecosystem, including marine and terrestrial environments. Therefore, nematodes play an important role in homeostasis, nutrient cycling and release of nutrients, which are for instance crucial for plant growth. With reference to the morphology of nematodes, they share numerous similarities within this high abundance of species. The morphology of nematodes is simple, consisting of an unsegmented bilaterally symmetrical body, which is composed of a hypodermis and a longitudinal muscle layer covered by a cuticle. Nematodes range in size, depending on the species, from several millimeters up to one meter [11]. They have been described as "a tube within a tube", referring to the alimentary canal which extends from the anterior (head) to the posterior end (tail). Nematodes feature several nervous, digestive, excretory and reproductive systems, but lack a respiratory system. Most species possess two sexes, but some are hermaphroditic, which are characterized by featuring male and female reproductive organs in the same individual. Sexual size dimorphism occurs in most of the species, resulting in increased length of female worms compared to male worms. Research has been focused on the parasitic forms due to their veterinary (domesticated animals, cattle-breeding), economic (crop plants) and medical importance. It is estimated that approximately 138 nematode species occur in humans [12]. Parasitic nematodes (hookworm, lungworm, pinworm, eelworm, and threadworm) occur mostly within the host at the circulatory, respiratory and alimentary systems. They are the mediators for several devastating diseases, such as lymphatic filariasis and onchocerciasis. *Onchocercidae* represent a family of nematodes, commonly termed as threadworms (~ 600 species) in the superfamily *Filarioidea.* These helminths belong to one of the major groups of human pathogenic parasites, being responsible for disabling diseases such as onchocerciasis, lymphatic filariasis or loiasis [13, 14].

1.3 Helminth infections: beneficial or harmful?

Although, the role of helminths in the incidence of infectious diseases is well established, there is unequivocal epidemiological data showing reduced incidence of allergies [15-17] and autoimmune diseases [18, 19] in regions with a high prevalence of helminth infections. Parasitic helminths are multicellular eukaryotic invertebrates, which have adapted to their host and developed diverse mechanisms to facilitate their maintenance and long term survival within the host, as "masters of regulation" [20, 21]. Long-term survival within the host is achieved by extenuating type 1 immune responses and eliciting a predominant type 2 immune milieu [20, 22]. During the last decades the incidence of infectious diseases decreased significantly due to improved standard of living, sanitation and medical progress. Therefore helminth infections mostly occur nowadays in the tropical and subtropical countries, affecting mainly the poor parts of the population [23-25].

In the past, several studies have shown a "beneficial" impact of helminth infections. Helminth-derived immunomodulatory products such as the small molecule analogs (SMA) of the excretory-secretory product 62 (ES-62) represent potential new therapeutic approaches to treat autoimmune and allergic symptoms, including experimental arthritis [26], systemic lupus erythematosus (SLE) [27], skin and lung allergy [28], type 1 diabetes (T1D) [29-32] and type 2 diabetes (T2D) [30, 33, 34]. Nevertheless helminths are also responsible to mediate several severe diseases such as lymphatic filariasis caused by *Wucheria bancrofti*, *Brugia malayi*, *Brugia timori* and onchocerciasis caused by *Onchocerca volvulus*. These diseases stigmatize the affected individuals by causing lymphedema in limbs (elephantiasis) and scrotum (hydrocele) in lymphatic filariasis patients and causing blindness and severe dermatitis in onchocerciais patients [8, 35-38]. Due to the chronic nature of these diseases and the inability of the affected patients to work, onchocerciasis and lymphatic filariasis represent a huge socio-economic problem [8, 35].

Furthermore, several studies demonstrated that helminth infection may increase the susceptibility of diverse diseases like malaria [39], HIV (human immunodeficiency virus) [40] and tuberculosis [41] and also impair vaccine responses [42, 43].

1.4 Mass drug administration (MDA)

As human-pathogenic filarial nematodes can cause debilitating diseases that stigmatize the affected individuals with vision impairment, blindness and severe dermatitis in onchocerciasis patients [44], lymphedema in limbs (elephantiasis) and scrotum (hydrocele) in lymphatic filariasis patients [8], mass drug admininistration programs were started to contain them. Both diseases represent neglected tropical diseases and it is estimated that around 120 million people are infected with filariae that cause lymphatic filariasis and an additional 17 million people suffer of onchocerciasis [45, 46]. The control of onchocerciasis and lymphatic filariasis solely relies on the repeated mass drug administration programs (MDAs) of ivermectin (IVM) exclusively for onchocerciasis patients and IVM plus albendazole (ALB) for lymphatic filariasis in Africa and diethylcarbamazine (DEC) plus ALB for lymphatic filariasis outside of Africa [8, 35]. The elimination of both diseases is hampered due to a lack of macrofilaricidal efficacy of IVM and DEC, which only temporarily inhibit the embryogenesis of female adult worms [8, 47]. Thus, these MDAs have to be given (bi-) annually for multiple years for the reproductive life span of the adult worms (onchocerciasis ~15 years) (lymphatic filariasis ~5 years), which depicts a huge challenge for health care systems [8].

New therapy approaches recommended by the WHO focus on a triple administration of DEC, IVM and ALB, resulting in a complete clearance of MF for a period of minimum two years [48], which may accelerate the elimination of lymphatic filariasis in specific countries non-endemic for onchocerciasis (outside of Africa) given an equable population coverage of >65%

[48, 49]. This clearance was associated with a decrease of circulating filarial antigen levels, which indicates a macrofilaricidal effect [50]. A recent study conducted in Papua New Guinea could show that a single regimen of a triple combination of IVM, DEC and ALB was able to clear significantly microfilaria from the blood for 3 years [48]. However, modelling studies predict impaired efficacy by the reduction of MDA rounds in areas of lower endemicity of lymphatic filariasis [49]. Nevertheless, reduced MDA rounds in areas of lower prevalence of onchocerciasis and lymphatic filariasis will improve the cost-effectiveness of community-based MDA programs [51]. Furthermore, it has to be taken in consideration that multiple drug administration's (triple therapy) [52] always harbor potential risks of upcoming resistance and of causing severe adverse events (SAE) in co-infections for instance in Africa with onchocerciasis and *Loa loa* [53]. SAE occur due to excessively rapid MF elimination by IVM in *Loa loa*-infected patients and during DEC treatment in onchocerciasis-infected patients. [8, 52, 54-56]. Therefore novel alternative strategies, including the further identification of new compounds eliciting macrofilaricidal or adult-worm sterilizing efficacy, should be developed and established [51, 57].

1.5 *Wolbachia*- a new promising target for filarial therapy

Wolbachia are common gram negative intracellular alpha-proteobacterial endosymbionts of terrestrial arthropods and nematodes, which belong to the order *Rickettsiales*. Most arthropods, including the majority of insect species, *arachnidas*, *crustaceans* and nematodes possess *Wolbachia* [58-60]. However, some filarial species do not harbor *Wolbachia*, for instance the rodent nematode *Acanthocheilonema viteae* [59] or the human pathogenic filaria *Loa loa* [61]. In arthropods they behave as reproductive parasites, whereas in nematodes they are mutualist symbionts, playing an essential role for filarial survival, fertility and larval molting [9, 37, 47, 62-65]. In filarial nematodes different strains of *Wolbachia* have been

classified into different super groups (C, D, J, and F) [66, 67]. Several studies have confirmed that *Wolbachia* are found primarily in the reproductive tract of adult female worms and in the hypodermis [68] including all life cycle stages (L1, L2, L3, L4, male and female adult worms) [59, 66, 69, 70] even in embryos, which are then transmitted transovarially [71, 72]. The density of *Wolbachia* diversifies depending on the colonized tissues and development stage. Therefore, MF (L1 larvae) possess less *Wolbachia* compared to higher larval (L2, L3, L4) and adult stages [70]. Interestingly, *Wolbachia* may induce inflammatory responses within the filariae-infected host [73-75], through TLR2/TLR6 activation [75], inducing Th1 cytokines such as TNF, Interleukin-6 (IL-6), IL-1β, IFN-γ, and IL-2, while reducing anti-inflammatory mediators such as Tregs, IL-10 and TGFβ [76, 77]. *Wolbachia* have been identified as a new promising target for anti-filarial therapy [60]. Depletion of *Wolbachia* with doxycycline or rifampicin leads to permanent sterilization of *O. volvulus* female adult worms and adult filariae causing lymphatic filariasis and result in a slow elimination of the adult worms [63, 78-81]. Recent studies have shown that *Wolbachia* provide essential metabolites and nucleotides and support the development and survival of the filariae [36, 82-84]. However, doxycycline is contraindicated for pregnant or lactating women and children below the age of 8 and has to be given at least for four to six weeks to achieve a permanent sterilization or macrofilaricidal efficacy [47, 54].

Collectively, there is a crucial demand for novel drugs and alternative treatments, which directly target adults and permanently impair filarial fertility and survival. New therapies, ideally as oral formulation or by a single parenteral administration, could contribute to the elimination of those filarial diseases and would allow their application in areas with upcoming drug resistance and in areas of onchocerciasis and/or *Loa loa* co-endemicity, avoiding severe adverse events due to the use of microfilaricidal drugs.

1.6 The Hygiene Hypothesis

During the last decades epidemiological studies confirmed an increased incidence of allergies such as dermatitis, rhinitis, asthma [85, 86], and autoimmune diseases, for instance rheumatoid arthritis, multiple sclerosis (MS), chronic inflammatory bowel disease and T1D in developed countries compared to developing countries [25, 29, 31, 86, 87]. Interestingly, there is an inverse correlation between the prevalence of helminth infections and the occurrence of allergies and autoimmune diseases [86], since the number of helminth-infected patients decreased significantly due to improved hygiene, sanitation and medical progress over the past decades in developed countries [24, 88]. Based on those observations the hygiene hypothesis was developed and states that a lack of infections during childhood results in an impaired adaptive immune system, favoring the development of allergies. Accordingly, children infected with *Schistosoma mansoni* [89-91] and *Schistosoma haematobium* are less prone to develop allergies [15, 16] and studies performed in areas with a low level of sanitation and a high prevalence of intestinal helminth infections (hookworm) revealed a decreased skin sensitization in children [17]. In addition, it has been shown that MS prevalence and progression was reduced by helminth infections [18, 19]. Interestingly, the clearance of helminth infections abrogated this helminth protective induced effect and resulted in an increased pathology [15, 92-94] and disease incidence [95, 96].

1.7 Diabetes- health challenge of the 21st century

In light of the emerging evidence that helminths protect against type 2 diabetes, the current deworming programs or MDAs against helminths in combination with other conventional risk factors might contribute to the development of diabetes [97]. Diabetes represents the fastest increasing long-term disease of the 21st century that affects millions of people worldwide, depicting a huge health problem.

The International Diabetes Federation (IDF) reported that around 387 million people were suffering from diabetes in 2014. This number is expected to increase up to 642 million patients by 2040. Around 90% of patients suffering from diabetes are due to T2D. Diabetes is a chronic metabolic disease impairing the production (T1D) or the sensitivity (T2D) to respond to the hormone insulin, resulting in elevated blood glucose levels [98]. T1D (autoimmune diabetes) has its onset commonly during childhood and is caused by the destruction of insulin-producing pancreatic β-islet cells by autoreactive T cells, wehereas T2D (metabolic diabetes) occurs during adulthood by decreasing insulin sensitivity. Insulin resistance is highly associated with ageing, obesity and physical inactivity [98]. The risk to develop T1D is strongly dependent on genetic and environmental criteria, whereas in T2D the life style and alimentation significantly influences T2D development.

Diabetes increases the risk of severe macrovascular (cardiovascular) and microvascular (retino- and nephropathy) blood vessel damage and therefore, severe heart diseases, eye, kidney and nerve damages [99, 100]. Furthermore, recent studies demonstrated an association between diabetes and several types of cancer [99-101].

Obesity is responsible for numerous chronic diseases, such as cardiovascular diseases, cancer and diabetes in high, middle and low-income countries. Recent papers have indicated an essential link between functional changes of innate immune cells during inflammation and insulin resistance [102]. In general, obesity leads to chronic inflammation and alterations of the cellular composition of the adipose tissue. Therefore, adipose tissue of slim individuals mainly constitutes of high frequencies of type 2-associated and anti-inflammatory, regulatory cells including eosinophils, AAMs, Th2 cells and Tregs. However, during obesity adipocytes increase in size and undergo apoptosis [103, 104] due to adipose tissue hypoxia [105, 106], which provides an inflammatory stimulus, leading to the infiltration of inflammatory cell

types such as CD8+ T cells and classically activated macrophages and a reduction of eosinophils and Tregs. Interestingly, recent studies highlighted an essential role of T cells during several processes between the adaptive immune system and obesity-induced systemic metabolic dysfunctions as well as insulin resistance [107, 108]. Inhibition of the insulin signaling cascade results in an impaired glucose uptake. Besides, it was also shown that the depletion of CD8+ T cells alleviated adipose tissue inflammation in obese mice and improved insulin resistance [109, 110]. Despite these findings less is known about the immunomodulatory capacity of T cells during obesity. high fat diet (HFD) induced obesity in mice is associated with a constantly increasing cell number (hyperplasia) and size of adipocytes (hypertrophy) [111], lipid accumulation and increased body weight. Adipocyte hypertrophy and hypoxia [105, 106] represent the most important mediators for local adipose tissue inflammation. This inflammation is associated with an increased production of several chemokines such as Regulated And Normal T cell Expressed and Secreted (RANTES), monocyte chemotactic protein 1 (MCP-1), cytokines (IL-6, TNF) and apoptosis, which further induce the infiltration of inflammatory cell types such as classically activated macrophages enhancing inflammation [112] and inhibiting the insulin signalling cascade [113, 114]. Accordingly, an inverse association between helminth infection and diabetes was observed in several human studies [115, 116]. Further animal studies showed that helminth infection or the repeated administration of crude adult worm extracts (LsAg) or helminth-derived products improve diet-induced insulin resistance [117, 118], which was associated with regulatory immune responses and a type 2 immune shift and counter-regulated inflammatory type 1 immune responses, leading to an immunoregulatory phenotype with an expansion of AAMs, eosinophils, regulatory T cells, type 2 innate lymphocytes (ILC2s) in the adipose tissue [30, 119].

A number of reports have shown that helminth infections, their extracts and products were able to prevent diabetes in a murine model of T1D (non-obese diabetic (NOD) mice). Extracts of adult *S. mansoni* as well as its eggs demonstrated a decreased T1D disease incidence and perpetuated islet cells [120]. Another study demonstrated that worm products from *Fasciola hepatica* were also shown to prevent the onset of diabetes, by peritoneal AAMs driven immune responses, which posesses the capacity of inducing a potent Treg response [121]. In regard to nematodes, Hübner *et al.* illustrated that the filarial model *L. sigmodontis* using L3 larvae, adult worms or LsAg protected NOD mice in developing T1D due to the generation of a Th2 immue responses as well as Treg responses [31]. However, it has to be noted that worm products and helminth belonging to different species may elicit different mechanism and therefore, revealing no beneficial impact in certain diseases like T1D. ES-62 represents a glycoprotein, which is derived from the filarial nematode *Acanthocheilonema viteae*. Prophylactical and therapeutical approaches by ES-62 have been reported in several diseases, such as SLE [122] and asthma [123, 124]. Nevertheless ES-62 or its synthetical SMAs were shown to have no impact on T1D development in NOD mice, suggesting a different mechanism of action. It seems to be more suitable as prophylactical and therapeutical therapy in strong systemic inflammatory diseases, instead in diseases with dominating organ-specific pathology [125]. Recent work of our group demonstrated (Surendar *et al. submitted*) that repeated i.p. administration of LsAg led to an increase of adipose tissue released adiponectin, a protein hormone produced by adipocytes and involved in numerous metabolic processes (glucose regulation, fatty acid oxidation) [126, 127]. Interestingly, other studies have shown that adiponectin in combination with leptin reverses insulin resistance in mice [128] and obesity as well as adiponectin concentrations are inversely correlated [127, 129, 130].

1.8 Calprotectin- S100A8/S100A9

Studying the protective effects of helminths in metabolic and autoimmune diseases can lead to helminth-based therapies. However, it is also important to better understand their mechanisms of pathogenesis in case of the tropical diseases caused by them. In this context, the role of *L. sigmodontis* infective larvae in early pulmonary phase of infection is recently being studied extensively. The recruitment of neutrophils along with an increase in the S100A8 and S100A9 proteins has been shown as the mechanism behind the pulmonary inflammation. Another recent study demonstrated that infective *L. sigmodontis* L3 larvae trigger pulmonary inflammation, which was associated with neutrophil recruitment, increased lung pathology as well as increased concentrations of S100A8/S100A9 in the bronchoalveolar lavage [131]. These results indicate Calprotectin (S100A8/S100A9) as potential marker of inflammation with an essential role on the outcome of filarial infection. Tissue injuries or infections result in a marked increase and release of damage-associated proteins from the S100 protein family [132-134]. These alarmins bind and activate damage-associated molecular patterns (DAMPs) via Toll-like receptor 4 (TLR4) [135, 136], a receptor for advanced glycation endproducts (RAGE) [137], heoaran sulphate proteoglycans (HSPG), G-protein coupled [138], scavenger [139], epidermal growth factor (EGF) [140], Gaq-coupled [141], human epidermal growth factor receptor 2 (HER2) [142], fibroblast growth factor receptor 1 (FGFR1) [143], dependent mechanism and function as early amplifiers of acute and chronic inflammatory immune responses [132, 136].

The S100 protein family has been shown to play a key role during the regulation of various cellular processes such as calcium homeostasis, cytoskeletal dynamics, transcription factors, enzymatic activities, phagocytosis activity, chemotaxis (neutrophils, monocytes, and macrophages), cell growth, survival and differentiation.

Currently 25 S100 proteins have been identified and two prominent members of the protein family (S100A8 and S100A9) constitute the heterodimer Calprotectin [144] (MRP8/MRP14). Calprotectin elicits a major role during inflammatory conditions [145] such as in numerous autoimmune diseases, neurodegenerative disorders, atherosclerosis and several types of cancer [145-148]. However, there is still a controversy ongoing whether calprotectin is pathogenic (pro-inflammatory) or protective (anti-inflammatory) [149]. S100A8 and S100A9 are constitutively expressed in circulating neutrophils and monocytes [133] with reduced expression levels during cell differentiation and maturation. Both proteins are released during infection, tissue damage, cellular necrosis, formation of neutrophil extracellular traps (NETs) [150] and can be also secreted passively [132, 133, 151].

1.9 Aryl hydrocarbon receptor

The aryl hydrocarbon receptor (AhR) represents a transcription factor in the pattern recognition receptor (PRR) group and belongs to the family of basic helix-loop-helix/PAS (bHLH PAS). It plays an important role in the sensing of environmental changes and is widely abundant in the immune system, including peripheral immune organs such as spleen and lymph nodes. Furthermore, AhR is highly expressed in mature immune cells at barrier sites (Th17, Tregs, γδ T cells, macrophages, dendritic cells) such as in the skin [152, 153], lung, liver and gastrointestinal tract [154]. AhR acts as environmental sensor ensuring immunosurveillance and primary defence against external harmful factors.

In the absence of a ligand, AhR is retained in an inactive complex located in the cytoplasm bound to actin filaments, consisting of various chaperone proteins such as heat shock protein 90 (HSP90) [155], AhR-interacting protein (AIP) [156, 157] and p23 [158]. HSP90 and p23 have been shown to be involved in DNA and ligand binding. Binding of a ligand results in a complex activation and therefore to a translocation into the nucleus [159], where AhR is

released from the complex and forms a heterodimer with its protein partner aryl hydrocarbon receptor nuclear translocator (ARNT) [160]. Afterwards AhR/ARNT binds to genomic regions containing its binding motif dioxin response element (DRE) [161] and leads to the expression of target genes for instance *CYP1A1*, *CYP1A2*, *CYP1B1* and AhR repressor (*AhRR*) [161, 162].

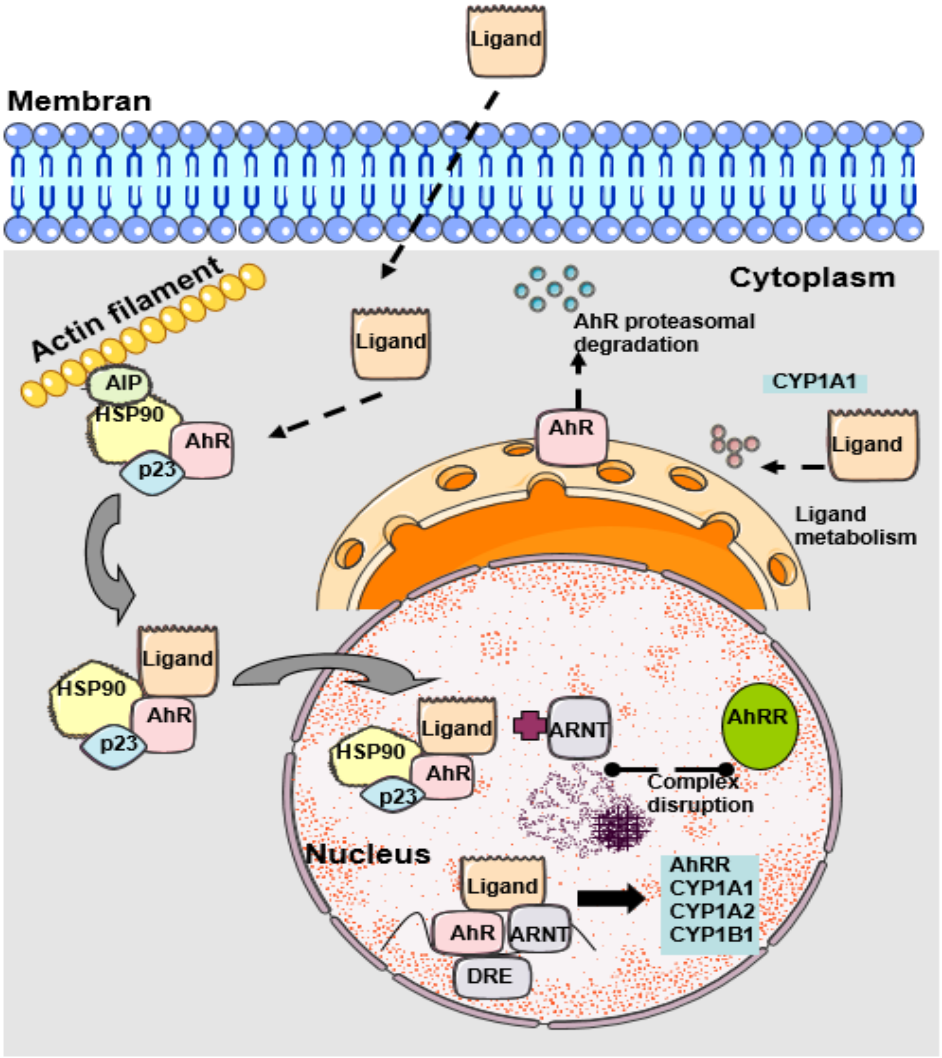

Fig. 1: The aryl hydrocarbon receptor pathway. In its inactived form AhR is bound to actin filaments in the cytoplasm and forms a complex with various chaperone proteins, such as HSP90, p23 and AIP. Binding of a ligand leads to translocation of the complex into the nucleus, where AhR is released from the complex and forms a heterodimer with its protein partner ARNT and binds to genomic binding motif regions (DRE). Afterwards target genes are expressed for instance as *CYP1A1*, *CYP1A2*, *CYP1B1*, and AhR repressor (*AhRR).* AhR signaling is regulated by AhR/ARNT complex disruption via AhRR, proteasomal degradation of AhR and ligand metabolism by CYP1A1 [163].

Besides, the multifunctional roles of AhR on the immune response, several studies demonstrated an essential role of AhR in the recognition and elimination of invading pathogens. AhR has been shown to be responsible for the orchestration of specific inflammatory immune responses towards the pathogen and therefore, reducing immunopathology to the host [164]. For instance AhR provide protection during enteropathogenic bacterial infection by its regulatory capacity on Th22 cells or more specifically on their IL-22 production [165, 166]. Furthermore, other reports highlighted that bacterial infections in $AhR^{-/-}$ mice with *Streptococcus pneumonia* [167] (extracellular pathogen) as well as *Listeria monocytogenes* (intracellular pathogen) [168] resulted in increased pathogen susceptibility. Interestingly, another report illustrated a regulatory property by AhR signaling in hematopoietic and non-hematopoietic compartments to the antibacterial response, revealing an important involvement of macrophages and neutrophils during *Pseudomonas aeruginosa* infection [169]. Due to the fact that $AhR^{-/-}$ mice are characterized by reduced numbers of skin and gut intraepithelial lymphocytes [170] as well as intestinal innate lymphoid cells (ILCs), it can be speculated that absence of AhR impairs immune responses within these barriers. Impaired immune responses facilitate pathogen invasion and lead to an increased susceptibility, which was further observed during *Citrobacter rodentium* infection [171, 172]. Although AhR is highly expressed in barrier sites, which are the entry points for helminths, nothing is known about its role during helminth infections.

1.10 *L. sigmodontis*: a laboratory rodent filariae model to investigate immune responses during filariasis

L. sigmodontis represents an excellent laboratory model to investigate parasitological and immunological responses during filarial infection [173-176]. BALB/c mice are susceptible to *L. sigmodontis* infection and the filariae can undergo its full life cycle under laboratory conditions [173, 177], whereas in C57BL/6 mice filarial development is impaired, leading to accelerated elimination of adult worms around 35dpi and to complete absence of MF [178]. Previous studies showed that the *L. sigmodontis* mouse model helped us to obtain a better understanding of the filarial immunomodulation [179, 180] and involved protective immune responses, since immunocompetent laboratory mice are non-permissive and exhibit high resistance to human pathogenic filariae (*Brugia* spp, *Onchocerca* spp) [178]. The *L. sigmodontis* mouse model in BALB/c, C57BL/6 and immunodeficient mice was used to identify and study local and time dependent immune responses during filarial infection [174, 181-185]. ***L. sigmodontis***-infected mice develop immune responses that resemble those of human filarial infections. During human filariasis patients develop type 2 immune response including eosinophilia and the release of eosinophil-associated molecules, increased production of type 2 cytokines such as IL-4 and IL-5 [186], elevated numbers of innate lymphocyte cells [187], as well as polarisation of classical activated macrophages into AAMs [188]. Human filariasis is further associated with regulatory immune responses that suppress both type 1 and type 2 immune responses due to the induction of IL-10 and expansion of regulatory T cells (Tregs) [189-191]. Those type 2 immune responses are linked to protection and the development of filarial pathology in patients with onchocerciasis [192, 193]. For instance some patients with onchocerciasis develop hyperreactive symptoms with severe skin disease and those exhibit strongest type 2 immune responses, which are associated with reduced MF levels [180, 194].

Similar observations were made in patients with lymphatic filariasis, whereas only 50% of patients develop microfilaremia. Those patients exhibited increased adaptive immune responses and elevated parasite-specific IL-5 levels [195]. On the other hand lymphedema has been associated with pronounced parasite-specific Th1 and Th17 responses [196].

In the *L. sigmodontis* model impaired type 2 immune responses due to the absence of essential cell types such as eosinophils, including eosinophil products like eosinophil peroxidase (EPO) and major basic protein (MBP) resulted in an increased *L. sigmodontis* worm burden. However, no development of MF occured in semi-resistant 129/SvJ background mice [182]. Mice deficient for eosinophil-associated chemokines such as Eotaxin 1 exhibited an increased *L. sigmodontis* adult worm burden [197]. Similar results were observed in IL-5 deficient mice due to the essential role of this type 2 cytokine, which is crucial for the differentiation and maintenance of eosinophils during *L. sigmodontis* infection. Furthermore, several studies illustrated a protective role of IL-4 during *L. sigmodontis* infection as semi-resistant C57BL/6 mice develop patent infections in the absence of IL-4 [183, 198]. It was shown that IL-4 deficient BALB/c mice exhibit increased MF levels compared to WT controls [183, 199]. Chronic helminth infections are known to establish an anti-inflammatory milieu within their host by increasing the frequency of regulatory T cells, AAMs and certain inhibitory cytokines such as IL-10 and/or TGFβ. Therefore, the absence of IL-4 may impair worm survival since IL-4 and IL-13 represent crucial mediators and play an essential role in the development of AAMs. Recent studies have shown a positive correlation between *L. sigmodontis* adult worm numbers and total counts of AAMs [200]. Interestingly, numerous studies have proven a beneficial impact of *L. sigmodontis* infection on allergic sensitization in asthma [201], type III hypersensitivity [202], vaccine modulation [203, 204] and T cell responses [205-207].

With regard to the immunmodulatory capacity of *L. sigmodontis*, repeated administrations of LsAg or infection with *L. sigmodontis* have been shown to provide a protective impact against T1D [29, 31, 208] and to ameliorate glucose tolerance in diet-induced obese mice [118]. Interestingly, in *E. coli*-induced sepsis, pathology was diminished during *L. sigmodontis* infection [209]. Besides, in co-infection models it was shown that *L. sigmodontis* led to a reduced mortality during *Plasmodium berghei* infection in mice [210] and was able to alleviate the pathology in *Mycobacterium tuberculosis* infected cotton rats [211]. In addition, *L. sigmodontis* has proven its excellent applicability for the screening and identification of potential anti-filarial drug and vaccination candidates as surrogate model for lymphatic filariasis and onchocerciasis [47, 79].

1.11 Life cycle of the murine filariae *L. sigmodontis*

The natural host of *L. sigmodontis* is the cotton rat (*Sigmodon hispidus*). Gerbils (*Meriones unguiculatus*) and BALB/c mice can be utilized as alternative hosts [173, 178]. *L. sigmodontis* is transmitted by an arthropod vector, the tropical rat mite (*Ornithonyssus bacoti*), which represents the obligate intermediate host. L1 stage larvae also known as MF molt within the mite to L2 (6-7 days) and infective L3 larval stages (10-12 days). During the blood meal of the vector, infective *L. sigmodontis* L3 larvae are transmitted into the host's skin, where they migrate via the blood and lymphatic system. After traversing the pulmonary capillaries L3 larvae reach the thoratic cavity, which represents the site of infection, where the filariae finally reside. Recently, it was demonstrated that *L. sigmodontis* migrating L3 larvae trigger a pulmonary inflammatory phase which is characterized by haemorrhages and granulomas due to endothelium and parenchyma damage. This transient lung inflammation was further associated with an elevated expression of S100A8/S100A9 in neutrophils [131]. Until 6dpi most of the L3 larvae reach the pleural cavity. Subsequently, L3 larvae will molt into L4

larval stages (8-12dpi). Around 30dpi L4 larvae molt into adult male and female worms, which can be differentiated by sexual (vulva or the spicule) and morphological dimorphisms (adult worm length: females 10-12cm, males 3-5cm). Adult worms reside within the pleural cavity for several months. Subsequent mating leads to the release of MF (80µm length), which enter the peripheral blood system from 50dpi [173, 178]. During the next blood meal MF are ingested by the mite vector and the life cycle starts over.

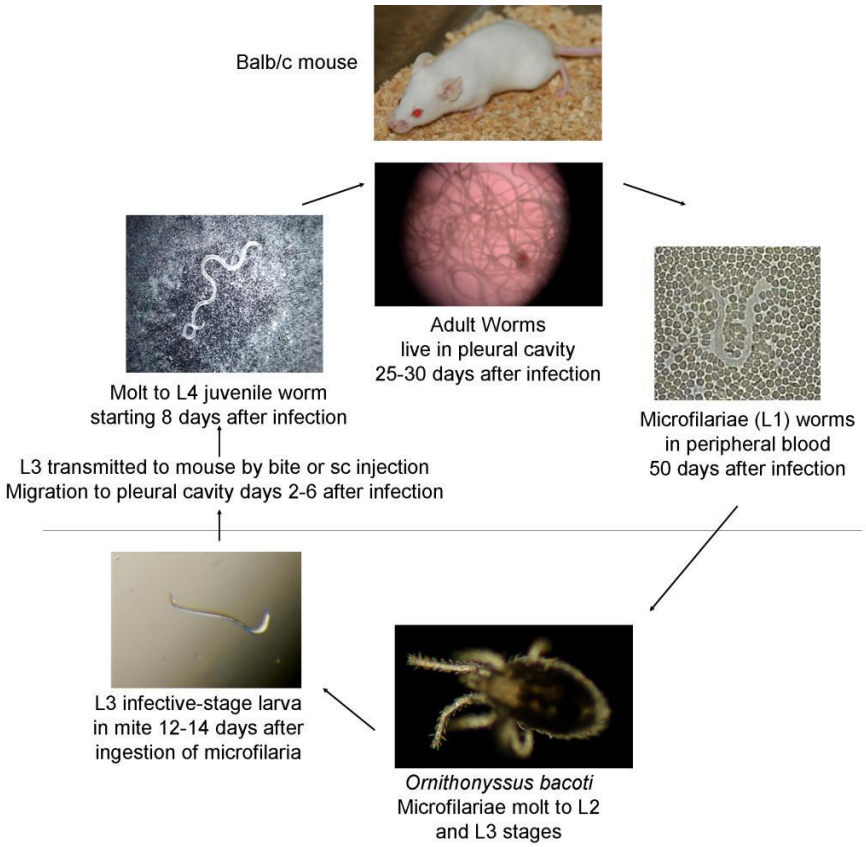

Fig. 2: Laboratory life cycle of *Litomosoides sigmodontis.* During the blood meal of the intermediate arthropod host *(Ornithonyssus bacoti)*, infective L3 larvae are transmitted into the murine host's skin. Larvae migrate via the blood and lymphatic system, passing the lung and reaching the site of infection, the thoracic cavity around 2-6 days post infection (dpi). Within the pleural cavity L3 larvae molt into L4 stages between 8-12dpi and then into adult worms around 30dpi. 50dpi fertilized female worms release their progeny (microfilariae) into the peripheral blood system [212].

1.12 Objectives of this thesis

A – Evaluation of protective immune responses during *L. sigmodontis* infection

Parasitic helminths are known to dampen type 1 specific immune responses and create a type 2 driven and regulatory milieu. Impaired type 1 and type 2 immune responses have been shown to increase parasite longevity and fertility. In this thesis the direct impact of eosinophils, IL-5, IL-4R, Aryl hydrocarbon receptor (AhR), and Calprotectin (S100A8/S100A9) during infection with the murine filarial nematode *L. sigmodontis* was investigated. To obtain a better understanding of the immunology involved and interaction between parasite and host, different mouse strains deficient for eosinophils (dblGATA), IL-5, IL-4R, IL-4R/IL-5, AhR and S100A8/100A9 were infected via different routes with *L. sigmodontis*; naturally (nat.), subcutaneously (s.c.), intravenously (i.v.), or intradermally (i.d.). To further determine protective immune responses, parasitological (parasite burden) and immunological (cytokine analysis, quantification of major immune cell types, histology) parameters at different time points post infection were analysed to allow conclusions on the role of these immunological components on *L. sigmodontis* infection.

B – Anti-inflammatory role of filarial extracts (LsAg) on T cell inflammation during diet-induced insulin resistance

Numerous epidemiological studies demonstrated an inverse relationship between allergies and infections. It is postulated that the loss of helminth infections and their beneficial immunomodulatory abilities due to improved hygiene, sanitation and medical progress led to an increased incidence of allergies and autoimmune diseases. A new approach to treat these diseases is the development of therapies based on filarial extract products and antigens. Worm-derived products have been shown to exhibit anti-inflammatory properties in the treatment of rheumatoid arthritis, multiple sclerosis, chronic inflammatory bowel disease

(IBD) and T1D. However, the impact of filarial infections and crude worm extracts on metabolic diseases like diet-induced insulin resistance is barely known.

Therefore, the next aim of this thesis was to investigate whether administration of LsAg protects against HF diet-induced insulin resistance in DIO mice by modulating T cell responses. Obesity is associated with a Th1-driven milieu and correlates with decreasing cell frequencies of Tregs, Th2 cells, AAMs and increased frequencies of classically activated macrophages, CD8+ T cells and pro-inflammatory cytokines. Thus, we hypothesized a reduction in the pro-inflammatory immune responses due to the anti-inflammatory properties of LsAg, which have been shown to improve glucose tolerance.

In summary, this project was performed to investigate the direct impact of LsAg on insulin sensitivity in DIO mice, to identify potential novel treatments and protective mechanisms against metabolic diseases such as diet-induced insulin resistance.

C – Identification of macrofilaricidal drug candidates

The control of lymphatic filariasis and onchocerciasis relies on the repeated administration of drugs (MDA) that solely target the filarial offspring, the MF, and temporarily inhibit the embryogenesis of adult female worms. Hence, these treatments have to be given on an annual to bi-annual basis for the reproductive lifespan (several years) of the female adult worms. Therefore, current efforts to eliminate filarial diseases are hampered by the lack of macrofilaricidal drugs. New drugs are required for the elimination of those filarial diseases. In collaboration with industry partners such potential candidates were identified using the *L. sigmodontis* rodent model.

2. Materials & Methods

2.1 Ethics Statement

Animal housing conditions and the procedures used in this work were performed according to the European Union animal welfare guidelines. All protocols were approved by the Landesamt für Natur, Umwelt und Verbraucherschutz, Cologne, Germany (87-51.04.2010A335, 84-02.04.2014.A327, 84-02.04.2016.A331 and 84-02.04.205.A507).

2.2 Mice

All animals (*Mus musculus*) were bred at the animal facilities of the University Hospital of Bonn (House for Experimental Therapy and the Institute for Medical Microbiology, Immunology and Parasitology, IMMIP) according to animal welfare guidelines and housed during the experiments at the animal facility of the IMMIP. Mice were kept, at 22°C in a 12h day-night cycle, in individually ventilated cages. All animals were provided free access to food pellets and water *ad libitum*. Experiments in this thesis were performed using following animal genotypes: BALB/c WT and IL-4R$^{-/-}$ mice, which lack the signaling via the IL-4R, which responds to IL-4 as well as IL-13, (BALB/c-Il4ratm1Sz/J) were purchased from Janvier (Saint-Berthevin, France) and Charles River (Erkrath, Germany), respectively. dblGATA BALB/c mice were originally obtained from The Jackson Laboratory (Bar Harbor, Maine, USA), IL-5$^{-/-}$ and IL-4R$^{-/-}$/IL-5$^{-/-}$ BALB/c mice from Prof. Dr. Klaus Matthaei (Matthaei, Stem Cell & Gene Targeting Laboratory, ANU College of Medicine, Biology and Environment), which lack eosinophils.

S100A8/A9$^{-/-}$ C57BL/6 mice were kindly provided from Prof. Dr. Thomas Vogl (Institute of Immunology, University of Münster, Germany). Corresponding C57BL/6 WT control mice were purchased from Charles River (Erkrath, Germany). AhR$^{-/-}$ and C57BL/6 WT control mice were obtained from the Life & Medical Sciences Institute (LIMES) (Prof. Dr. Irmgard

Förster, University Bonn, Germany). For diet-induced insulin resistance experiments, male C57BL/6 (WT) mice were used (Charles River, Erkrath, Germany). HFD, consisting of 60% of calories from fat, was acquired from Research Diets (Inc. Brogaarden, Denmark). HFD was started at 6-8 weeks of age for a total duration of 18 weeks. For all experiments, age and sex-matched mice were used.

2.3 Euthanasia of mice

At determined time points mice were euthanized per inhalation of an overdose of Isoflurane (1-cloro-2,2,2-trifluoroethyldifluoro-methylether; Forene®, Abbolt, Wiesbaden) in a sealed plastic box. Afterwards mice were examined for vital signs and reflexes to assure exitus. Euthanasia of BALB/c WT, IL-4R$^{-/-}$ (BALB/c-Il4ratm1Sz/J), dblGATA, IL-5$^{-/-}$ and IL-4R$^{-/-}$ /IL-5$^{-/-}$ was performed on 71 and 119dpi. Necroscopsies of S100A8/A9$^{-/-}$ and corresponding C57BL/6 control mice were performed on 12 and 29dpi. AhR$^{-/-}$ and C57BL/6 mice were euthanized and analyzed on 5 and 12dpi. For diet-induced insulin resistance experiments male C57BL/6 mice were euthanized after 4 weeks of repeated administration of LsAg after 18 weeks of HFD.

2.4 Life cycle *Litomosoides sigmodontis*

The life cycle of the filarial nematode *L. sigmodontis* as well as the infection of the animals is maintained and performed in an isolated area of the animal facilities of the IMMIP. *Ornithonyssus bacoti*, the tropical rat mite, is used as an obligate intermediate host. Breeding of mites were performed in plastic basins covered with fine litter, in incubators at 28°C and 80% air humidity to mimic the natural environmental conditions of the mites. Feeding of mites with fresh blood was performed thrice a week.

The life cycle of *L. sigmodontis* is maintained by placing the mites to its natural host, the cotton rat (*Sigmodon hispidus*). Cotton rats were periodically examined for MF load in the

peripheral blood. A small portion of blood taken from the orbital vein was used to determine MF numbers. During infection, the fine litter containing mites was mixed and transferred to special mite basins, whereupon a cotton rat was centrally placed, completely surrounded by the fine litter. Thereupon, uninfected mites fed on the MF containing blood of the cotton rats, leading to infection of the mites. Subsequently, fed mites leave the cotton rat and return to the fine litter, covering the surface of the basin. Afterwards, the fine litter was congregated in a glass Erlenmeyer-flask and covered with an artificial polyamide gaze. The flasks were placed in basins filled with soap water and stored in the incubator. After completing the infection, the cotton rat was returned to the plastic basin, covering the surface with soap water in order to remove remaining mites. The following day, cotton rats were placed in new cages until the next infection. Within the intermediate host, MF will develop and molt into infective L3 larvae around 8-9dpi. Several mites were frequently analysed for L3 larvae count in order to maintain an estimation of the parasitemia [181, 183].

2.5 Infection with *L. sigmodontis*

Experimental animals were infected in different ways; natural, subcutaneous, intradermal or intravenous. Nat. infection was performed via mites that were fed on microfilaremic cotton rats 10-12 days ago. Those mites were allowed to feed over night on 8-week-old mice, thereby transmitting infective L3 larvae to the mice. Therefore, mice were placed into the plastic basin, ground covered with mite-containing bedding.

To ensure comparability, all animals were exposed to the same population of mites. During the blood meal of the intermediate host, infective L3 larvae are transmitted into the skin of the mice. Fed mites returned to the fine litter, covering the bottom basin. The following day, the bedding was removed and discarded. Afterwards, infected mice were placed for 24h above soap water to further remove mites that fall into the water. The next day, mice were placed in

new cages, containing fresh bedding, food and water. To achieve further mites removal, cage bedding was replaced on a daily basis for five days. On the sixth day post infection mice were relocated to a different facility, part of the IMMIP animal facilities and remained there until the day of necropsy.

For i.d., s.c. and i.v. injection of infectious L3 *L. sigmodontis* larvae mites were dissected under the binocular microscope. Vital L3 larvae were isolated and collected. During s.c. injections, 40 L3 larvae in 100µl PBS media (PAA Laboratories GmbH, Pasching, Austria) were injected into the neck fold of the mice. Corresponding control mice were injected under the same conditions.

Two days prior to i.d. injections, the upper hind leg region of mice was shaved using commercially available depilatory crème (Veet). For i.d. injections 10 L3 larvae in 100µl PBS or 30µg LsAg were injected. Control mice were injected with 100µl PBS

For i.v. injections 40 L3 larvae in 100µl PBS were injected into the caudal vein of the mice. Same conditions were performed for corresponding control mice. During i.d., s.c. and i.v. injections the applied PBS was pre-warmed.

2.6 LsAg preparation

L. sigmodontis adult worms were isolated under sterile conditions from the thoracic cavities of infected mongolian gerbils. Thereupon, worms were collected in a petri dish and afterwards mechanically minced into a homogenized solution on ice using endotoxin-free PBS. The supernatant was taken and protein quantification was performed by Bradford assay (PAA, Pasching, Austria). LsAg aliquots were stored at -80°C.

2.7 Determination of worm burden

The thoracic cavity of euthanized mice were analysed to determine differences in the worm burden between IL-4R$^{-/-}$, dblGATA, IL-5$^{-/-}$, IL-4R$^{-/-}$/IL-5$^{-/-}$, S100A8/A9$^{-/-}$, AhR$^{-/-}$ and

corresponding BALB/c and C57BL/6 control mice. Therefore, 10ml of pleural lavage was filtered using sterile 40µm gaze filter in order to isolate the worms. Afterwards the gaze filter was placed in a petri dish. Furthermore, the peritoneal cavity was checked for additional remaining worms. Adult male and female worms were counted and morphologically distinguished**.**

2.8 Determination of microfilariae load

L. sigmodontis-infected mice were periodically (starting from 50dpi) examined for MF load in the peripheral blood (50µl) taken from the *vena facialis* and resuspended in 1ml of red blood lysis buffer (10x RBC lysis buffer, eBioscience, San Diego, USA) at room temperature (RT). The blood was centrifuged at 400g for 5min at RT (Eppendorf Centrifuge 5810R). Afterwards, the supernatant was discarded and the pellet resuspended. MF load was then evaluated by the use of a light microscope, utilizing 10 x magnification.

2.9 Analysis of female worm embryogenesis

Embryonic stages (egg, morula, pretzel, stretched MF) were determined and enumerated from two female worms per animal (total of 10 worms per group). Worms were isolated from WT, IL-4R$^{-/-}$, dblGATA, IL-5$^{-/-}$, IL-4R$^{-/-}$/IL-5$^{-/-}$ mice at 71 days post *L. sigmodontis* infection. Worms were individually homogenized by using a mortar in 80µl PBS and 20µl Hinkelmann solution (0.5% eosin Y, 0.5% phenol, 0.185% formaldehyde in destilled water). Embryonic stages in 10µl were determined and counted under a light microscrope (10 x magnification).

2.10 Plasma isolation

Before euthanasia of the mice blood was taken via the *vena facialis* using lancets (Goldenrod, Fisher Scientific, USA) and was directly transferred into EDTA tubes. Afterwards the isolated blood was centrifuged at 6000g/min at RT. Plasma was thereafter taken and stored at -20°C for further analysis.

2.11 Isolation of thoracic cavity cells

Experimental animals were euthanized per inhalation of an overdose of Isoflurane, disinfected with 70% ethanol and fixed dorsally on a surgical board. Subsequently, the thoracic cavity was dissected by conducting a gentle incision starting at the abdomen up to the thorax. The skin was fixed marginally with pins. Within the exposed diaphragm, a small cut was performed. Afterwards the thoracic cavity was flushed utilizing a sterile Pasteur pipette with media (RPMI 1640, Gibco, Thermo Fisher Scientific Inc., Carlsbad, CA, USA) or PBS to isolate cells. Each flushing step was performed with a volume of 1ml and filtered through gauze to isolate the worms in case of *L. sigmodontis*-infected mice. The first ml was transferred into an Eppendorf tube and centrifuged for 5min at 400g at RT. The supernatant was kept in a deepwell plate and stored at -20°C for further cytokine/chemokine analysis. The pellet was combined with the volume of the ensuing flushing steps, in total 9ml and added to a 15ml falcon placed on ice for FACS analysis.

2.12 Isolation of bronchoalveolar cells

The trachea was surgically exposed and a small incision was performed at the cervico-thoracic junction and a venous catheter (Vasofix Braunüle- B Braun, Germany) was inserted, followed by several washing steps of the bronchoalveolar space with 10ml of cold PBS. The first ml was collected in an Eppendorf tube and centrifuged at 400g for 5min at 4°C. The supernatant was added into a deepwell plate and stored at -20°C for further cytokine/chemokine and enzyme analysis. The pellet was pooled with the volume of the ensuing flushing steps (9ml) and added to a 15ml falcon placed on ice for FACS analysis. Afterwards, the cells were centrifuged at 400g for 5min at 4°C. At last, cell numbers were determined by Casy® Cell Counter (Hoffmann-La Roche Ltd, AG, Basel, Switzerland) and adjusted for further FACS analysis or cell culture stimulation experiments.

2.13 Isolation of splenocytes

The spleen of dissected mice were removed surgically and added to a 15ml Falcon filled with 5ml of media (RPMI 1640) or PBS and kept on ice. Afterwards, each spleen was grinded and pressed through a 70µm cell strainer (Miltenyi, Bergisch Gladbach, Germany) by utilizing a 10ml syringe plunger. The flow-through was collected in a 15ml Falcon tube. Strainer and petri dish were flushed several times with RPMI medium to ensure higher isolation of cells. Next, cells were washed and centrifuged at 400g for 10min at 4°C. The supernatant was discarded and the pellet was resuspended with 1ml of red blood cell lysis buffer (Thermo Fisher, San Diego, USA) for 5min at RT. Lysis was stopped by adding further 9ml of RPMI medium and washed again by centrifugation at 400g for 10min and 4°C. The supernatant was discarded and the pellet was resuspended in 10ml of RPMI cell culture medium. Cell numbers were determined by Casy® Cell Counter and adjusted for further FACS analysis or cell culture stimulation experiments.

2.14 Stromal vascular fraction (SVF) and liver cell isolation

Mice were anaesthetized (Rompun - Bayer, Ketamin – WDT, Germany) and fixed on a surgical board for tissue and organ removal. The skin and peritoneum were gently dissected and mice were intracardially perfused for 5min with 1x PBS to remove non-adhering, non-infiltrating erythrocytes and blood-lymphocytes. Subsequently, visceral adipose tissue (VAT) from the intraabdomen and liver was removed and collected in DMEM-low glucose medium (Gibco, life technologies, USA) containing 1g/L D-glucose (Sigma Aldrich, Steinheim, Germany), 4mM L-Glutamine, 25mM HEPES, 1g/ml BSA and 1% penicillin-streptomycin (all PAA Laboratories GmbH, Pasching, Austria). Resected tissue was minced by scissors and transferred to 15ml falcons, containing 4ml medium of 1.5mg/ml Collagenase-P (Roche, Mannheim, Germany).

Thereupon tissue suspension was incubated at 37°C for 30min with continuous shaking. During half of the incubation period samples were mixed thoroughly by hand. After a 30min incubation step samples were washed with MACS buffer (Miltenyi, Bergisch Gladbach, Germany) and centrifuged at 400g for 5min at RT. Supernatant was discarded and red blood lysis was performed (Thermo Fisher Scientific, San Diego, USA) by adding 1ml lysis buffer for 5min at RT. Lysis reaction was stopped by adding 9ml of MACS buffer. Samples were filtered through a 100µm filter and then centrifuged at 400g for 5min at RT. Afterwards, the supernatant was discarded and cell numbers were determined by Casy® Cell Counter and adjusted for further FACS analysis or cell culture stimulation experiments.

2.15 Freezing of cells

FixPerm Substrat® was diluted (1:3) with FixPerm Diluent® (Thermo Fisher Scientific, San Diego, USA). Cells were fixed in 300µl FixPerm® buffer overnight at 4°C. The next day, a washing step was performed by adding 1ml of PBS and centrifuged at 400g for 10min at 4°C. The supernatant was removed and the cell pellet was resuspended in 1ml PBS/10% DMSO (Sigma-Aldrich, Steinheim, Germany). Cells were frozen and stored at -20°C.

2.16 Neutrophil Purification - Percol

Mice were euthanized per inhalation of an overdose of Isoflurane. Afterwards, the femurs of S100A8/A9$^{-/-}$ and corresponding WT controls were removed surgically and the remaining tissue was detached. The condyles of the bones were cut and subsequently the bone marrow was flushed with 5ml of cold sterile PBS by utilizing a 10ml syringe and a 27G needle. The flow-through was filtered immediately and collected in a 15ml falcon tube. Next, a centrifugation step was performed at 400g for 5min at 4°C and the supernatant was removed. Red blood cell lysis was performed by adding 1ml RBC lysis buffer for 5min at RT. Lysis was stopped by adding an additional 9ml of cold sterile PBS. Afterwards, the cells were

washed and centrifuged again at 400g for 10min at 4°C. The supernatant was discarded and the cell pellet was resuspended in 3ml of PBS. Neutrophil purification was conducted by a 3-layer Percoll gradient method. A stock solution of 100% Percoll (GE Healthcare Life Sciences, Munich, Germany) was prepared by adding 9 volumes of pure Percoll and one volume of 10x PBS. Further, Percoll solutions at 72%, 64% and 52% were prepared by diluting 100% Percoll solution.

RPMI media was used for better visible separation of the different layers. Each layer consists of 3ml and was added carefully into a 15ml falcon tube in a percentage dependent manner 1) 72% → 2) 64% → 3) 52% → 4) cells. Afterwards, the tube was centrifuged for 30min at 1500g at RT without brake. Neutrophils are found at the interface between the 72% and 64% layers and were recovered by a soft Pasteur pipette. Next, cells were washed with PBS and centrifuged at 400g for 5min at RT. After the centrifugation step, the supernatant was removed and cells were resuspended in 1ml of PBS. Cell numbers were determined by Casy® Cell Counter and adjusted for further FACS analysis or cell culture stimulation experiments.

2.17 Bronchoalveolar cell and splenocytes stimulation

Splenocytes were isolated as previously described under 2.13 and cultured in 1ml of media (RPMI 1640) containing 10% FCS, 1% L-Glutamine 100U / mL Penicillin-Streptomycin under different conditions for 72h at 37°C (5% CO_2, 80% humidity). Each condition consisted of $2x10^6$ cells. Cells were stimulated with either Concanavalin A (ConA) (2.5µg/ml) (Sigma-Aldrich, St. Louis, MO, USA) or LsAg (25µg/ml). Unstimulated cells were used as control. After 72h of incubation the supernatant was recovered and frozen at -20°C for further cytokine analysis.

2.18 Conditioned media culture of CD4+ and CD8+ T cells

Splenocytes were isolated as described under 2.13 splenic CD4+ and CD8+ T cells were separated by magnetic MACS beads according to the manufacturer´s protocol (Milteny Biotec, Bergisch Gladbach, Germany). CD4+ and CD8+ T cells from obese mice were cultured for 4h in adipocyte conditioned media from LsAg and PBS-administrated mice with a cocktail containing PMA (50ng/ml), ionomycin (1µg/ml) (Sigma-Aldrich, St. Louis, MO, USA), Golgi Plug and Golgi Stop (0.66µg/ml) (BD Bioscience, Franklin Lakes, USA). Adipocyte conditioned media was assessed by daily i.p. (in total 4 weeks) injections of 2µg LsAg and PBS as corresponding controls in mice fed for 10-12 weeks with normal food diet (NFD) or either HFD. In summary, 100mg of adipose tissue was isolated and digested with collagenase. After three washing steps, old media was replaced with fresh media. Ddipocytes from NFD or HFD were cultured with purified splenic CD4+ or CD8+ T cells as described previously.

2.19 Neutrophil cell culture conditions

Bone marrow-derived neutrophils were isolated as previously described under 2.16. Each condition consisted of $1x10^5$ neutrophils and was performed in triplicates. Neutrophils were cultured in 200µl of RPMI 1640 media containing 10% FCS, 1% L-Glutamine, 100U/mL Penicillin-Streptomycin for 2h and 6h at 37°C (5% CO_2, 80% humidity) . Cells were stimulated with LPS Ultrapure (100ng/ml) (InvivoGen, San Diego, USA) and crude worm *L. sigmodontis* extract LsAg (50µg/ml). Unstimulated cells were used as control. After 7h of culture the supernatant was recovered and frozen at -20°C for further cytokine, chemokine and enzyme analysis. Cells were taken for FACS analysis.

2.20 Neutrophil depletion within the lung

Mice were treated intranasally with 250µg/ml anti-Ly6G antibody (Clone 1A8) (BioXCell, West Lebanon, USA) to deplete neutrophils within the lung. Depletion was performed 18h prior to infection with *L. sigmodontis* and repeated every other day until 5dpi. Corresponding control mice were treated with an IgG2a isotype antibody (Clone C1.18.4) (BioXCell, West Lebanon, USA). Neutrophil depletion within the bronchoalveolar lavage was confirmed via flow cytometry.

2.21 Enzyme-linked immunosorbent assay (ELISA)

Determination of cytokine, chemokine and enzyme concentrations in pleural, bronchoalveolar lavage and cell culture supernatants was performed utilizing the Sandwich-ELISA method. ELISAs were performed in duplicates according to the manufacturer's kit protocols (Thermo Fisher Scientific: IL-4, IL-5, IL-6, IL-13, IFN-γ, TNF, IL-1β) (Thermo Fisher Scientific, Waltham, USA) (R&D systems: CXCL-1, CXCL-2, CXCL-5, elastase, adiponectin) (R&D, Minneapolis, USA). ELISA plates (Greiner Bio-One, Solingen, Germany) were coated with primary antibody (capture), diluted in either coating buffer (10x coating buffer (1:10 dilution dest. water) (Thermo Fisher Scientific, Waltham, USA) or PBS (R&D) overnight at 4°C. The following day, plates were washed thrice with washing buffer (PBS/0,05% Tween20® (Sigma-Aldrich, St. Louis, MO, USA)) and subsequently blocked with either 1x Assay diluent (Thermo Fisher Scientific, Waltham, USA) or PBS/1% BSA (R&D) for 2h at RT. Afterwards, plates were washed thrice, corresponding serial dilutions of standards and samples were added in duplicates overnight at 4°C. 1x Assay diluent or PBS/1% BSA was used as blank controls. On the third day, plates were washed for five times and the second antibody (detection) was added for a further duration of 1h at RT. After five washing steps the enzyme horseradish peroxidise (R&D, Minneapolis, USA) or avidin peroxidase (Thermo Fisher Scientific, Waltham, USA) was added for 1h at RT.

Plates were washed again for five times. Subsequently tetramethylene benzidine (TMB) (Thermofisher, Inc., San Diego, CA, USA) was added until the color change occurred. Further change in color was stopped by adding 25 µl of 1M H_2SO_4 (Merck, Darmstadt, Germany). Determination of the concentration was evaluated by the optical density (OD) at 450nm and 650nm was used as reference using SpectraMAX 340 Pc plate reader (Molecular Devices, Ismaning, Germany).

2.22 Flow cytometry - Fluorescence activated cell scan (FACS)

To analyze cellular composition, cell activation and intracellular cytokines within the thoracic cavity, spleen, skin and lung, the single cell suspensions were stained for cell surface markers and analyzed via flow cytometry by subdividing a cell population into sub-populations based on size (Forward Scatter (FSC)), granularity (Sideward Scatter (SSC)) and fluorescent labeling. Prior to the analysis, isolated cells were washed and blocked in PBS containing 1% BSA and rat Ig (1µg/ml, Sigma-Aldrich, St. Louis, MO, USA) for 1h. Cells were then centrifuged at 400g for 5min at 4°C and stained by fluorescent-marked monoclonal antibodies in FACS tubes. Compensation was performed via BD compensation beads. Gate setting for specific cell populations was based on the Fluorescence minus one (FMOs) approach, which lacks one of the utilized antibodies.

For intracellular staining of RELMα or intracellular cytokines, isolated cells were incubated in 300µl fixation and permeabilization buffer overnight at 4°C. Next day, cells were washed and centrifuged at 400g for 5min at 4°C. Afterwards, fixed cells were incubated in 300µl permeabilization buffer (Thermo Fisher Scientific, San Diego, USA) for 20min at RT. Next, cells were washed during a centrifugation step and subsequently blocked in PBS/1% BSA containing rat Ig (1µg/ml) for 1h at 4°C. After two further washing steps in permeabilization

buffer for 10min at 400g, cells were stained or prepared for cell culture simulation (LPS, ConA, LsAg, PMA/ Ionomycin with Golgi Plug & Golgi Stop).

For RELMα staining, fixed and permeabilized cells were stained with rabbit-anti-mouse RELMα (Peprotech, Rocky Hill, NJ, USA) for 1h at 4°C in the dark. Cells were then washed in permeabilization buffer and centrifuged at 400g for 5min at 4°C. Subsequently, cells were stained with the corresponding secondary antibody (goat anti-rabbit Alexa488, Invitrogen, Carlsbad, CA, USA) for 30min at 4°C in the dark. Measurement and analysis was acquired using the BD Canto (BD Biosciences, Heidelberg, Germany) and BD FACSDiva software.

2.23 Glucose tolerance test

Six hours before performing the glucose tolerance test (GTT), C57BL/6 mice were fasted. Fasting blood glucose levels were measured from the tail vein using a blood glucose meter (Accu-Check Advantage, Roche Diagnostics GmbH, Mannheim, Germany). During glucose challenge mice were injected i.p. with a dose of 2g glucose monohydrate (Merck, Darmstadt, Germany) solution per kg body weight. Periodically at 15, 30, 60, 90, and 120min post glucose injection, blood was taken by the tail vein and glucose concentrations were determined.

2.24 Insulin tolerance test

Four hours before performing the insulin tolerance test (ITT), C57BL/6 mice were fasted by removing NFD and HFD. After 4h, fasting blood glucose levels were measured from the tail vein using a blood glucose meter (Accu-Check Advantage, Roche Diagnostics GmbH, Mannheim, Germany). During insulin challenge, mice were injected i.p. with a dose of 0.001U/g body weight of insulin. At 15, 30, 60, 90, and 120min post insulin injection, blood was taken from the tail vein and glucose concentrations were determined.

2.25 Lung histology and immunhistology

S100A8/A9$^{-/-}$ and C57BL/6 WT naive and infected mice (nat., s.c., i.v. infection) were sacrificed at 12dpi. The bronchoalveolar space was flushed several times as described previously. Next, the lung was fixed in 4% formalin overnight. The following day, the fixative was renewed for another 24h. Afterwards, lungs were placed in 70% alcohol for 2-7 days before paraffin embedding. Five-micron-thick serial sections were prepared. Each lung was stained with a haematoxylin-eosin (H&E) solution. The peri-vascular space (PVS) was analysed by utilizing a Masson's trichrome staining (Sigma-Aldrich, St. Louis, MO, USA) to visualize and pictorially accentuate collagen fibers according to the manufacturer protocols. Immunostained serrations were washed in PBS and subsequently tissue peroxidase was blocked by utilizing a dual endogenous enzyme block (Dako, Les Ulis, France) and biotin/avidin by a biotin blocking kit (Vector, Malakoff, France). Neutrophils were first stained in a 1/200 dilution with a primary antibody against Ly-6G (rat monoclonal AB, clone NIMP-R14, Hycult Biotech, Uden, Netherlands) dissolved in blocking serum (Vectastain kit, Vector, Malakoff, France). Antigen recovery was performed by using an antigen unmasking solution (Vector, Malakoff, France) at pH 6. Afterwards, S100A9 was stained with the primary antibody against S100A9 (rat monoclonal Ab, clone MU14-2A5, Hycult Biotech 1:200) in blocking serum (Vectastain kit, Vector, Malakoff, France). A proteinase K solution (0.004%), diluted in a 1:1 glycerol-modified Tris Buffer (EDTA 3.7%, Triton X-100 0.5%, pH 8), was used for antigen retrieval for 10min at 37°C. S100A9 detection was conducted by the Vectastain Elite ABC kit (Vector, Malakoff, France). Disclosure was performed with a high sensitivity AEC substrate (Dako, Les Ulis, France), which was subsequently counterstained with a Mayer's hematoxylin solution (Merck, Semoy, France).

2.26 Vascular permeability assay

In vivo vascular permeability was assessed via the intracutaneous injection of 10µg LsAg or of PBS as corresponding control in the ears of mice. After 3min mice were injected i.v. with 30mg/kg body weight of Evans Blue (Sigma-Aldrich, St. Louis, MO, USA) in 200µl of NaCl 0.9%. After a subsequent incubation time of 10min, mice were euthanized and ears were removed and transferred into 500µl of >99% formamide (Sigma-Aldrich, St. Louis, MO, USA) and incubated at 56°C for 24h. Evans Blue leakage was quantified by determing optical density at 620nm (Molecular Devices, Ismaning, Germany).

2.27 *L. sigmodontis* L3 larvae *in vitro* assay

10 L3 larvae were cultured with $1x10^5$ WT and S100A8/A9$^{-/-}$ neutrophils in triplicates in enriched media (RPMI 1640 media + 10% FCS, 1% L-Glutamine, 100U/mL Penicillin-Streptomycin) for 48h at 37°C (5% CO_2 ,90% humidity). Motility was assessed daily by a five point scoring system; Score 4: vigorous, fidgeting movements. Score 3: slightly impaired vigorous movements. Score 2: impaired motility/slow movements. Score 1: mostly immobile/single movements. Score 0: fully immobile within 20s observation period.

2.28 Statistics

Data were analyzed for statistical significance using GraphPad Prism 5.03 software (GraphPad Software, La Jolla, California, USA). Differences between two unpaired groups were tested for statistical significance with the Mann-Whitney-U-test. Normal distribution of the data was tested with D'agostino test. Parametrically distributed data were analyzed by one-way ANOVA followed by Dunnett's test, whereas non-parametrically distributed data were analyzed by Kruskal-Wallis test followed by Dunn's posthoc test. P-values of <0.05 were considered statistically significant.

3. Results

3.1 Role of IL-4R, IL-5 and eosinophils on *L. sigmodontis* infection

3.1.1 IL-4R, IL-5 and eosinophils are essential for control of the occurrence of microfilaremia, whereas IL-5 and eosinophils impair adult worm survival, embryogenesis and maintenance of microfilaremia

Previous studies confirmed that type 2 immune response, involving eosinophils, IL-5 and IL-4, exhibit protective immune responses against *L. sigmodontis*. In the present project the impact of eosinophils, IL-5, and the IL-4R was directly compared on the outcome of *L. sigmodontis* infection during the peak of microfilaremia in WT animals (71dpi) and a late phase of infection (119dpi) after IL-4R$^{-/-}$/IL-5$^{-/-}$ mice showed a first decline in microfilaremia and most WT animals cleared the infection. Therefore, microfilarial burden and frequency of animals developing microfilaremia were analyzed over time. During necroscopies at 71 and 119dpi total adult worm numbers and worm lengths were determined. Furthermore, analysis of the cytokine production from thoracic cavity lavage, the site of adult worm residence, embryogenesis and major immune cell types were performed within the thoracic cavity and spleen. MF counts revealed increased numbers of peripheral MF throughout the infection in all tested immunocompromised mice (IL-4R$^{-/-}$, IL-5$^{-/-}$, IL-4R$^{-/-}$/IL-5$^{-/-}$ and dblGATA BALB/c mice) compared to WT controls (Fig. 3A). Furthermore, the onset of microfilaremia into the peripheral blood in all immune-deficient mouse strains was observed much earlier (56dpi) compared to WT controls (64dpi). IL-4R$^{-/-}$/IL-5$^{-/-}$ mice exhibited the highest MF counts during the whole time period. At 56dpi, 90% of IL-4R$^{-/-}$and 95% of IL-4R$^{-/-}$/IL-5$^{-/-}$ mice were positive for MF, whereas microfilaremia occurred in 39% of IL-5$^{-/-}$ and 66% in dblGATA mice in comparison to merely 10% of the WT controls (Fig. 3B). The peak of microfilaremia was observed in WT (~6 MF/50µl blood) and dblGATA mice at 78dpi (~746 MF/50µl

blood), in IL-4R$^{-/-}$ (~294 MF/50µl blood) at 70dpi, and in IL-5$^{-/-}$ (~639 MF/50µl blood) and IL-4R$^{-/-}$/IL-5$^{-/-}$ at 97dpi (~4600 MF/50µl blood) (Fig. 3A).

Microfilaremia persisted in IL-4R$^{-/-}$/IL-5$^{-/-}$, dblGATA, and IL-5$^{-/-}$ mice for >120dpi, while microfilaremia declined in IL-4R$^{-/-}$ and WT controls following 78dpi (Fig. 3A). All immune-deficient mice exhibited a substantially higher frequency of MF positive animals (dblGATA, IL-4R$^{-/-}$/IL-5$^{-/-}$ mice: 100%, IL-5$^{-/-}$ mice: 58.5%, IL-4R$^{-/-}$ mice: 100%) compared to WT controls (30%; Fig. 3B).

Adult worm counts were determined and showed an increase in all analysed immune-deficient mouse strains (dblGATA, IL-5$^{-/-}$, IL-4R$^{-/-}$/IL-5$^{-/-}$) except for IL-4R$^{-/-}$ mice compared to WT controls. For IL-5$^{-/-}$ and dblGATA mice at 71 and 119dpi, the differences were statistically significant in comparison to WT mice (Fig. 3C, D). At 119dpi an increased number of granuloma was observed in the IL-4R$^{-/-}$/IL-5$^{-/-}$ mice, which hampered the exact worm counts and may explain the lower worm numbers in comparison to the dblGATA and IL-5$^{-/-}$ mice.

To elucidate, whether the increased MF counts in IL-4R$^{-/-}$/IL-5$^{-/-}$, dblGATA and IL-5$^{-/-}$ mice are due to an enhanced embryogenesis of female adult worms in comparison to WT controls, embryograms were performed. Embryograms from 71dpi demonstrate that female adult worms from IL-4R$^{-/-}$/IL-5$^{-/-}$ animals had significantly higher numbers of all embryonal stages (eggs, morulae, pretzel, and stretched MF) compared to WT animals and of the later embryonal stages (pretzel and stretched MF) in comparison to IL-5$^{-/-}$ mice. In contrast, female adult worms from dblGATA and IL-5$^{-/-}$ mice exhibited significant increased numbers of the early embryonal stages (eggs: $p<0.01/p<0.05$; morulae: $p>0.05$), but no significantly increased number of stretched MF. These data indicate that the highest MF count in IL-4R$^{-/-}$/IL-5$^{-/-}$ animals is in part due to an enhanced embryogenesis (Fig. 3E).

Worm lengths of adult male and female worms were significantly longer in all tested immune compromised mouse strains compared to worms from WT controls at 71dpi (mean female worm length: WT 4.82cm, IL-4R$^{-/-}$ 5.54cm, dblGATA 5.62cm, IL-5$^{-/-}$ 5.30cm, IL-4R$^{-/-}$/IL-5$^{-/-}$ 6.51cm; mean male worm length: WT 1.54cm, IL-4R$^{-/-}$ 1.97cm, dblGATA 1.62cm, IL-5$^{-/-}$ 1.68cm, IL-4R$^{-/-}$/IL-5$^{-/-}$ 2.11cm ; Fig. 3F, G). Filariae lengths of adult male and female worms at 119dpi did not show any statistical differences between all utilized mouse strains (Fig. 3H, I). Besides, the ratio of male and female adult worms on 71 and 119dpi was not altered in any of the mouse strains tested (data not shown).

These results indicate that the release and maintenance of microfilaremia is efficiently regulated by IL-4R and IL-5/eosinophils. IL-5/eosinophils affect adult worm survival and thereby the maintenance of microfilaremia. This effect on microfilaremia was further promoted by the combined deficiency of IL-4R and IL-5.

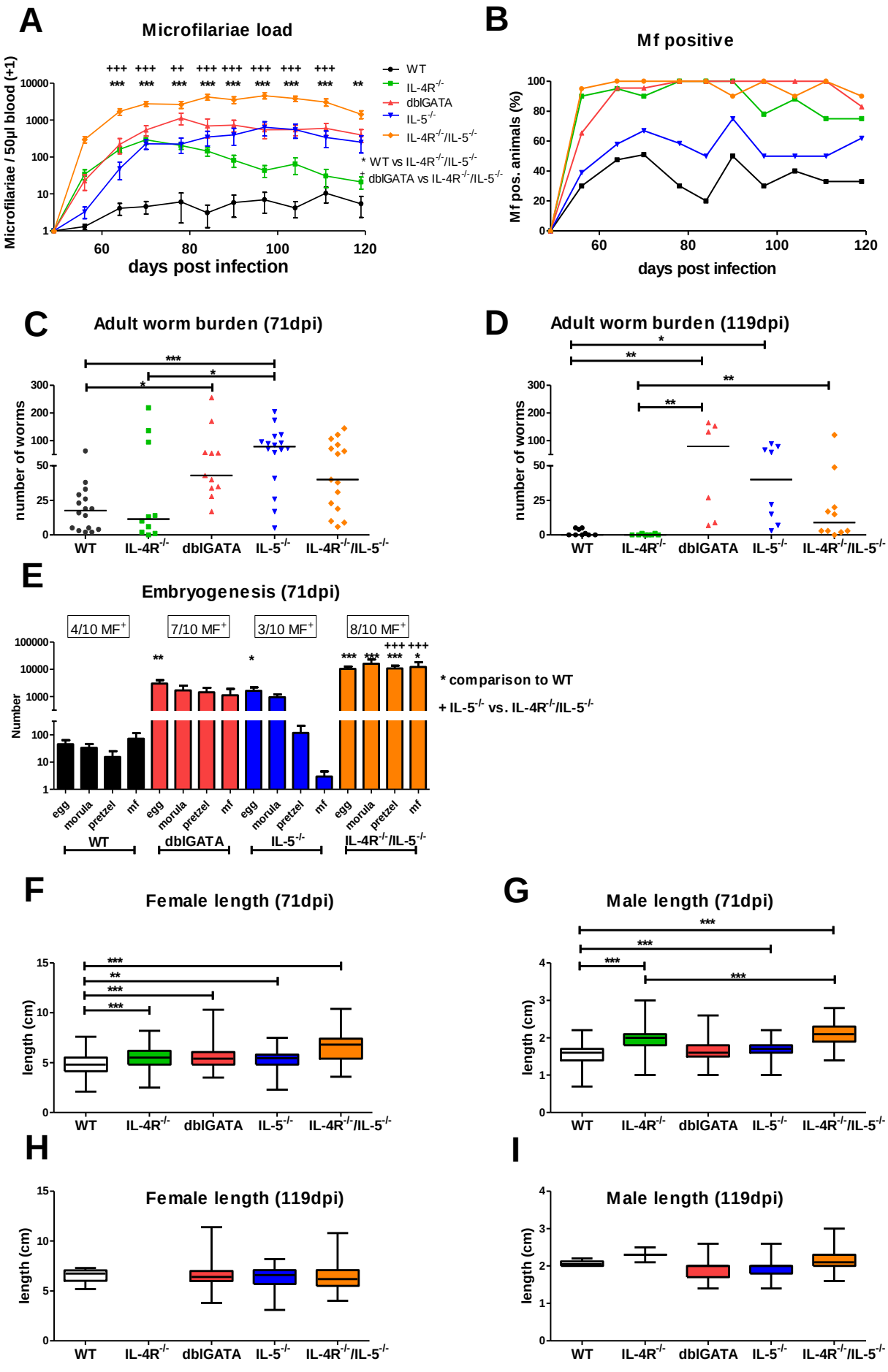
A
Microfilariae load
Microfilariae / 50µl blood (+1)
days post infection
WT
IL-4R-/-
dblGATA
IL-5-/-
IL-4R-/-/IL-5-/-
* WT vs IL-4R-/-/IL-5-/-
+ dblGATA vs IL-4R-/-/IL-5-/-
B
Mf positive
Mf pos. animals (%)
days post infection
C
Adult worm burden (71dpi)
number of worms
D
Adult worm burden (119dpi)
number of worms
E
Embryogenesis (71dpi)
4/10 MF+
7/10 MF+
3/10 MF+
8/10 MF+
Number
egg
morula
pretzel
mf
* comparison to WT
+ IL-5-/- vs. IL-4R-/-/IL-5-/-
F
Female length (71dpi)
length (cm)
G
Male length (71dpi)
length (cm)
H
Female length (119dpi)
length (cm)
I
Male length (119dpi)
length (cm)

Fig. 3: IL-4R and IL-5/eosinophils control microfilaremia, whereas IL-5 and eosinophils impair adult worm survival and maintenance of microfilaremia. (**A**) Microfilariae count per 50µl of peripheral blood throughout *L. sigmodontis* infection and (**B**) frequency of wildtype (WT) controls, IL-4R$^{-/-}$, dblGATA, IL-5$^{-/-}$, IL-4R$^{-/-}$/IL-5$^{-/-}$ mice that develop microfilaremia. Adult worm burden (**C, D**), embryogenesis of female adult worms staged as eggs, morulae, pretzel and stretched microfilariae at 71 days post infection (dpi) with numbers of female worms containing stretched microfilariae within their uteri indicated above the different mouse strains (**E**), and female (**F, H**) and male worm length (**G, I**) at 71 (**C, F, G**) and 119 (**D, H, I**) dpi. Results are shown as means ± SEM (**A, B, E**), medians (**C, D**), and box & whisker plots with minimum and maximum (**F-I**). Data were analyzed using two-way ANOVA followed by Bonferroni's post-test (**A**), one-way ANOVA followed by the Dunnett's test (**F**) and Kruskal-Wallis test followed by the Dunn's multiple comparison test (**C-E, G-I**).*p<0.05, **p<0.01, ***p<0.001. Data shown in (**A-C**) are pooled from two independent experiments at 71dpi with a total of 10-16 mice per group. Data shown in (**D, F-I**) are from one experiment with 6-10 mice per group and data shown in (**E**) from a single experiment with 5 mice per group and analysis of 2 female worms per mouse.

3.1.2 Negative association between thoracic cavity eosinophils and adult worm survival as well as AAMs with microfilaremia

Helminth infections are associated with increases of several cell frequencies such as eosinophils during chronic infections leading to eosinophilia or an increased frequency of AAMs. Therefore, potential correlations between different frequencies of immune cell populations with the pronounced number of MF and adult worms in immune-deficient mice were determined. Therefore, thoracic cavity and spleen cells of WT, IL-4R$^{-/-}$, dblGATA, IL-5$^{-/-}$, and IL-4R$^{-/-}$/IL-5$^{-/-}$ mice on 71 and 119 days post *L. sigmodontis* infection were assessed and analysed by flow cytometry. Total numbers of thoracic cavity cells were lower in dblGATA, IL-5$^{-/-}$ and IL-4R$^{-/-}$/IL-5$^{-/-}$ mice compared to WT controls at 71dpi, reaching statistical significance for IL-5$^{-/-}$ and IL-4R$^{-/-}$/IL-5$^{-/-}$ mice (Fig. 4A). Thoracic cavity cell counts at 119dpi were comparable and did not show any statistical differences between WT and immune-compromised mice (Fig. 4B). The absence of IL-4R at 71 and 119dpi resulted in

reduced absolute numbers of macrophages (Fig. 4C, D) and a lack of AAMs (Fig. 4E, F) within the thoracic cavity of IL-4R$^{-/-}$ and IL-4R$^{-/-}$/IL-5$^{-/-}$ mice. As expected total numbers of eosinophils in IL-5 and dblGATA deficient mice were barely present (Fig. 4G, H).

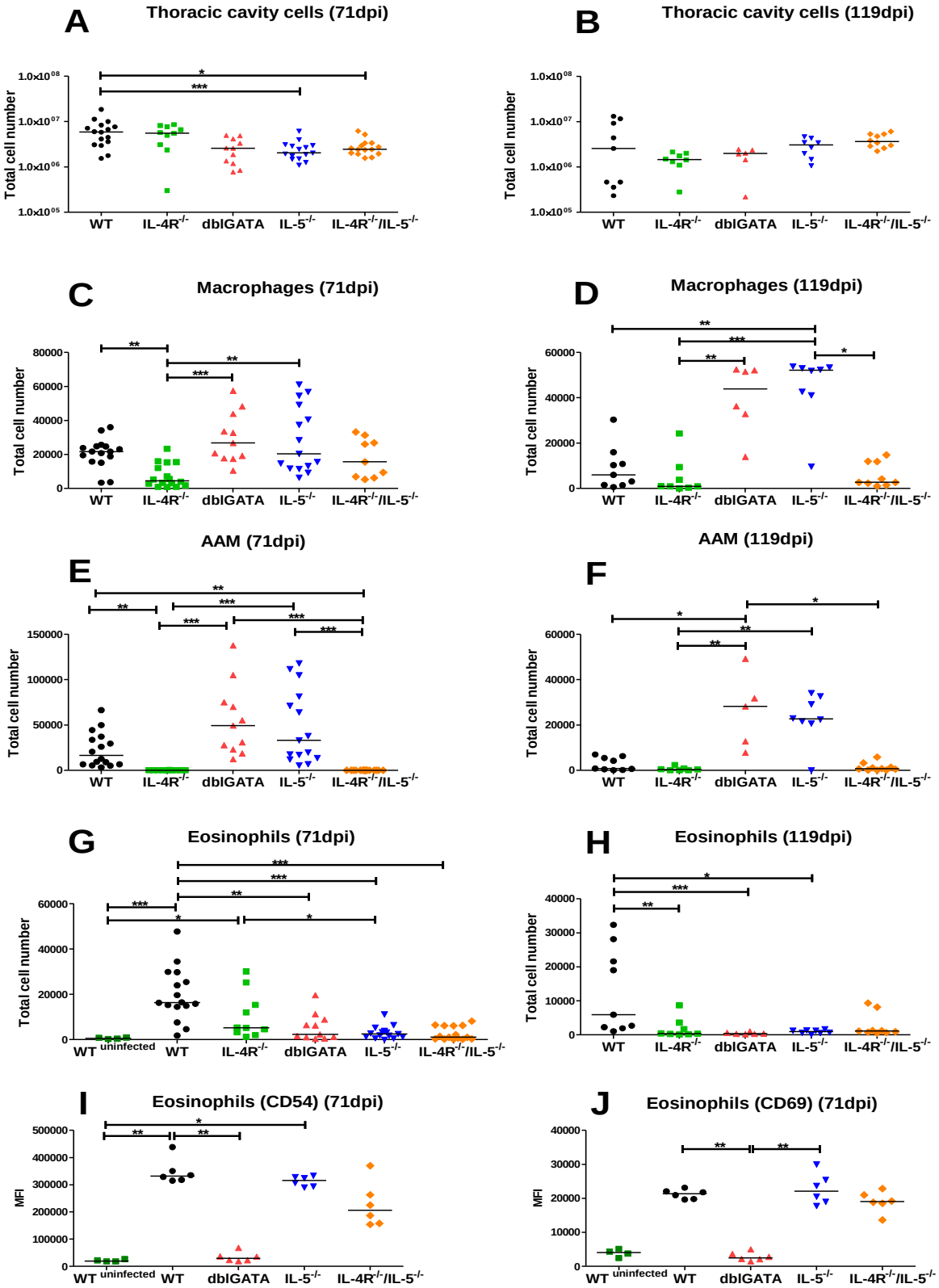

Fig. 4: Thoracic cavity cells of *L. sigmodontis*-infected IL-5$^{-/-}$, dblGATA and IL-4R$^{-/-}$/IL-5$^{-/-}$ mice lack eosinophils and IL-4R$^{-/-}$ and IL-4R$^{-/-}$/IL-5$^{-/-}$ mice lack alternatively activated macrophages. Total number of thoracic cavity cells in IL-4R$^{-/-}$, dblGATA, IL-5$^{-/-}$, IL-4R$^{-/-}$/IL-5$^{-/-}$ mice and wildtype (WT) controls 71 (**A**) and 119 days (**B**) post *L. sigmodontis* infection. Total thoracic cavity macrophage numbers (**C, D**), RELMα positive alternatively activated macrophage (AAM, **E, F**) and eosinophil numbers (**G, H**) at 71 and 119 days post *L. sigmodontis* infection (**A-H**), as well as expression of CD54 (**I**) and CD69 on eosinophils (**J**) at 71 days post *L. sigmodontis* infection and naïve WT controls (**G-J**). Results are shown as medians. Data were analyzed using one-way ANOVA followed by the Dunnett's test (**C, G, H**) and Kruskal-Wallis followed by the Dunn's multiple comparison test (**A, B, D, E, F, I, J**).*p<0.05, **p<0.01, ***p<0.001. Data shown in (**A, C, E, G**) are pooled from two independent experiments at 71dpi with 10-16 mice per group. Remaining figures (**B, D, F, H**) are from one experiment at 119dpi with 6-10 mice per group. Figures (**I, J**) are representative of one independent experiment at 71dpi with 4-6 mice per group.

Absolute numbers of thoracic cavity CD4+ T cells, CD8+ T cells and neutrophils were determined on 71 and 119dpi (Fig. 5). At 71dpi, absolute CD4+ T cell numbers were increased in IL-5$^{-/-}$ mice (Fig. 5A) and neutrophil numbers were significantly increased in IL-4R$^{-/-}$/IL-5$^{-/-}$ mice in comparison to the corresponding control group (Fig. 5E). Those differences in CD4+ T cell and neutrophil numbers were not observed anymore at 119dpi (Fig. 5B, F). Absolute CD8+ T cell numbers did not show any statistical differences between all tested mouse strains at 71 and 119dpi (Fig. 5C, D).

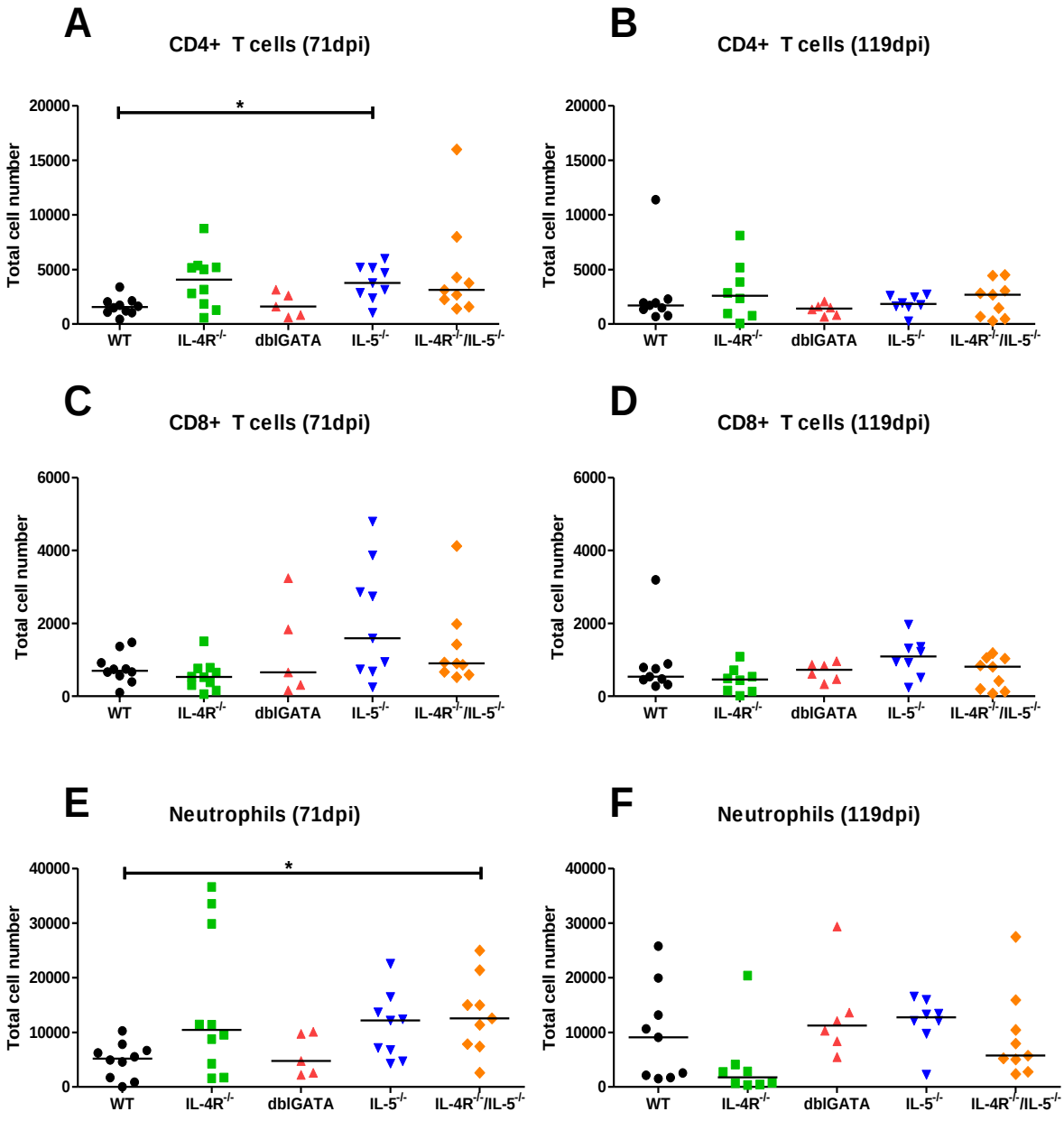

Fig. 5: Mice deficient for IL-5, dblGATA, IL-4R and IL-4R/IL-5 show no strong influence on CD4+ T cells, CD8+ T cells and neutrophil numbers within the thoracic cavity. Total thoracic cavity CD4+ T cell numbers (**A**, **B**), CD8+ T cell numbers (**C**, **D**) and neutrophil numbers (E, F) at 71 and 119 days post *L. sigmodontis* infection in IL-4R$^{-/-}$, dblGATA, IL-5$^{-/-}$, IL-4R$^{-/-}$/IL-5$^{-/-}$ mice and wildtype (WT) controls. Results are shown as medians. Data were analyzed using one-way ANOVA followed by the Dunnett's test (**A, E**) and Kruskal-Wallis followed by the Dunn's multiple comparison test (**B, C, D, F**).*$p<0.05$. Data shown in (**A, C, E**) are pooled from two independent experiments at 71dpi with 10-16 mice per group. Remaining figures (**B, D, F**) are from one experiment at 119dpi with 6-10 mice per group.

Spearman correlation analysis revealed a strong negative correlation between thoracic cavity eosinophil numbers and adult worm counts at 71dpi (r= -0.61; p=0.0001; Fig. 6A), which was not present anymore at 119dpi (r= -0.07; p=0.61; Fig. 6B). Furthermore, thoracic cavity eosinophil numbers negatively correlated to the MF load at 71 (r= -0.46; p=0.005) and 119dpi (r= -0.24; p=0.13; Fig. 6C, D).

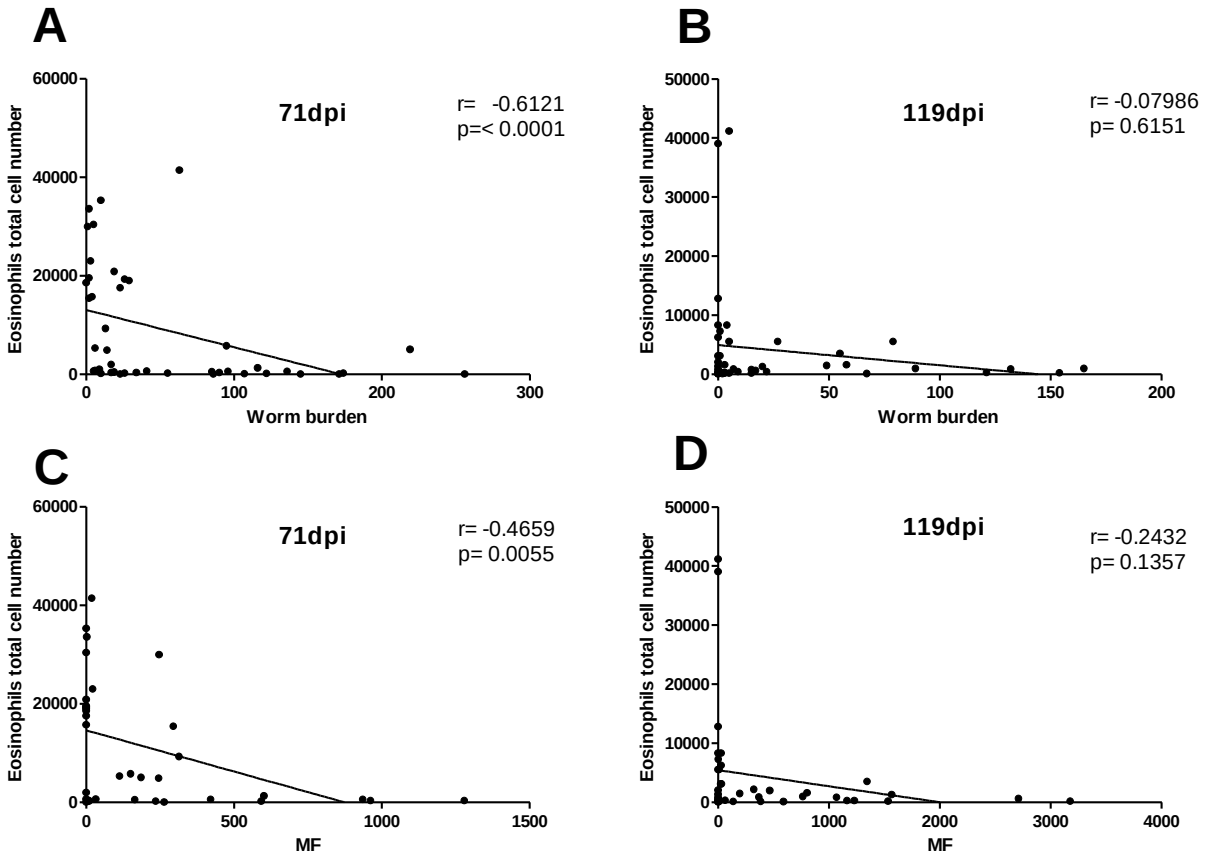

Fig. 6: Negative correlation of thoracic cavity eosinophil numbers and adult worm burden as well as MF counts. Correlation of the total thoracic cavity eosinophil numbers and adult worm burden (**A, B**) and peripheral blood MF counts (**C, D**) at 71 (**A, C**) and 119 days (**B, D**) post *L. sigmodontis* infection in IL-4R$^{-/-}$, dblGATA, IL-5$^{-/-}$, IL-4R$^{-/-}$/IL-5$^{-/-}$ mice and wildtype controls. Spearman correlation. Data shown in (**A, C**) are pooled from two independent experiments at 71dpi with 10-16 mice per group. Remaining figures (**B, D**) are from one experiment at 119dpi with 6-10 mice per group.

Thoracic cavity AAM counts did not show any correlation with adult worm counts at 71dpi (r=0.08; p=0.57; Fig. 7A), but a positive correlation at 119dpi (r= 0.70; p=0.0001; Fig. 7B). Interestingly, AAM numbers correlated negatively with the MF load 71dpi (r= -0.34; p=0.02; Fig. 7C), but disappeared during the late phase (119dpi) of *L. sigmodontis* infection (r= 0.14; p=0.38; Fig. 7D).

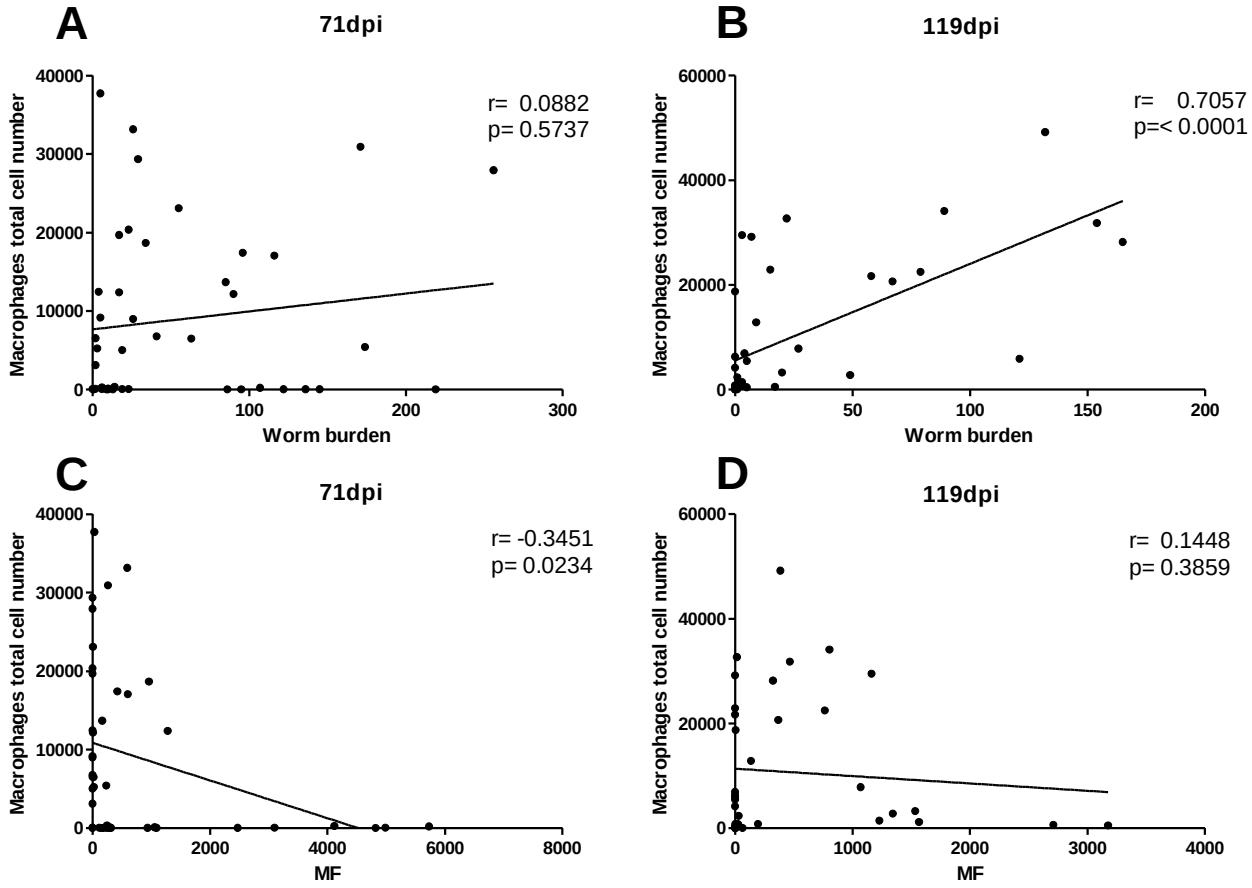

Fig. 7: Contrasting correlation of thoracic cavity alternatively activated macrophage numbers and adult worm burden and MF counts. Correlation of the total thoracic cavity RELMα-positive macrophage numbers and adult worm burden (**A, B**) and peripheral blood MF counts (**C, D**) at 71 (**A, C**) and 119 days (**B, D**) post *L. sigmodontis* infection in IL-4R$^{-/-}$, dblGATA, IL-5$^{-/-}$, IL-4R$^{-/-}$/IL-5$^{-/-}$ mice and wildtype controls. Spearman correlation. Data shown in (**A, C**) are pooled from two independent experiments at 71dpi with 10-16 mice per group. Remaining figures (**B, D**) are from one experiment at 119dpi with 6-10 mice per group.

The aforementioned results support an essential role of thoracic cavity eosinophils for adult worm and MF elimination, whereas AAMs correlated with reduced MF counts.

3.1.3 Positive association of splenic neutrophils with adult worm and MF survival

Splenocytes of all immune-deficient mouse strains and WT controls were assessed and immunological analysis was performed via flow cytometry. Absolute spleen cell counts were increased in the immune-compromised mice compared to WT controls at 71dpi, reaching statistical significance for IL-4R$^{-/-}$/IL-5$^{-/-}$ mice (Fig. 8A). During the late phase of *L. sigmodontis* infection at 119dpi, spleen cell numbers of dblGATA mice were significantly increased compared to WT controls (Fig. 8B). Numbers of neutrophils were significantly increased in spleens of IL-5$^{-/-}$ and IL-4R$^{-/-}$/IL-5$^{-/-}$ mice on 71dpi (Fig. 8C) and in IL-4R$^{-/-}$/IL-5$^{-/-}$ mice at 119dpi compared to WT controls (Fig. 8D). A strong positive correlation was observed for neutrophil counts in the spleen with MF load at 71 ($r= 0.47$; $p=0.001$; Fig. 8E) and 119dpi ($r= 0.40$; $p=0.01$; Fig. 8F) as well as adult worm burden at both time points (71dpi: $r= 0.43$; $p=0.003$; 119dpi: $r= 0.45$; $p=0.002$; Fig. 8G, H).

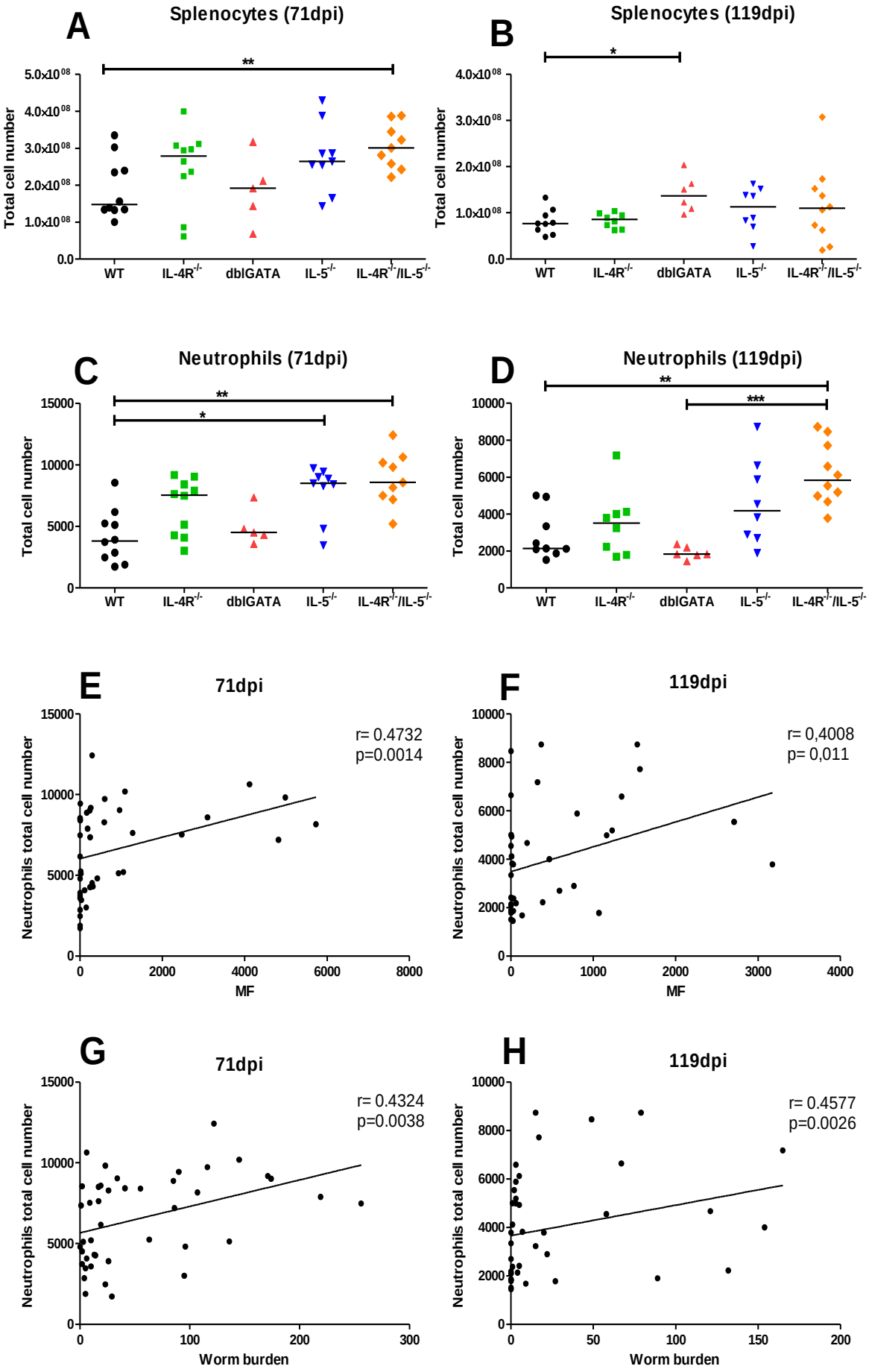
A
Splenocytes (71dpi)
**
Total cell number
5.0x10^08
4.0x10^08
3.0x10^08
2.0x10^08
1.0x10^08
0.0
WT
IL-4R-/-
dblGATA
IL-5-/-
IL-4R-/-/IL-5-/-
B
Splenocytes (119dpi)
*
Total cell number
4.0x10^08
3.0x10^08
2.0x10^08
1.0x10^08
0.0
WT
IL-4R-/-
dblGATA
IL-5-/-
IL-4R-/-/IL-5-/-
C
Neutrophils (71dpi)
**
*
Total cell number
15000
10000
5000
0
WT
IL-4R-/-
dblGATA
IL-5-/-
IL-4R-/-/IL-5-/-
D
Neutrophils (119dpi)
**
***
Total cell number
10000
8000
6000
4000
2000
0
WT
IL-4R-/-
dblGATA
IL-5-/-
IL-4R-/-/IL-5-/-
E
71dpi
r= 0.4732
p=0.0014
Neutrophils total cell number
15000
10000
5000
0
0
2000
4000
6000
8000
MF
F
119dpi
r= 0,4008
p= 0,011
Neutrophils total cell number
10000
8000
6000
4000
2000
0
0
1000
2000
3000
4000
MF
G
71dpi
r= 0.4324
p=0.0038
Neutrophils total cell number
15000
10000
5000
0
0
100
200
300
Worm burden
H
119dpi
r= 0.4577
p=0.0026
Neutrophils total cell number
10000
8000
6000
4000
2000
0
0
50
100
150
200
Worm burden

Fig. 8: Neutrophil numbers in the spleen correlate positively with the adult worm burden and microfilariae load. Total numbers of spleen cells (**A, B**) and neutrophils (**C, D**) in IL-4R$^{-/-}$, dblGATA, IL-5$^{-/-}$, IL-4R$^{-/-}$/IL-5$^{-/-}$ mice and wildtype (WT) controls 71 and 119 days post *L. sigmodontis* infection. Spearman correlation of the total neutrophil spleen cell numbers and peripheral blood microfilariae counts (**E, F**) and adult worm burden (**G, H**) at 71 and 119 days post *L. sigmodontis* infection in IL-4R$^{-/-}$, dblGATA, IL-5$^{-/-}$, IL-4R$^{-/-}$/IL-5$^{-/-}$ mice and wildtype controls. Results are shown as medians (**A, B, C, D**) and Spearman correlation (**E, F, G, H**). Differences were analyzed for statistical significance using the one-way ANOVA followed by the Dunnett's test (**B, C, D**) and Kruskal-Wallis test followed by the Dunn's multiple comparison test (**A**).*p<0.05, **p<0.01, ***p<0.001. Data in (**A, C, E, G**) are pooled from two independent experiments at 71dpi with 10-16 mice per group. Remaining figures (**B, D, F, H**) are from one experiment at 119dpi with 6-10 mice per group.

Total numbers of CD4+ T cells, CD8+ T cells, neutrophils, macrophages and eosinophils were determined within the spleen on 71 and 119dpi (Fig. 9). A significant decrease of absolute CD4+ T cell numbers was observed for IL-4R$^{-/-}$ and IL-5$^{-/-}$ deficient mice at 71dpi (Fig. 9A), whereas CD4+ T cells were lower in dblGATA and IL-5$^{-/-}$ mice compared to WT controls at 119dpi (Fig. 9B). CD8+ T cell numbers were significantly decreased in IL-4R$^{-/-}$, IL-5$^{-/-}$ and IL-4R$^{-/-}$/IL-5$^{-/-}$ on 71dpi (Fig. 9C) and continued to decrease at 119dpi for IL-4R$^{-/-}$ and IL-4R$^{-/-}$/IL-5$^{-/-}$ deficient mice compared to WT controls (Fig. 9D). Absolute macrophage cell counts at 71dpi were significantly increased in IL-4R$^{-/-}$/IL-5$^{-/-}$ compared to corresponding WT mice (Fig. 9E). At 119dpi no differences in macrophage numbers were present in all tested mouse strains (Fig. 9F). A statistically significant increase of eosinophils (Fig. 9G) was observed at 71dpi in IL-4R$^{-/-}$ mice compared to WT controls. Absolute eosinophil counts were significantly decreased in dblGATA and IL-5$^{-/-}$ animals compared to WT mice (Fig. 9H).

Eosinophil numbers within the spleen did not correlate with the MF load at 71 (r= 0.12; p=0.42; Fig. 9I) and 119dpi (r= -0.26; p=0.10; Fig. 9J), but correlated negatively with the adult worm counts at 119dpi (r= -0.49; p=0.001; 71 dpi: r= -0.23; p=0.12; Fig. 9K, L).

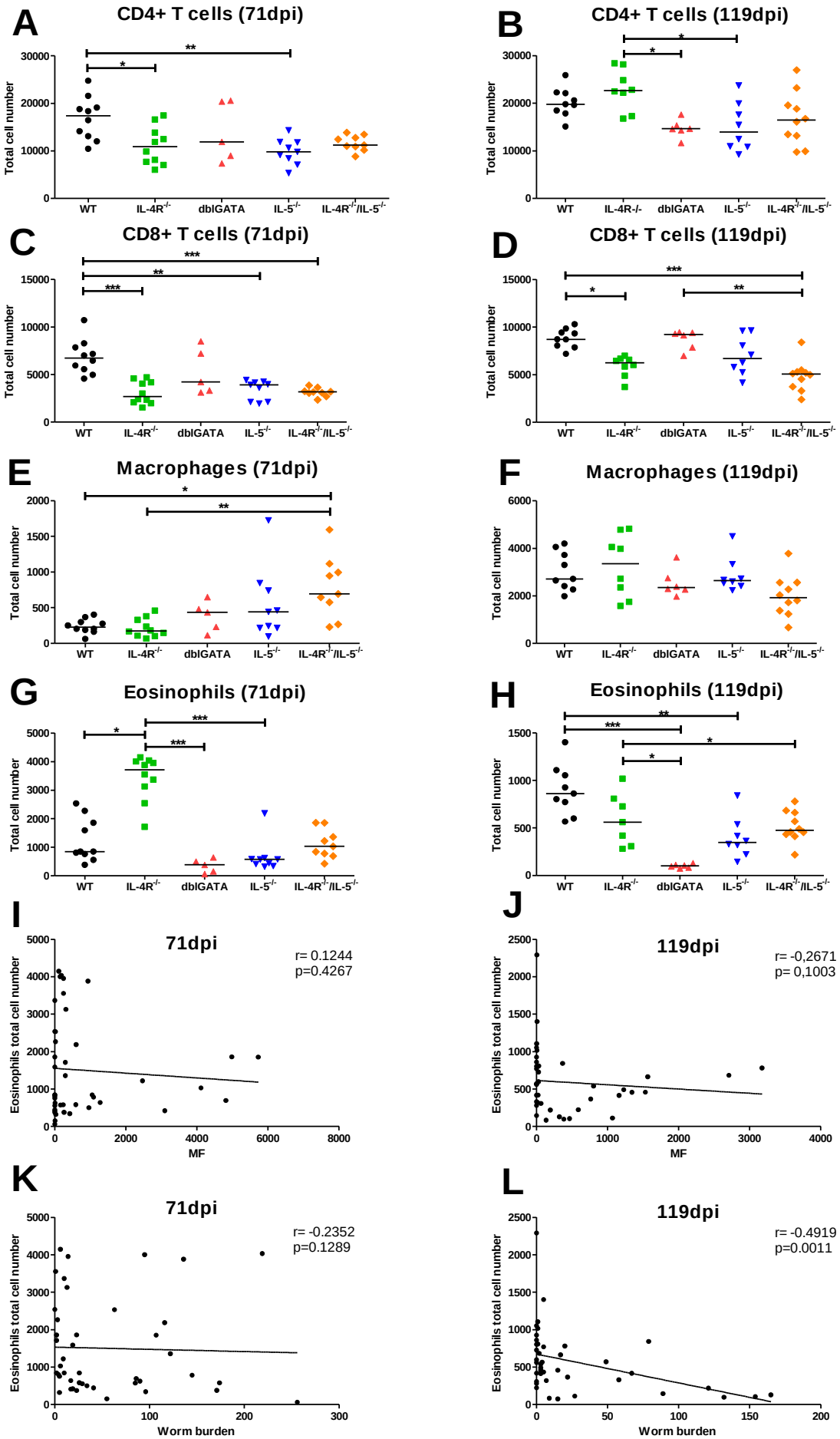
A
CD4+ T cells (71dpi)
Total cell number
WT
IL-4R-/-
dblGATA
IL-5-/-
IL-4R-/-/IL-5-/-
B
CD4+ T cells (119dpi)
C
CD8+ T cells (71dpi)
D
CD8+ T cells (119dpi)
E
Macrophages (71dpi)
F
Macrophages (119dpi)
G
Eosinophils (71dpi)
H
Eosinophils (119dpi)
I
71dpi
r= 0.1244
p=0.4267
Eosinophils total cell number
MF
J
119dpi
r= -0,2671
p= 0,1003
K
71dpi
r= -0.2352
p=0.1289
Worm burden
L
119dpi
r= -0.4919
p=0.0011

Fig. 9: Impact of the lack of IL-5, dblGATA, IL-4R and IL-4R/IL-5 on CD4+ T cell, CD8+ T cell, macrophage and eosinophil numbers in the spleen of *L. sigmodontis*-infected mice. Total spleen cell CD4+ T cell (**A, B**), CD8+ T cell (**C, D**), macrophage (**E, F**) and eosinophil numbers (**G, H**) at 71 and 119 days post *L. sigmodontis* infection in IL-4R$^{-/-}$, dblGATA, IL-5$^{-/-}$, IL-4R$^{-/-}$/IL-5$^{-/-}$ mice and wildtype (WT) controls. Spearman correlation of the total eosinophil spleen cell numbers and peripheral blood microfilariae counts (**I, J**) and adult worm burden (**K, L**) at 71 and 119 days post *L. sigmodontis* infection. Results are shown as medians (**A**-**H**) and Spearman correlation (**I**-**L**). Differences were analyzed for statistical significance using the one-way ANOVA followed by the Dunnett's test (**A, D**) and Kruskal-Wallis test followed by the Dunn's multiple comparison test (**B, C, E, F, G, H**).*p<0.05, **p<0.01, ***p<0.001. Data in (**C, E, G, I, K**) are pooled from two independent experiments at 71dpi with 10-16 mice per group; data shown in (**A**) is a representative of two independent experiments with 5-10 mice per group, as it did not pass the test for homodesticity. Remaining figures (**B, D, F, H, J, L**) are from one experiment at 119dpi with 6-10 mice per group.

3.1.4 Thoracic cavity IL-6 cytokine concentration correlates negatively with MF loads

Immunological changes within the thoracic cavity cytokine milieu were analysed and quantified by lavage, namely the Th1 cytokines IFN-γ and IL-6, as well as the type 2 cytokines IL-4, IL-5 and IL-13 (Fig. 10) in order to investigate potential correlations between those cytokines and microfilaremia as well as adult worm burden. At 71dpi, IFN-γ levels were elevated in all tested immune-deficient mouse strains compared to WT controls (Fig. 10A) and remained high in IL-4R$^{-/-}$/IL-5$^{-/-}$ mice at 119dpi (Fig. 10B). Interestingly, IL-6 cytokine levels (Fig. 10C, D) showed a strong negative correlation with the MF load (71dpi: r= -0.43, p=0.004; 119dpi: r=0.30 p=0.06). No correlations were observed between IL-6 levels and adult worm burden at the onset of microfilaremia and the late phase of *L. sigmodontis* infection (71dpi: r= -0.02, p=0.90; 119dpi: r= 0.16, p=0.30). IFN-γ, IL-4, IL-5, and IL-13 cytokine levels did neither correlate with adult worm burden nor MF load and correlations are summarized in table 1. These results indicate that thoracic cavity cytokine levels did not

correlate with the adult worm burden and solely IL-6 correlated negatively with the MF counts at 71dpi (Table 1).

Table 1: Negative correlation of IL-6 thoracic cavity concentrations with the MF load. Spearman correlation of IL-4, IL-5, IL-6, IL-13, and IFN-γ cytokine levels within the thoracic cavity lavage at 71 and 119 days post *L. sigmodontis* infection with total worm numbers and MF load.

Cytokine	**Microfilariae 71dpi**		**Microfilariae 119dpi**	
IL-4	r=0.34	p=0.04	r=-0.04	p=0.79
IL-5	r=0.10	p=0.62	r=-0.33	p=0.13
IL-6	r=-0.43	p=0.001	r=0.30	p=0.06
IL-13	r=0.18	p=0.26	r=0.36	p=0.02
IFN-y	r=0.03	p=0.84	r=0.16	p=0.34
Cytokine	**Worm burden 71dpi**		**Worm burden 119dpi**	
IL-4	r=0.01	p=0.95	r=0.06	p=0.73
IL-5	r=0.19	p=0.35	r=-0.34	p=0.11
IL-6	r=-0.02	p=0.90	r=0.16	p=0.30
IL-13	r=0.01	p=0.93	r=0.19	p=0.23
IFN-y	r=0.07	p=0.65	r=-0.04	p=0.81

High IL-13 concentrations in the thoracic cavity lavage were observed in the absence of AAMs in IL-4R$^{-/-}$ as well as IL-4R$^{-/-}$/IL-5$^{-/-}$ mice at 71dpi (Fig. 10I, J), reaching statistically significant difference in IL-4R$^{-/-}$/IL-5$^{-/-}$ mice compared to WT controls at 119dpi (Fig. 10J). However, lack of eosinophils in IL-5$^{-/-}$, IL-4R$^{-/-}$/IL-5$^{-/-}$ and dblGATA mice did not alter IL-4, IL-5, IL-6, or IL-13 cytokine levels (Fig. 10C-J).

Collectively, these data demonstrate that IL-4R$^{-/-}$/IL-5$^{-/-}$ mice exhibited the highest susceptibility for *L. sigmodontis* infection due the combined lack of AAMs and eosinophils, which resulted in an earlier onset of microfilaremia, development of microfilaremia in all animals with highest MF loads, and an extended adult worm survival.

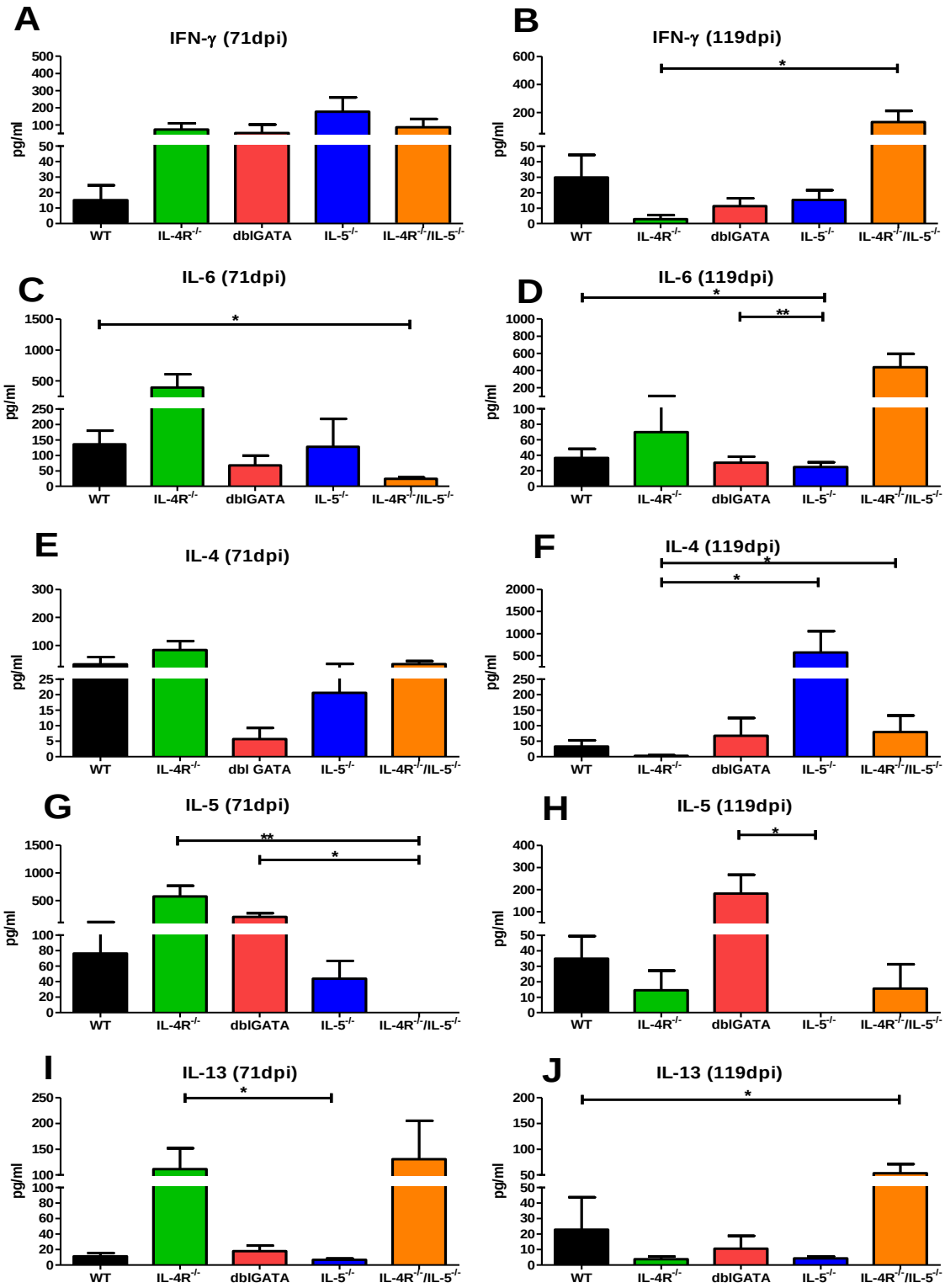

Fig. 10: Impact of the lack of IL-5, dblGATA, IL-4R and IL-4R/IL-5 on the thoracic cavity cytokine milieu in *L. sigmodontis*-infected mice. Cytokine concentrations of IFN-γ (**A, B**), IL-4 (**C, D**), IL-5 (**E, F**), and IL-13 (**G, H**) in the thoracic cavity lavage 71 and 119 days post *L. sigmodontis* infection of wild type (WT), IL-4R$^{-/-}$, dblGATA, IL-5$^{-/-}$ and IL-4R/IL-5$^{-/-}$ mice. Results are shown as median. Differences were analyzed for statistical significance using the Kruskal-Wallis test followed by the Dunn's multiple comparison test. *$p<0.05$, **$p<0.01$. Data shown in (**A, C, E, G**) are pooled from two independent experiments at 71dpi with 10-16 mice per group. Remaining figures (**B, D, F, H**) are from one experiment at 119dpi with 6-10 mice per group.

3.2 Impact of S100A8/A9 on *L. sigmodontis* infection

3.2.1 Migrating L3 larvae mediate pulmonary inflammation

A recent study has shown that the migratory phase of infective L3 *L. sigmodontis* larvae was associated with elevated expression of the alarmins S100A8/S100A9 (Calprotectin) in neutrophils within the bronchoalveolar lavage. Therefore, the direct impact of Calprotectin during *L. sigmodontis* infection in C57BL/6 mice lacking S100A8/A9 compared to C57/BL6 WT controls was investigated.

During the blood meal of the natural arthropod vector *O. bacoti*, infectious L3 *L. sigmodontis* larvae are transmitted into the skin of the rodent host and migrate via the blood and lymphatic system, reaching the pulmonary capillaries and finally the thoracic cavity, where the filarial worms reside. As they are known to induce transient pulmonary inflammation during the migratory phase, the lung pathology between uninfected (Fig. 11A) and *L. sigmodontis*-infected animals was compared (Fig. 11B). Histology was performed by our cooperation partner (Dr. Frédéric Fercoq) in Paris. Lungs of *L. sigmodontis*-infected mice elicited a considerable increase of inflamed blood vessels and goblet cells, which were further characterized by a higher mucus production (Fig. 11C). The number of congested blood vessels (Fig. 11D) and goblet cells was associated with the number of worms reaching the site of infection (Fig. 11E) compared to lungs of uninfected animals. Furthermore, the perivascular space (PVS) revealed an elevated number of infiltrating immune cells such as neutrophils (Fig. 11F, G) and eosinophils (Fig. 11H, I).

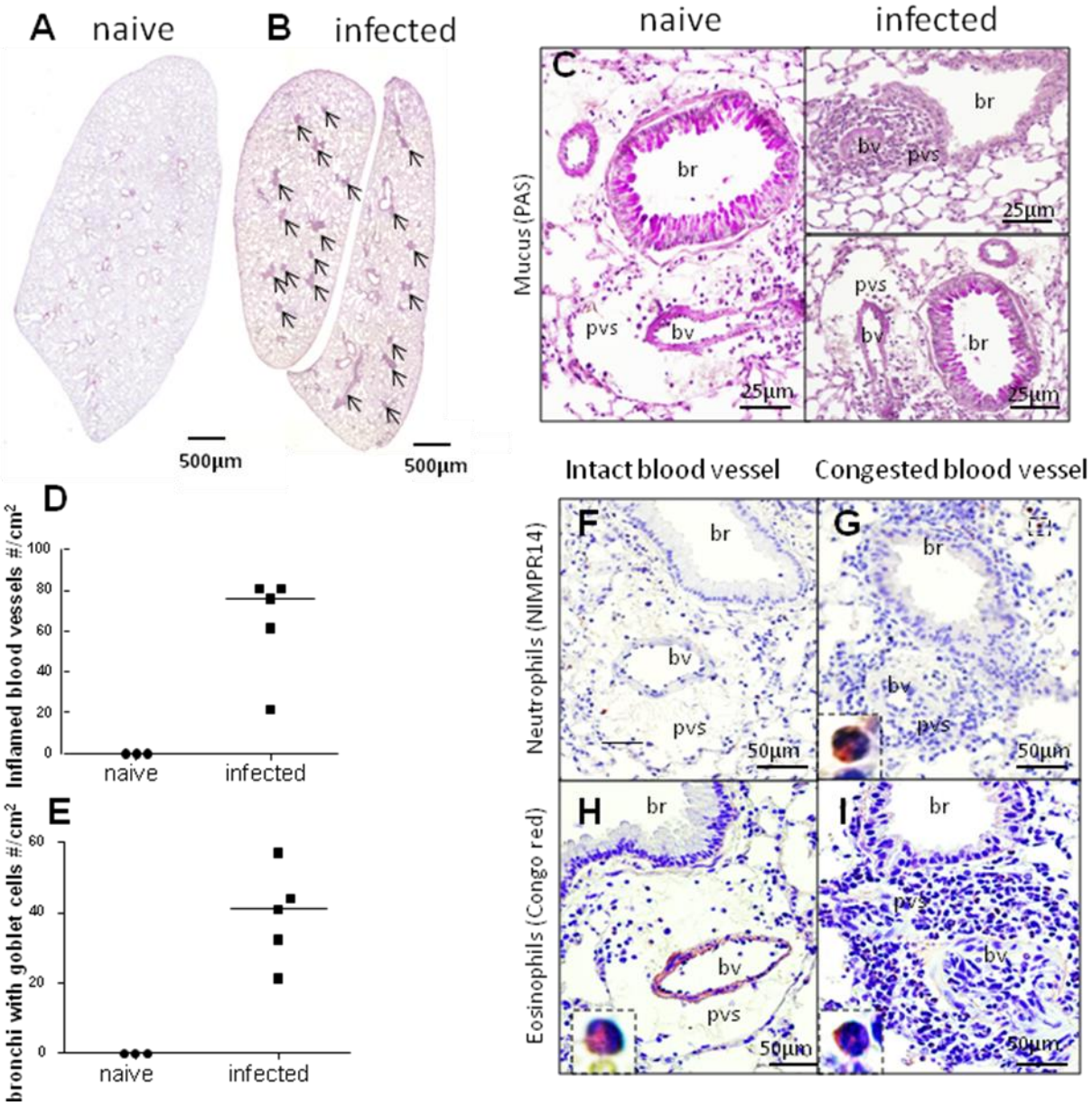

Fig. 11: Migrating L3 larvae cause transient pulmonary inflammation. C57BL/6 WT and S100A8/A9$^{-/-}$ mice were naturally infected with *L. sigmodontis*. Representative pictures of a lung from an uninfected WT mouse (**A**) and a lung 12 days post natural *L. sigmodontis* infection of a WT mouse (**B**) are shown. Number of inflamed blood vessels (**C**, **D**) and inflamed goblet cells (**C**, **E**) from naïve and 12-day *L. sigmodontis* infected mice. Influx of neutrophils (**F**, **G**) and eosinophils (**H**, **I**) in the perivascular space (PVS) of an intact and congested blood vessel. The figures are representative from two experiments with at least 1-3 mice per group.

First, the abundance of the damage-associated protein S100A9 was confirmed by histology in WT animal lung parenchyma and its absence in S100A8/A9$^{-/-}$ mice lungs (Fig. 12)

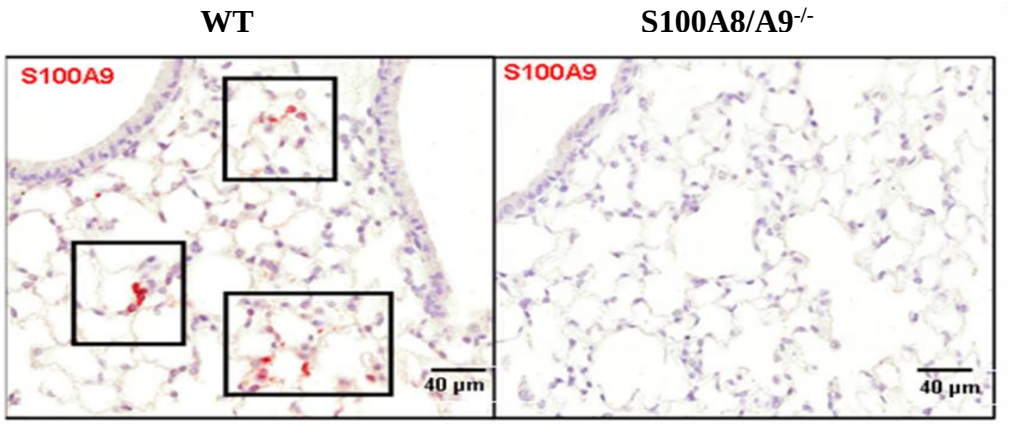

Fig. 12: S100A9 expression in the lung parenchyma. Representative figure of S100A9 expression in uninfected WT (**A**) and S100A8/A9$^{-/-}$ mice (**B**) lung parenchyma.

3.2.2 S100A8/A9$^{-/-}$ mice show decreased worm burden and increased inflammation

To investigate the role of S100A8/A9 during filarial infection, WT and S100A8/A9$^{-/-}$ mice were infected nat. with *L. sigmodontis* via the bite of the tropical rat mite. Necropsy at 12dpi included enumeration of the worm burden and analysis of the lung pathology by histology, the cellular composition, the cytokine profile and enzymes. S100A8/A9$^{-/-}$ mice revealed a significantly reduced worm burden compared to WT controls (Fig. 13A). Interestingly, S100A8/A9$^{-/-}$ mice suffered less lung pathology, probably due to the decreased worm burden, which was further characterized by a reduction of inflamed blood vessels per cm^2 in comparison to corresponding WT animals (Fig. 13B). S100A8/A9$^{-/-}$ exhibited an increased number of total thoracic cavity cells compared to WT controls (Fig. 13C). Flow cytometry analysis of the thoracic cavity revealed that frequencies of CD4+ T cells, CD8+ T cells, neutrophils, macrophages and eosinophils were comparable between the two tested groups (Fig. 13D). However, an increase of neutrophil-associated chemokines CXCL-1 (Fig. 13E),

CXCL-2 (Fig. 13F), CXCL-5 (Fig. 13G), and elastase (Fig. 13H) was observed in the thoracic cavity lavage of S100A8/A9$^{-/-}$ mice compared to WT controls.

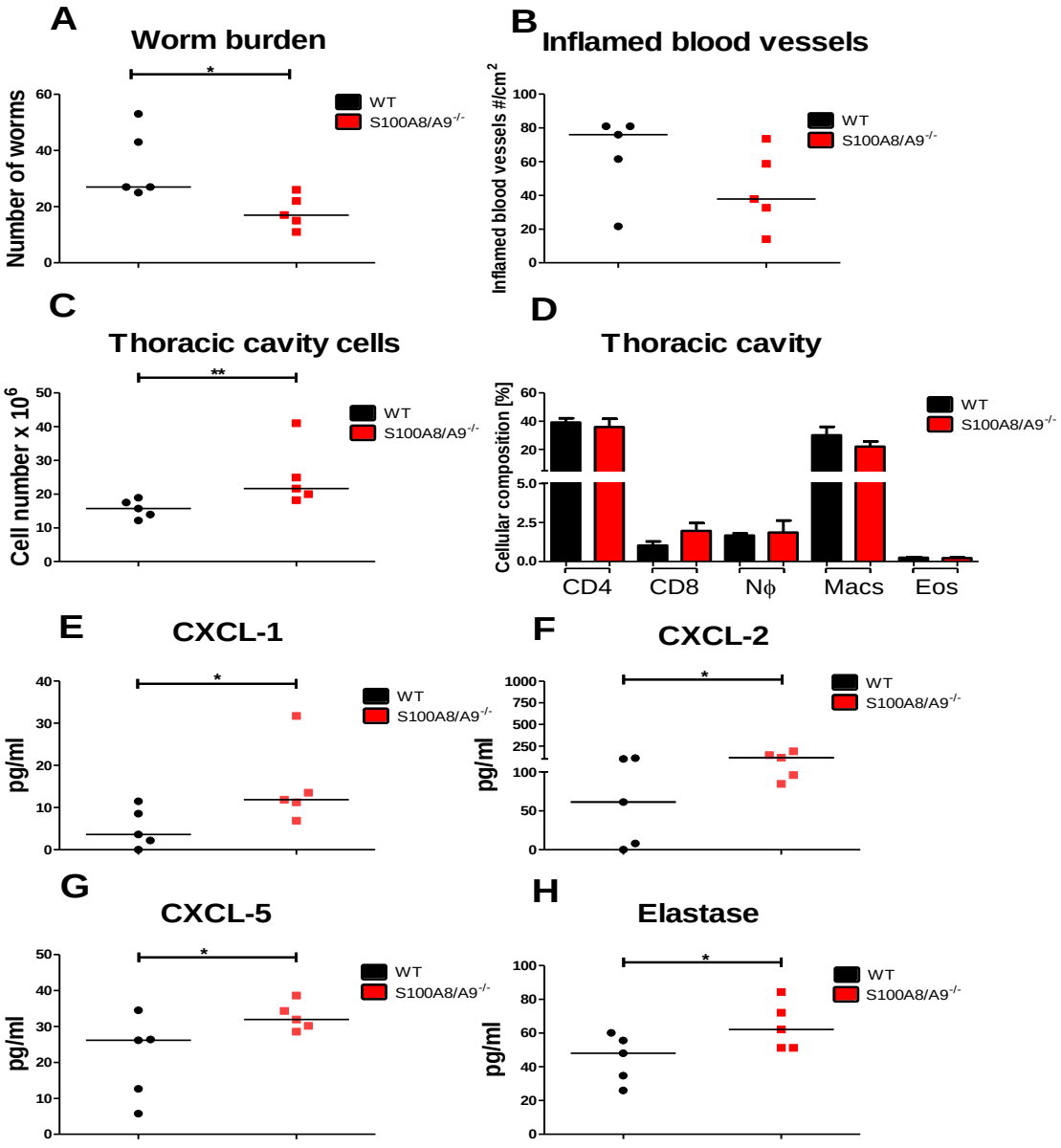

Fig. 13: Reduced worm burden and lung pathology, but increased neutrophil mediator release following L3 migration in S100A8/A9$^{-/-}$ mice. Worm burden following natural *L. sigmodontis* infection in WT and S100A8/A9$^{-/-}$ mice at 12 days post infection (**A**). Total number of inflamed blood vessels (**B**), number of thoracic cavity cells (**C**) and cellular composition of the thoracic cavity lavage 12 days post *L. sigmodontis* infection in WT and S100A8/A9$^{-/-}$ mice (**D**). Concentrations of CXCL-1 (**E**), CXCL-2 (**F**), CXCL-5 (**G**), and elastase (**H**) in the thoracic cavity lavage 12 days post *L. sigmodontis* infection in WT and S100A8/A9$^{-/-}$ mice. Results are shown as median (**A-C**, **E-H**) or mean with SEM (**D**). Differences were analyzed for statistical significance using the Mann-Whitney U-test *p<0.05, **p<0.01. Data shown are from one experiment with 5 mice per group.

3.2.3 Subcutaneous infection with L3 larvae results in a reduced worm burden in S100A8/A9$^{-/-}$ mice

In order to elucidate whether the observed protective effect in S100A8/A9$^{-/-}$ mice occurs within the skin as the first barrier, WT and S100A8/A9$^{-/-}$ animals were s.c. inoculated with infective L3 larvae. S.c. infection of *L. sigmodontis* L3 larvae resulted in a similar outcome as during nat. infection, revealing again a reduced worm burden in S100A8/A9$^{-/-}$ mice (Fig. 14A). To confirm that the S100A8/A9 dependent mechanism did not occur within the skin, immune responses within the skin were assessed 3h after both mouse strains were injected i.d. with 10 L3 larvae. I.d. injections of *L. sigmodontis* L3 larvae in WT and S100A8/A9$^{-/-}$ mice led to an increased influx of cells to the site of infection compared to PBS-treated corresponding controls. Interestingly, S100A8/A9$^{-/-}$ mice exhibited more cells after PBS and L3 injection compared to WT animals (Fig. 14B). Frequencies of eosinophils (Fig. 14C) were increased after L3 injection in S100A9$^{-/-}$ mice as well as the frequency of neutrophils (Fig. 14D) in both mice strains. However, no statistical significant differences between WT and S100A8/A9$^{-/-}$ animals were observed following L3 injection with regard to the frequency of eosinophils (Fig. 14C), neutrophils (Fig. 14D) and macrophages (Fig. 14E). To assess differences in the cell activation, MHCII expression was determined in the measured cell frequencies. MHCII expression was increased in eosinophils (Fig. 14F), macrophages (Fig. 14G) in the skin of L3 larvae injected S100A8/A9$^{-/-}$ animals compared to cells of PBS treated S100A8/A9$^{-/-}$ animals. With regard to the cell activation of neutrophils, MHCII expression did not differ between PBS and L3 larvae treated WT and S100A8/A9$^{-/-}$ mice (Fig. 14H).

Collectively, these data revealed that S100A8/A9 does not markedly impacts or increases protective immune responses within the skin.

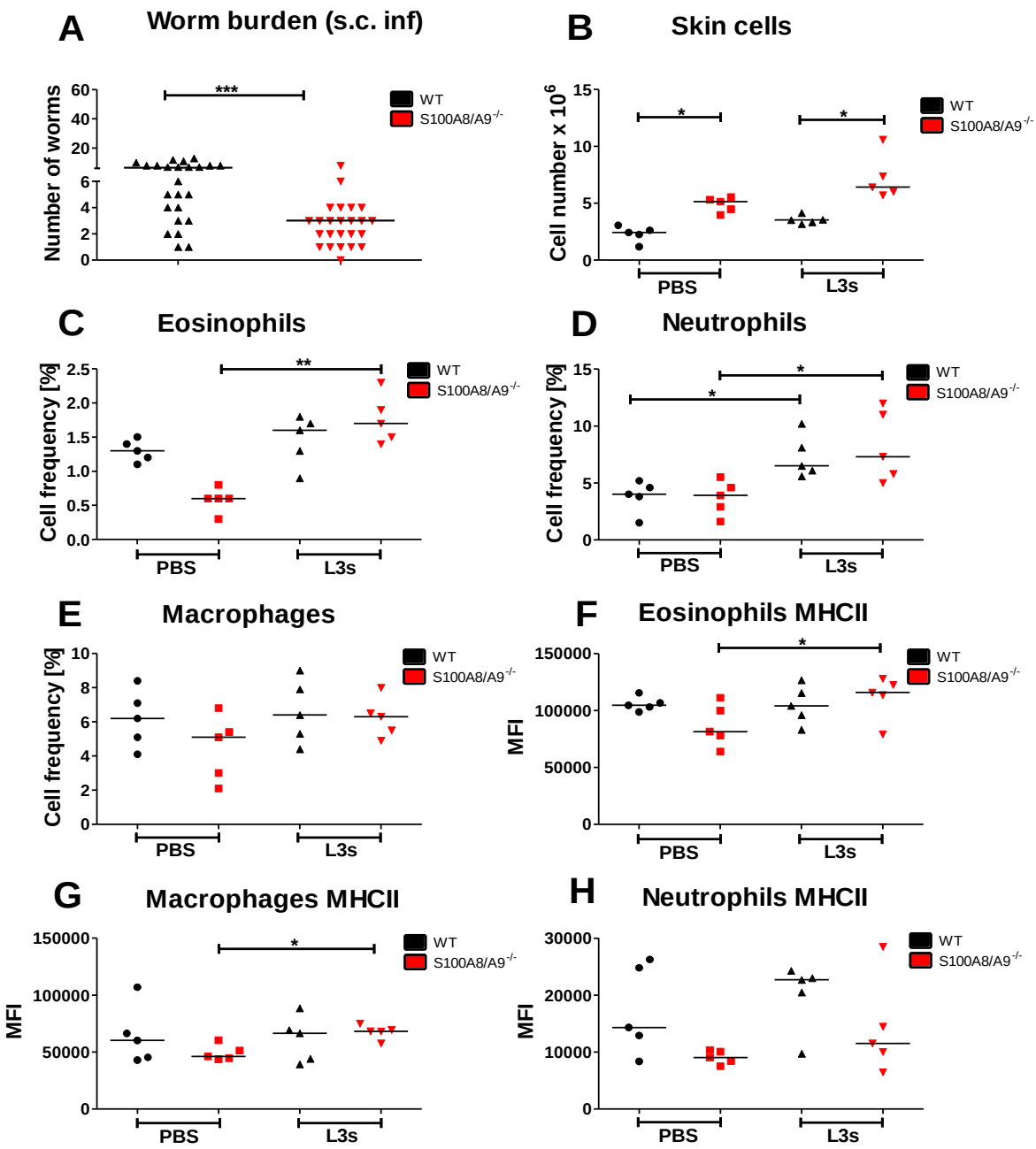

Fig. 14: Subcutaneous inoculation of infective *L. sigmodontis* L3 larvae leads to a reduced worm burden in S100A8/A9$^{-/-}$ mice. Worm burden after subcutaneous *L. sigmodontis* infection in WT and S100A8/A9$^{-/-}$ mice 12 days post infection (**A**). Total number of skin cells (**B**), frequency of eosinophils (**C**), neutrophils (**D**) and macrophages (**E**) and their respective MHCII expression (**F-H**) in WT and S100A8/A9$^{-/-}$ mice 3h post intradermal *L. sigmodontis* injection. Results are shown as median. Differences were analyzed for statistical significance using the Mann-Whitney U-test (**A**). Statistical significance of not normally distributed data (**B-H**) was analyzed by Kruskal-Wallis followed by Dunn's multiple comparison test *p<0.05, **p<0.01, ***p<0.001. Data shown are pooled from two experiments with 8 mice per group (**A**) and remaining figures from one experiment with 5 mice per group (**B**, **C**, **D**, **E**, **F**, **G**, **H**).

To determine a potential role of S100A8/9 within the spleen during *L. sigmodontis* infection and parasite clearance, flow cytometry and splenocyte culture was performed. Absolute spleen cell numbers were significantly increased in S100A8/A9$^{-/-}$ animals compared to WT mice during nat. infection (data not shown) and s.c. infection (Fig. 15A). No differences were observed in the frequencies of CD4+ T cells, CD8+ T cells, macrophages and eosinophils between the S100A8/A9$^{-/-}$ mice and WT controls. However, the frequency of neutrophils was elevated in S100A8/A9$^{-/-}$ animals compared to corresponding WT mice (Fig. 15B). Upon LsAg stimulation for 72h cultured splenocytes of S100A8/9$^{-/-}$ mice produced higher amounts of IFN-γ (Fig. 15C) and TNF (Fig. 15D) compared to WT cultured splenocytes.

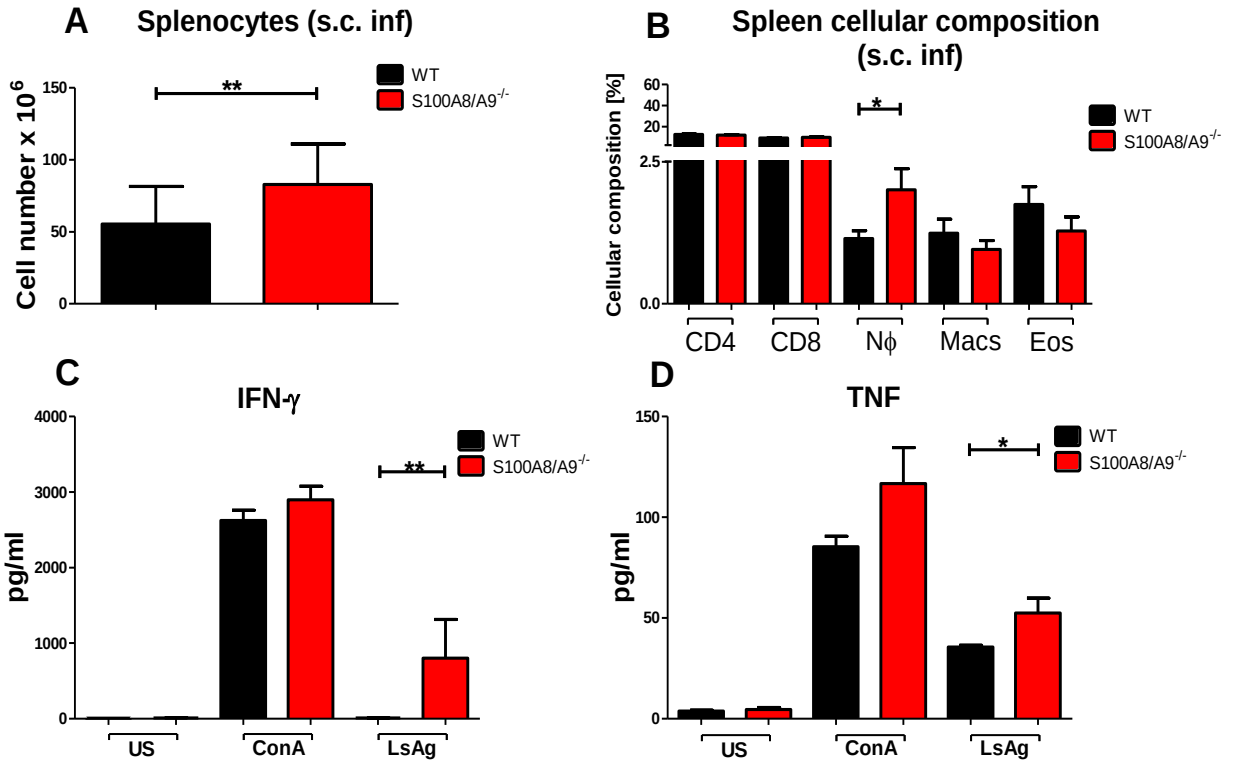

Fig. 15: Total number of spleen cells in WT and S100A8/A9$^{-/-}$ mice at 12 days post subcutaneous *L. sigmodontis* infection. Total number of spleen cells in WT and S100A8/A9$^{-/-}$ mice (**A**). Cellular composition in spleen (**B**). Cytokine concentrations of IFN-γ (**C**) and TNF (**D**) in 72h spleen culture supernatant upon ConA (2.5µg/ml) and LsAg stimulation (25µg/ml). Results are shown as median. Differences were analyzed for statistical significance using the Mann-Whitney U-test *p<0.05, **p<0.01. Data shown are pooled from two independent experiments with 8 mice per group (**A**, **B**) and 4 mice per group (**C**, **D**).

Furthermore, s.c. infection of *L. sigmodontis* L3 larvae revealed an increased thoracic cavity cell count (Fig. 16A) and no major differences in major cell frequencies (Fig. 16B) within the thoracic cavity as observed earlier during nat. *L. sigmodontis* infection. Total bronchoalveolar cell numbers were comparable between WT and S100A8/A9$^{-/-}$ mice (Fig. 16C). However, all analysed cell frequencies within the bronchoalveolar lavage were increased in S100A8/A9$^{-/-}$ mice (Fig. 16D).

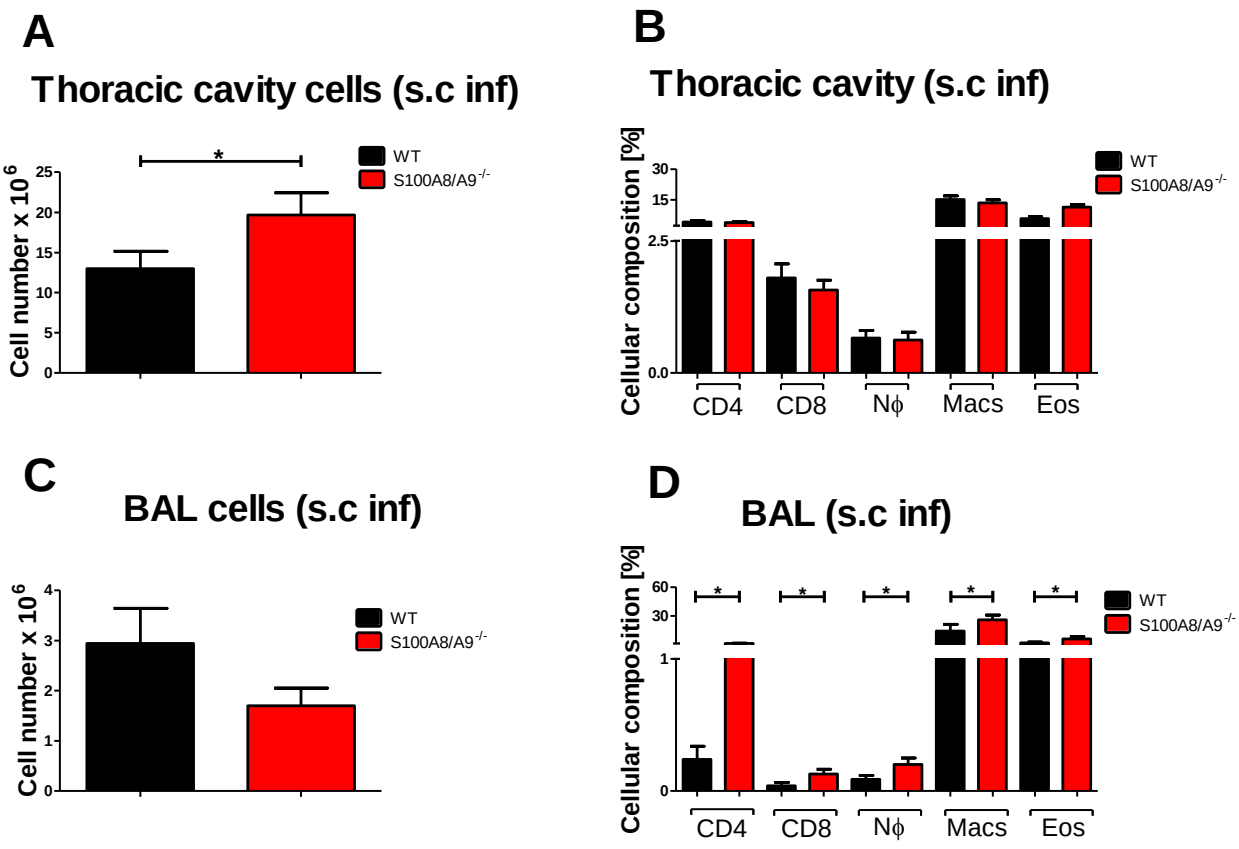

Fig. 16: Subcutaneous inoculation of infective *L. sigmodontis* L3 larvae does not impair immune responses at the site of infection. Thoracic cavity cells after subcutaneous *L. sigmodontis* infection in WT and S100A8/A9$^{-/-}$ mice 12 days post infection (**A**). Thoracic cavity cellular composition (**B**). Total bronchoalveolar cell count (**C**) and cellular composition (**D**). Results are shown as median. Differences were analyzed for statistical significance using the Mann-Whitney U-test *p<0.05. Data shown are pooled from two independent experiments with 4-8 mice per group.

3.2.4 Absence of S100A8/A9 within the lung increases pulmonary inflammation during migration of infective *L. sigmodontis* L3 larvae

To elucidate how S100A8/A9 deficiency impacts immune responses during the migration of *L. sigmodontis* L3 larvae within the lung, we first determined absolute bronchoalveolar cell numbers in *L. sigmodontis*-infected WT and S100A8/A9$^{-/-}$ mice following nat. infection. Total bronchoalveolar cell numbers were significantly decreased in S100A8/A9$^{-/-}$ mice (Fig. 17A). However, an increase of CD4+ T cell, CD8+ T cell, neutrophil, macrophage, and eosinophil frequencies in S100A8/A9$^{-/-}$ mice were observed compared to corresponding WT mice (Fig. 17B). Bronchoalveolar cell numbers and worm numbers positively correlated at 12dpi in WT and S100A8/A9$^{-/-}$ animals during nat. or s.c. *L. sigmodontis* infection (Fig. 17C). Additionally, a strong positive correlation was observed between congested blood vessel counts and worm burden (Fig. 17D). Levels of CXCL-1 (Fig. 17E), CXCL-2 (Fig. 17F), CXCL-5 (Fig. 17G), and elastase (Fig. 17H) were significantly increased in BAL of S100A8/A9$^{-/-}$ animals compared to corresponding WT controls. These results indicate that the lung may be involved in the protective immune responses against migrating *L. sigmodontis* L3 larvae.

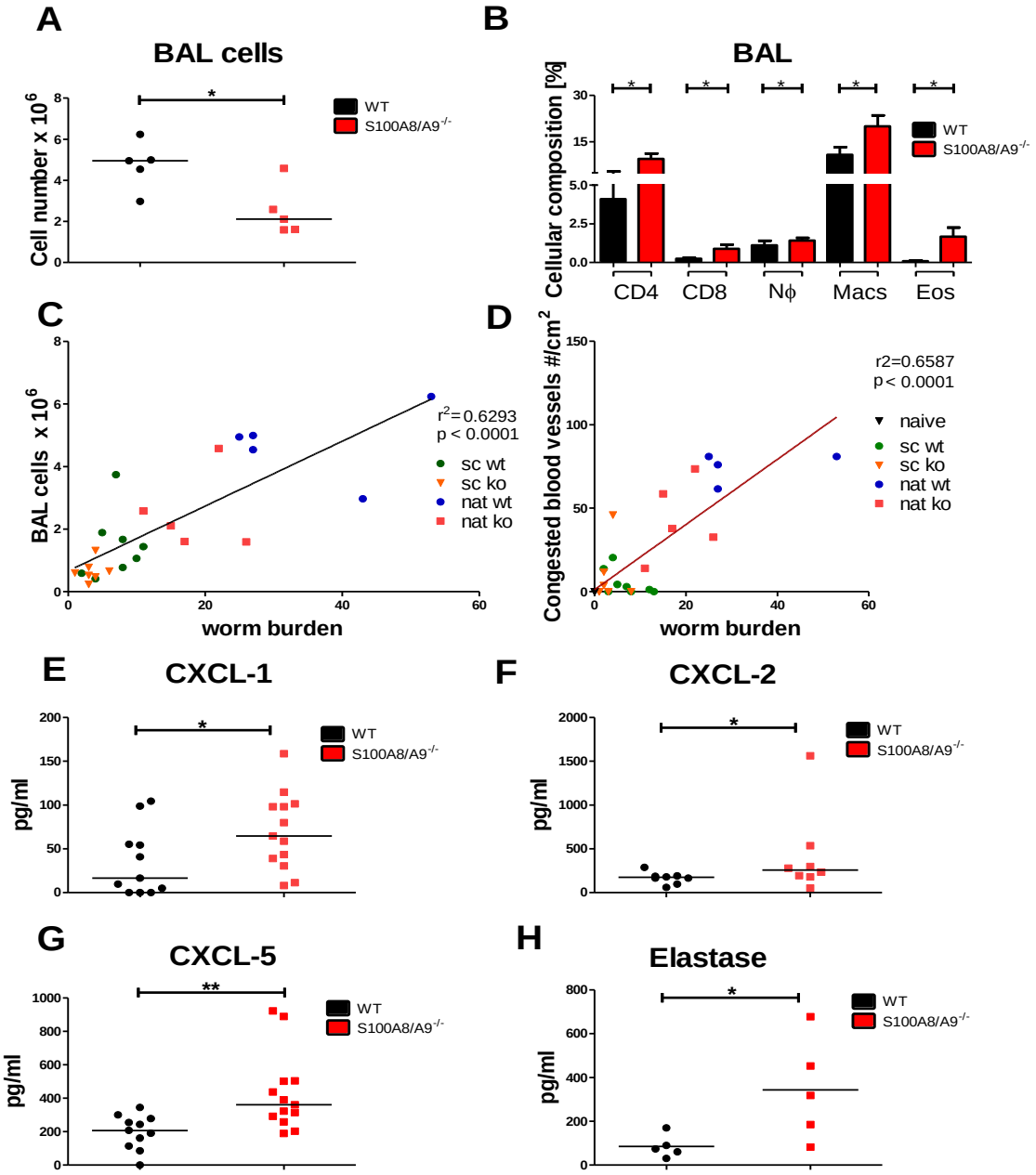

Fig. 17: Immune responses to migrating *L. sigmodontis* L3 larvae within the BAL are increased in S100A8/A9$^{-/-}$ mice. Total numbers of bronchoalveolar cells (**A**) and cellular composition including CD4+ T cells, CD8+ T cells, neutrophils, macrophages, and eosinophils (**B**) in WT and S100A8/A9$^{-/-}$ mice 12 days post *L. sigmodontis* infection. Spearman correlation of total bronchoalveolar cells and worm counts (**C**) as well as congested blood vessels and worm counts (**D**) obtained 12 days post *L. sigmodontis* infection. Concentrations of CXCL-1 (**E**), CXCL-2 (**F**), CXCL-5 (**G**), and elastase (**H**) in the bronchoalveolar lavage 12 days post *L. sigmodontis* infection of WT and S100A8/A9$^{-/-}$ mice. Results are shown as median (**A**, **C**-**H**) or mean with SEM (**B**). Differences were analyzed for statistical significance using the Mann-Whitney U-test *p<0.05, **p<0.01. Data shown in figure (**A**) and (**B**) are pooled from two experiments with 2-3 mice per group. Remaining figures consist of two or three independent experiments with 3-8 mice per group.

As the frequency of neutrophils and production of neutrophil-associated chemokines in the BAL and thoracic cavity were increased in S100A8/A9$^{-/-}$ animals, the neutrophil activation of S100A8/A9$^{-/-}$ and WT mice was assessed. Neutrophils isolated 12dpi from the BAL of S100A8/A9$^{-/-}$ mice did not show any differences in the expression of CD40 (Fig. 18A). However, bone-marrow-derived neutrophils of S100A8/A9$^{-/-}$ animals showed a statistical significant increased expression of CD40 upon LPS and LsAg stimulation (Fig. 18B). CD86 showed a statistical significant increase (Fig. 18C) following *in vitro* stimulation with LPS and even under unstimulated conditions compared to WT mice. The increased activation of S100A8/A9$^{-/-}$ neutrophils was associated with an increased apoptosis, revealing an elevated frequency of dying and dead neutrophils lacking S100A8/A9 (Fig. 18D). Additionally, an elevated level of myeloperoxidase (MPO), an enzyme which is abundantly expressed in neutrophils and elicits protective properties in the elimination of bacteria and other pathogens, was observed from neutrophils of S100A8/A9$^{-/-}$ animals compared to WT neutrophils following LPS and LsAg stimulation as well as under unstimulated conditions (Fig. 18E). In order to investigate whether these changes in neutrophil activation may affect NET formation and L3 larvae motility, which represent an essential tool in the capture and elimination of invading pathogens, L3 larvae were cultured in the presence of neutrophils from WT and S100A8/A9$^{-/-}$ mice. Interestingly, S100A8/A9$^{-/-}$ neutrophils revealed an earlier inhibition of L3 larvae motility in comparison to L3 larvae cultured with neutrophils of WT mice. In order to investigate DNA dependency of the inhibitory effect of S100A8/A9$^{-/-}$ neutrophils, DNAse was added. The addition of DNAse improved L3 motility in the presence of S100A8/A9$^{-/-}$ neutrophils (Fig. 18F). Similar to above mentioned results on neutrophil activation, S100A8/A9$^{-/-}$ neutrophils cultured with L3 larvae had an increased MHCII expression compared to neutrophils of WT animals (Fig. 18G). Collectively, these data indicate that

neutrophils from S100A8/A9$^{-/-}$ animals exhibit an increased activation and inhibit L3 larvae motility more effectively.

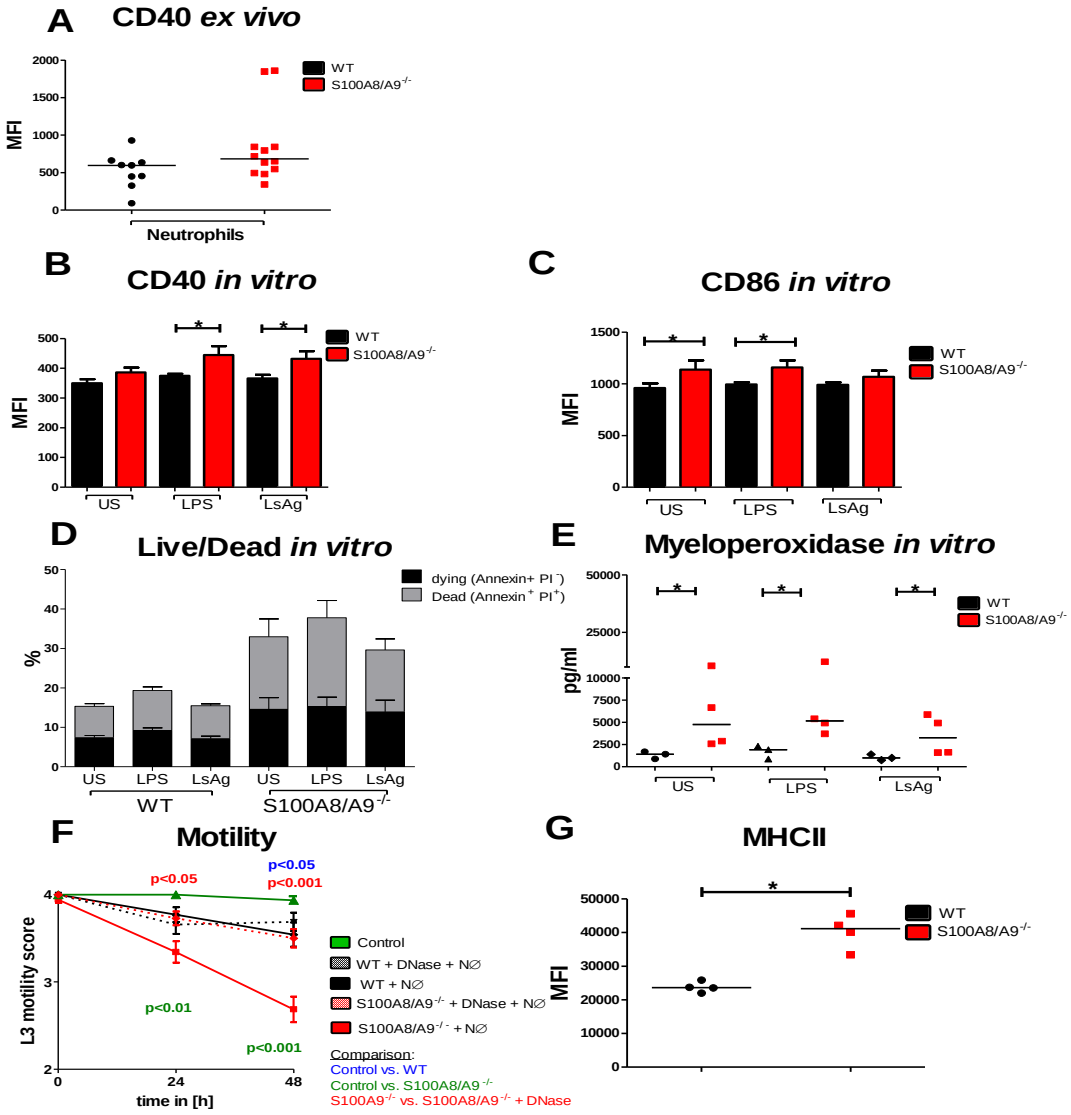

Fig. 18: Increased activation and apoptosis of S100A8/A9$^{-/-}$ neutrophils. *Ex vivo* CD40 expression of neutrophils 12 days post *L. sigmodontis* infection of WT and S100A8/A9$^{-/-}$ mice (**A**). CD40 (**B**) and CD86 (**C**) expression as well as apoptosis (**D**) of bone marrow-derived neutrophils from WT and S100A8/A9$^{-/-}$ mice after 7h of *in vitro* culture without stimulation (US) or with LPS or LsAg stimulation. Myeloperoxidase concentration of WT and S100A8/A9$^{-/-}$ neutrophils upon 7h LPS and LsAg *in vitro* stimulation (**E**). Motility score of L3 larvae cultured in the presence of WT or S100A8/A9$^{-/-}$ neutrophils +/- DNAse (**F**) and MHCII expression (**G**) from WT and S100A8/A9$^{-/-}$. Results are shown as median (**A**, **F**, **G**), mean with SEM (**B**-**D**). Differences were analyzed for statistical significance using the Mann-Whitney U-test *p<0.05, **p<0.01, ***p<0.001. Data shown in (**A**, **B**, **C**) are pooled from 2-3 independent experiments with at least 2-3 mice per group. Remaining figures consist of one experiment with 3-4 mice per group.

3.2.5 Depletion of neutrophils of the lung abrogates the S100A8/A9-mediated protective effect

As S100A8/A9$^{-/-}$ neutrophils exhibited an increased activation and inhibition of L3 motility *in vitro*, depletion of neutrophils within the lung was performed by intranasal injection of an anti-Ly6G antibody during the early phase of *L. sigmodontis* infection. Neutrophil depletion was performed in order to investigate whether neutrophil absence abrogates the protective effect on the worm burden. Control animals were treated with an isotype control. As expected, isotype treated S100A8/A9$^{-/-}$ animals exhibited a reduced worm burden compared to WT mice at 12dpi (Fig. 19A). Interestingly, the depletion of neutrophils in S100A8/A9$^{-/-}$ mice led to a significant increase of worm recovery compared to isotype treated S100A8/A9$^{-/-}$ controls, revealing a similar worm burden compared to isotype-treated WT mice (Fig. 19A). Furthermore, an association was observed between the increased worm burden in neutrophil-depleted S100A8/A9$^{-/-}$ mice, the elevated number of inflamed blood vessels (Fig. 19B) and an increased lung pathology (Fig. 19C). In summary, these findings suggest that bronchoalveolar neutrophils mediate protective immune responses against invading L3 larvae in S100A8/A9$^{-/-}$ animals.

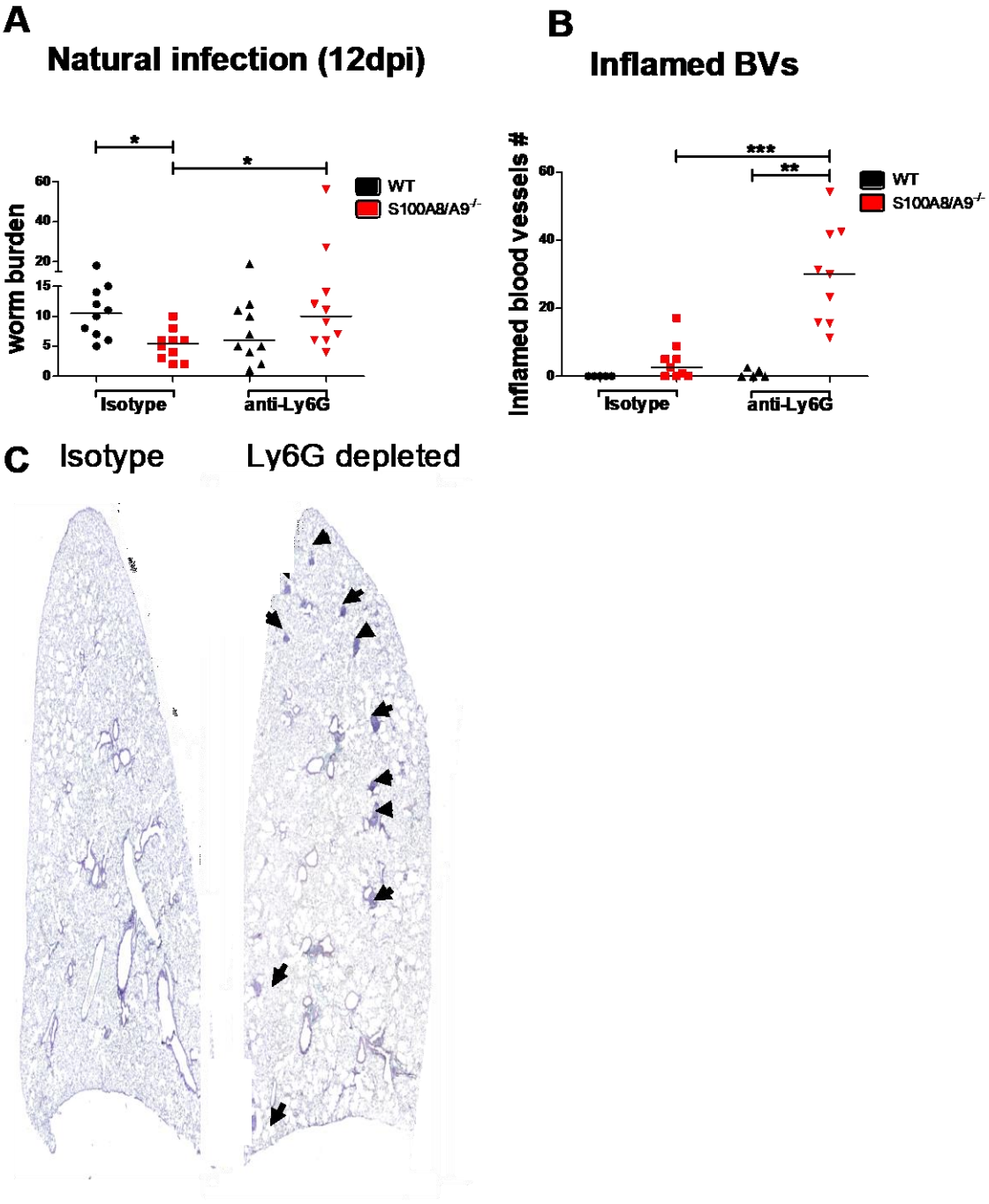

Fig. 19: Depletion of neutrophils during the early phase of *L. sigmodontis* infection abrogates the S100A8/A9-mediated reduction in worm burden. Worm burden 12 days post *L. sigmodontis* infection of WT and S100A8/A9$^{-/-}$ mice intranasally treated with anti-Ly6G to deplete lung neutrophils and isotype-treated controls (**A**) and total number of inflamed blood vessels (**B**). Representative picture of a lung isolated from a 12-day *L. sigmodontis*-infected S100A8/A9$^{-/-}$ mouse treated with isotype controls or anti-Ly6G (**C**). Statistical significance of not normally distributed data was analyzed by Kruskal-Wallis followed by Dunn's multiple comparison test (**A**, **B**). Data shown are pooled from two independent experiments with at least 5 mice per group.

3.2.6 Increased worm burden in S100A8/A9$^{-/-}$ mice upon intravenous injection of L3 larvae

To determine, if the protective mechanism observed in S100A8/A9$^{-/-}$ mice resulting in a decreased worm burden, is induced due to the consecutive entrance of L3 larvae from the pulmonary capillaries into the thoracic cavity, WT and S100A8/A9$^{-/-}$ mice were infected i.v. with 40 L3 larvae. I.v. injection of L3 larvae revealed an increased worm burden in S100A8/A9$^{-/-}$ animals compared to WT mice (Fig. 20A). This phenotype may occur due to the simultaneous entrance of the L3 larvae within the pulmonary capillaries into the thoracic cavity, preventing the timely initiation of protective immune responses against invading L3 larvae. During nat. and s.c. infection, infective L3 larvae reach the thoracic cavity between 2-6dpi, enabling the generation of protective immune responses against larvae that enter at a later time-point. Although i.v. infected S100A8/A9$^{-/-}$ mice exhibited an increased worm burden, similar immune responses within the thoracic cavity were observed following nat. and s.c. infection. Thoracic cavity cells (Fig. 20B) were increased as well as levels of elastase (Fig. 20C) and CXCL-2 (Fig. 20D) within the pleural lavage.

Total bronchoalveolar cell counts did not show any differences between WT and S100A8/A9$^{-/-}$ mice (Fig. 20E). However, elevated levels of CXCL-1 (Fig. 20F) and CXCL-5 (Fig. 20G) were observed within the bronchoalveolar lavage of S100A8/A9$^{-/-}$ compared to WT controls. These results indicate that the protective effect observed in S100A8/A9$^{-/-}$ mice is abrogated after i.v. infection.

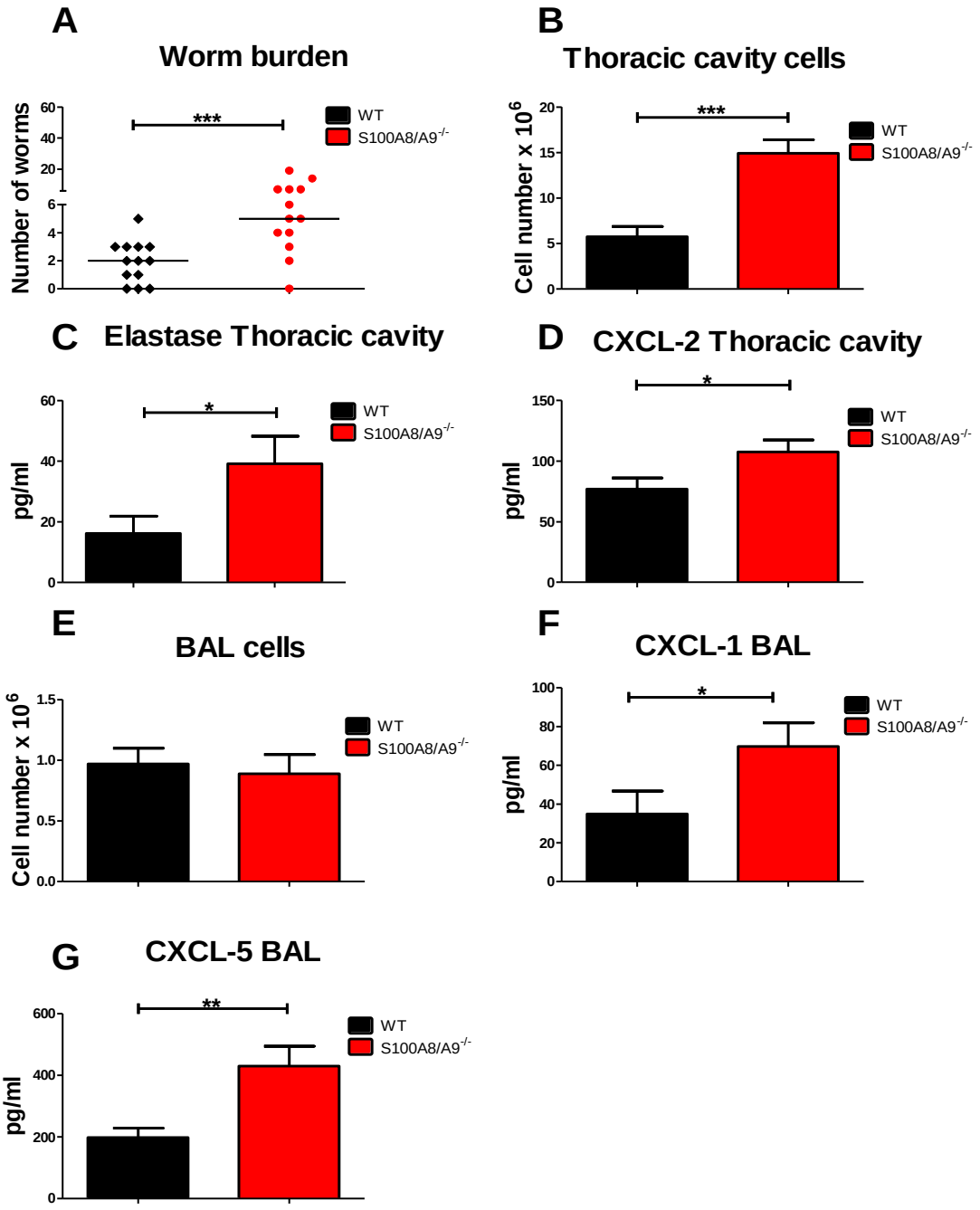

Fig. 20: Simultaneous entry of infective *L. sigmodontis* L3 larvae during intravenous injection leads to an increased worm burden in S100A8/A9$^{-/-}$ mice. Total number of worms in WT and S100A8/A9$^{-/-}$ mice 12 days post intravenous infection (**A**). Total number of thoracic cavity cells (**B**), concentrations of elastase (**C**) and CXCL-2 (**D**) in the thoracic cavity lavage as well as total number of bronchoalveolar cells (**E**), concentrations of CXCL-1 (**F**) and CXCL-5 (**G**) in BAL of 12-day *L. sigmodontis*-infected WT and S100A8/A9$^{-/-}$ mice. Figure **A** is shown as median. Remaining figures are shown as mean with SEM. Differences were analyzed for statistical significance using the Mann-Whitney U-test *p<0.05, **p<0.01, ***p<0.001. Data shown are pooled from two independent experiments with 5-8 mice per group.

3.2.7 Decreased inflammation in S100A8/A9$^{-/-}$ mice during the late phase of *L. sigmodontis* infection

Next, the role of S100A8/A9 during the molting of L4 *L. sigmodontis* larvae into adult worms (29dpi) was investigated. Analysis included worm counts, immune responses within the bronchoalveolar and thoracic cavity lavage at a time point at which L4 larvae molt in WT mice into adult male and female worms.

Comparable to the results at 12dpi the worm burden was significantly decreased in S100A8/A9$^{-/-}$ animals compared to WT mice at 29dpi (Fig. 21A). Furthermore, a lower amount of infiltrated cells, especially eosinophils, was observed in the perivascular space of WT mice, indicating a reduction in lung pathology (Fig. 21B). Analysis of the thoracic cavity lavage showed a significantly increased cell count in S100A8/A9$^{-/-}$ animals compared to WT controls (Fig. 21C). Frequencies of eosinophils, neutrophils and macrophages within the thoracic cavity at 29dpi were significantly decreased in S100A8/A9$^{-/-}$ mice in comparison to WT mice (Fig. 21D). Furthermore, no differences were observed for total bronchoalveolar cell numbers (Fig. 21E) and frequencies of eosinophils, neutrophils and macrophages (Fig. 21F) between both mouse strains. Interestingly, neutrophils in S100A8/A9$^{-/-}$ mice within the thoracic cavity (Fig. 21G) and bronchoalveolar lavage (Fig. 21H) were less activated compared to neutrophils of WT mice.

Collectively, these results indicate that at day 29dpi S100A8/A9 is rather involved during the early time point of infection, especially during the transient pulmonary inflammation caused by migrating infective L3 *L. sigmodontis* larvae.

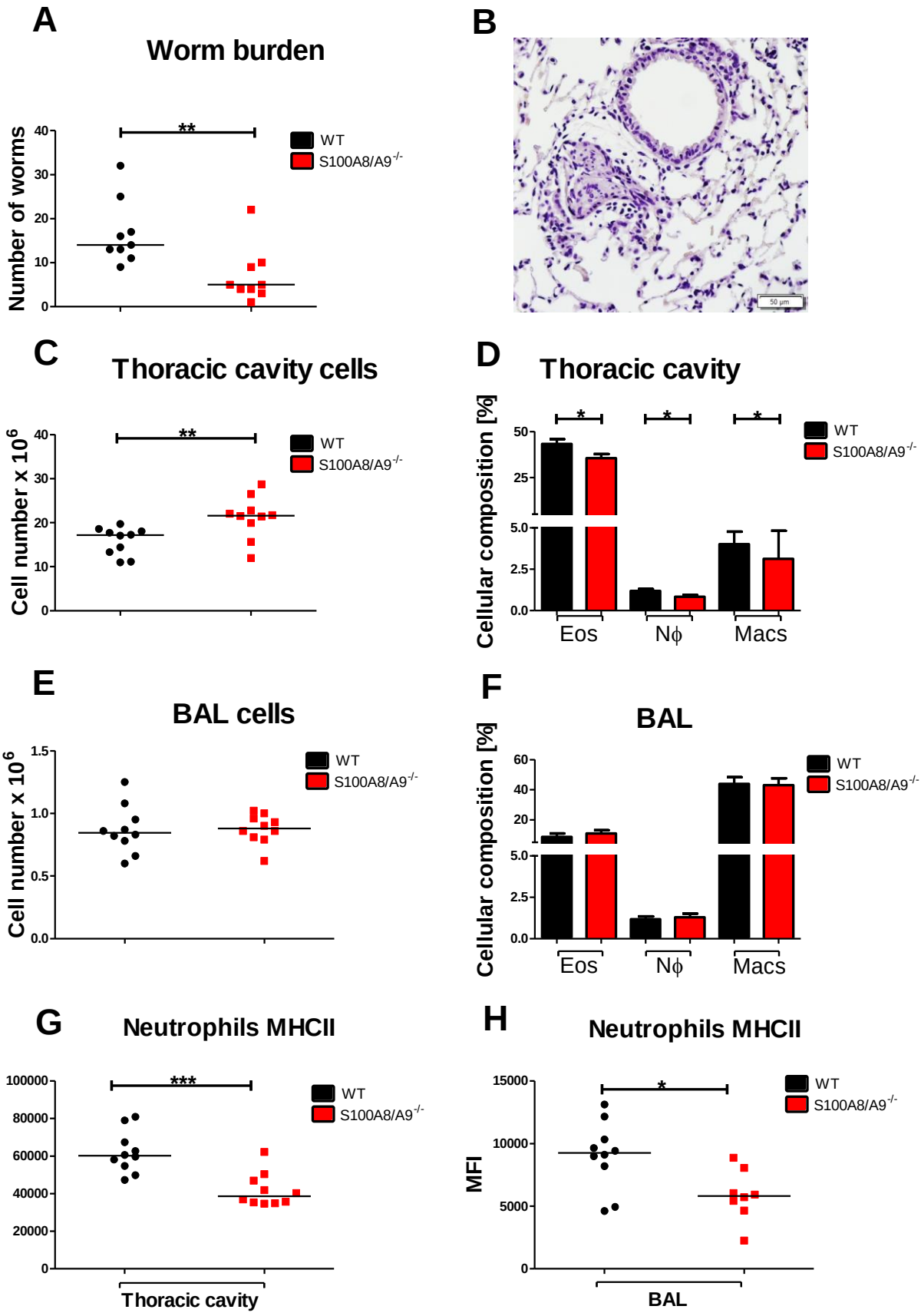
A
Worm burden
Number of worms
40
30
20
10
0
**
WT
S100A8/A9-/-
B
50 µm
C
Thoracic cavity cells
Cell number x 10^6
40
30
20
10
0
**
WT
S100A8/A9-/-
D
Thoracic cavity
Cellular composition [%]
50
25
5.0
2.5
0.0
*
*
*
WT
S100A8/A9-/-
Eos
Nϕ
Macs
E
BAL cells
Cell number x 10^6
1.5
1.0
0.5
0.0
WT
S100A8/A9-/-
F
BAL
Cellular composition [%]
60
40
20
5.0
2.5
0.0
WT
S100A8/A9-/-
Eos
Nϕ
Macs
G
Neutrophils MHCII
MFI
100000
80000
60000
40000
20000
0
***
WT
S100A8/A9-/-
Thoracic cavity
H
Neutrophils MHCII
MFI
15000
10000
5000
0
*
WT
S100A8/A9-/-
BAL

Fig. 21: Impact of S100A8/A9 on worm recovery and cellular responses in the thoracic cavity and bronchoalveolar lavage 29 days post *L. sigmodontis* infection. Worm burden in WT and S100A8/A9$^{-/-}$ mice 29 days post natural *L. sigmodontis* infection (**A**) and inflamed pulmonary blood vessels 29 days following *L. sigmodontis* infection in WT mice (**B**). Total number of thoracic cavity (**C**) and bronchoalveolar cells (**E**) as well as frequencies of indicated cell populations in thoracic cavity lavage (**D**) and bronchoalveolar lavage (**F**) as well as neutrophil MHCII expression in thoracic cavity (**G**) and bronchoalveolar lavage (**H**) in WT and S100A8/A9$^{-/-}$ mice 29 days post natural *L. sigmodontis* infection. Results are shown as median. Differences were analyzed for statistical significance using the Mann-Whitney U-test *p<0.05, **p<0.01, ***p<0.001. Data shown are from one experiment with 9 mice per group.

In summary, the data of this project demonstrate a pulmonary protective role of S100A8/A9 that inhibits L3-induced inflammation within the lung by decreasing chemokine production, granulocyte recruitment and furthermore neutrophil activation *in vitro* and *ex vivo*, reducing transient inflammatory responses and therefore facilitating larval migration.

3.3 Impact of AhR on *L. sigmodontis* infection

3.3.1 Deficiency of the aryl hydrocarbon receptor increases *L. sigmodontis* susceptibility

In the course of evolution eukaryotes developed different kind of cellular sensors including AhR, for the perception of external agents such as harmful agents, pathogens and toxins. As AhR is widely expressed within lung and skin, which represent the migration pathway of infective L3 *L. sigmodontis* larvae, it was aimed to identify its role during filarial infection. Therefore, AhR$^{-/-}$ mice were nat. infected with the murine filarial nematode *L. sigmodontis*. During necropsies at 5 and 14dpi worm numbers were assessed and the immune responses at the site of infection, the thoracic cavity, within the lung as well as spleen were analyzed. The worm burden was statistically significant increased in AhR$^{-/-}$ mice at 5 (median values AhR$^{-/-}$: 7/ WT: 5.2) and 14dpi (median values AhR$^{-/-}$: 18.6/ WT: 10.6) compared to WT controls (Fig. 22).

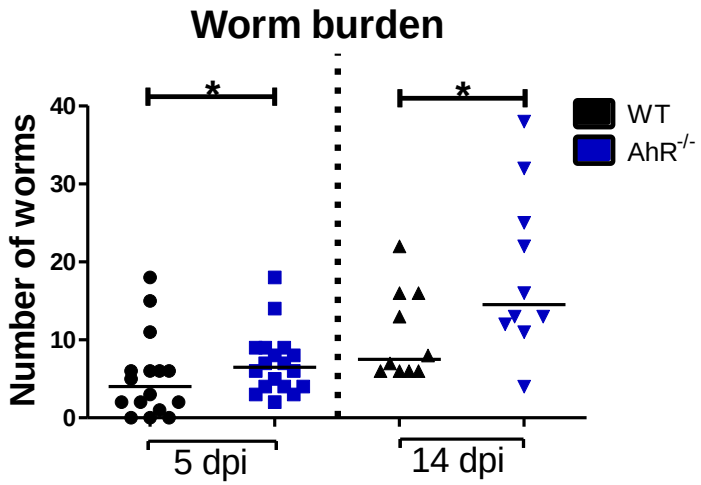

Fig. 22: Increased *L. sigmodontis* worm burden in AhR$^{-/-}$ mice. Worm burden following natural *L. sigmodontis* infection in WT and AhR$^{-/-}$ mice at 12 days post infection. Results are shown as median. Differences were analyzed for statistical significance using the Mann-Whitney U-test. *p<0.05. Data shown are pooled from 2-3 independent experiments with 5-7 mice per group.

3.3.2 AhR deficiency impairs immune responses within the thoracic cavity, lung and spleen

In order to investigate whether AhR-related changes in cellular composition and cytokine milieu are associated with the increased worm burden in $AhR^{-/-}$ mice, thoracic cavity, bronchoalveolar and spleen cells were analyzed by flow cytometry as well as cytokine profiles from the lavages at 5 and 14dpi. Uninfected $AhR^{-/-}$ mice did not show any differences in major immune cell frequencies of the thoracic cavity lavage compared to WT controls except for CD4+ T cell frequencies, which were significantly lower compared to WT CD4+ T cell frequencies (Fig. 23A). Thoracic cavity cell counts were significantly increased in $AhR^{-/-}$ mice in comparison to WT controls at 5 and 14dpi (Fig. 23B). This increase was associated with a higher frequency of macrophages in $AhR^{-/-}$ mice compared to WT controls during both time points (Fig. 23C, E). In contrast, frequencies of CD4+ T cells ($p<0.001$), eosinophils ($p<0.05$) and neutrophils ($p<0.05$) within the thoracic cavity were decreased in $AhR^{-/-}$ mice at 5dpi (Fig. 23C), reaching statistical significant differences at 14dpi compared to corresponding WT controls (Fig. 23E). Interestingly, MHCII expression was significantly lower for eosinophils, neutrophils and macrophages in $AhR^{-/-}$ mice at 5dpi compared to WT controls, indicating a reduced activation (Fig. 23D). MHCII expression in macrophages of $AhR^{-/-}$ animals was still decreased at 14dpi compared to WT mice (Fig. 23F).

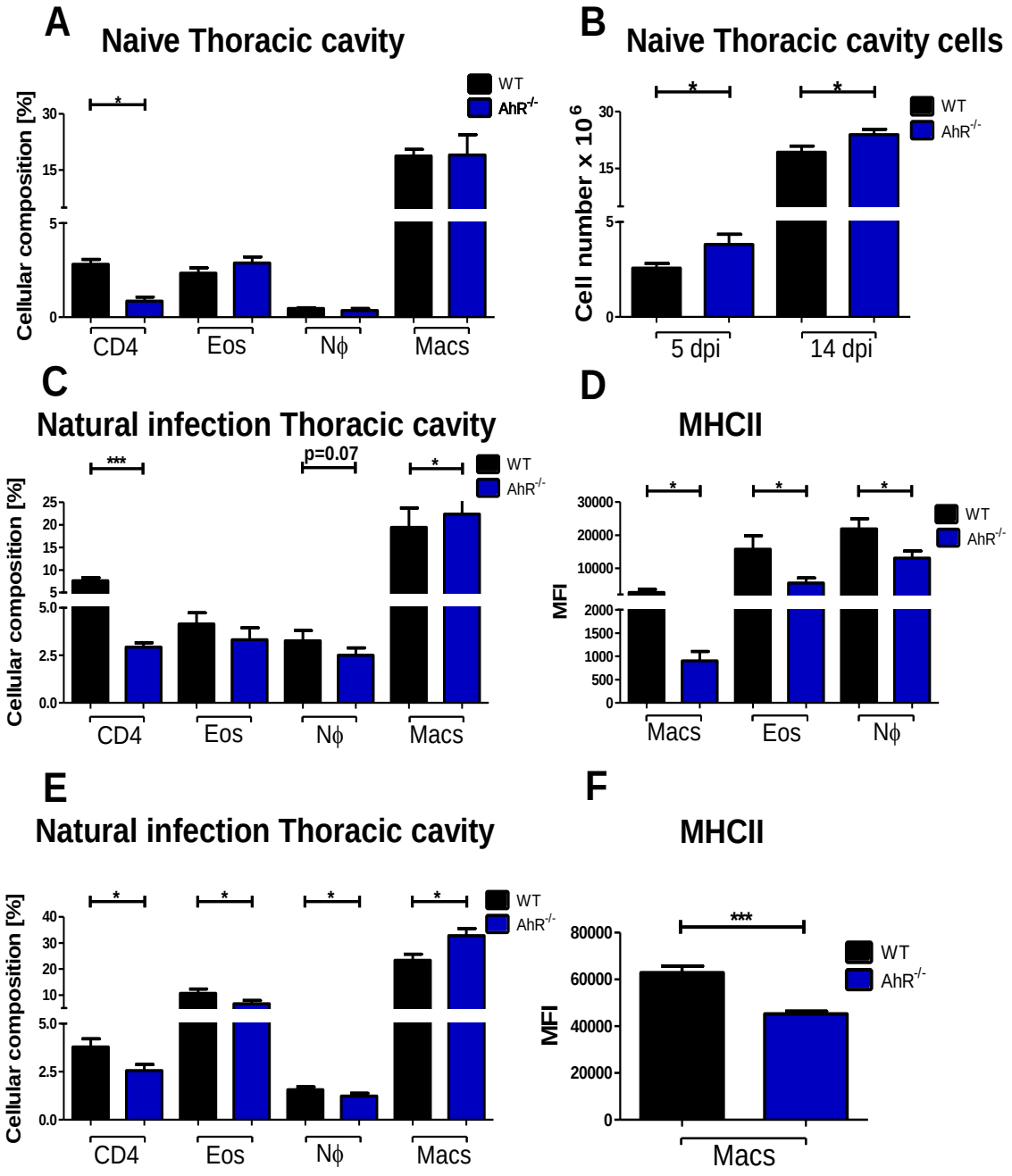

Fig. 23: Impaired immune responses in the thoracic cavity of AhR$^{-/-}$ mice. Cellular composition of the thoracic cavity lavage in naive WT and AhR$^{-/-}$ mice (**A**). Total number of thoracic cavity cells (**B**) and cellular composition of the thoracic cavity lavage (**C**) in 5 day *L. sigmodontis* infected mice as well as MHCII expression of macrophages, eosinophils and neutrophils (**D**). Cellular composition of the thoracic lavage (**E**) 14 days post *L. sigmodontis* infection and MHC expression of macrophages (**F**). Results are shown as mean with SEM. Differences were analyzed for statistical significance using the Mann-Whitney U-test *p<0.05, ***p<0.001. Data shown are pooled from two independent experiments with 5-7 mice per group.

Cytokine analysis of the pleural lavage for IL-4, IL-5, IL-6, IL-13, IFN-γ, TNF, and IL-1β were under the detection limit for naïve and infected WT and AhR$^{-/-}$ animals (data not shown). As AhR has been known to play a crucial role during attraction of several cell types during inflammatory processes, two prominent and AhR-associated chemokines were measured. Concentrations of CCL17 showed comparable values for AhR$^{-/-}$ and WT mice at 5dpi, but was significantly lower in AhR$^{-/-}$ at 14 dpi (Fig. 24A). In contrast, CXCL-10 was significantly increased at 5dpi in AhR$^{-/-}$ mice compared to WT controls, which was still elevated at 14dpi (Fig. 24B).

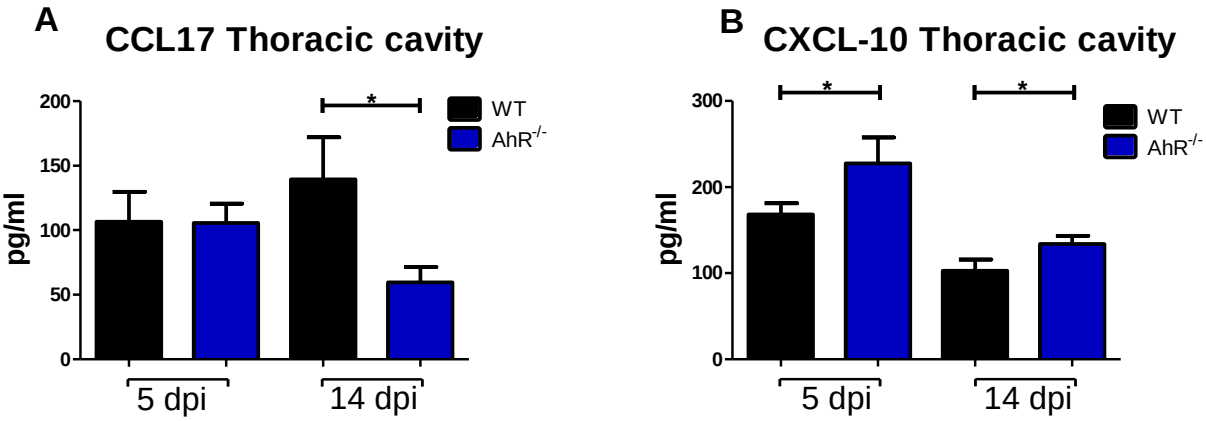

Fig. 24: AhR deficiency decreases CCL17 and increases CXCL-10 concentrations in the thoracic cavity lavage of *L. sigmodontis* infected mice. Concentrations of CCL17 (**A**) and CXCL-10 (**B**) in 5 and 14-day *L. sigmodontis* infected WT and AhR$^{-/-}$ mice. Results are shown as mean with SEM. Differences were analyzed for statistical significance using the Mann-Whitney U-test *p<0.05. Data shown are pooled from two independent experiments with 5-7 mice per group.

Similar to the pleural cavity cells, isolated bronchoalveolar and spleen cells were analyzed. Total bronchoalveolar cell counts (Fig. 25A) and cellular composition, including frequencies of CD4+ T cells, eosinophils, neutrophils and macrophages were comparable between uninfected AhR$^{-/-}$ and WT animals (Fig. 25B). At 5dpi bronchoalveolar frequencies of macrophages and eosinophils were decreased in AhR$^{-/-}$ mice compared to WT controls, whereas frequencies of neutrophils were increased in AhR$^{-/-}$ animals (Fig. 25C). The

decreased frequency of macrophages in AhR$^{-/-}$ at 5dpi was further associated with an increased MHCII expression in AhR$^{-/-}$ mice in comparison to WT animals. However, MHCII expression in neutrophils and eosinophils at 5dpi were comparable between both mouse strains (Fig. 25D).

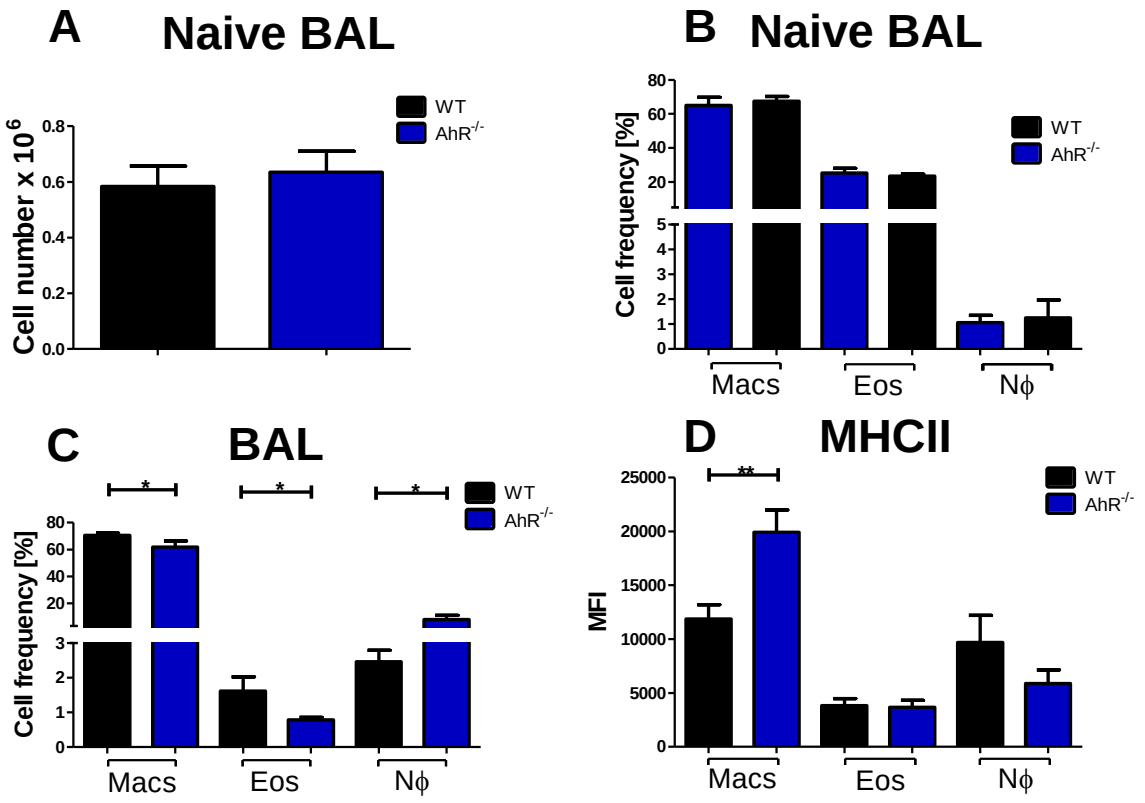

Fig. 25: Absence of AhR impairs the influx of macrophages and eosinophils during early *L. sigmodontis* infection within the bronchoalveolar lavage. Total number of bronchoalveolar cells (**A**). Cellular composition of the bronchoalveolar lavage in uninfected animals (**B**). Cellular composition of the bronchoalveolar lavage (**C**) and MHCII expression of macrophages, neutrophils and eosinophils (**D**) 5 days post *L. sigmodontis* infection of WT and AhR$^{-/-}$ mice. Results are shown as mean with SEM. Differences were analyzed for statistical significance using the Mann-Whitney U-test *p<0.05, **p<0.01. Data shown (**A**, **B**) consist of one experiment with 4 mice per group. Remaining data shown are pooled from two independent experiments with 3-4 mice per group (**C**, **D**).

ELISA results from the bronchoalveolar lavage revealed statistically significant lower concentrations of CCL17 (Fig. 26A) and CXCL-10 (Fig. 26B) at 5dpi in AhR$^{-/-}$ compared to

WT mice. The difference vanished during the later time point of infection at 14dpi (data not shown).

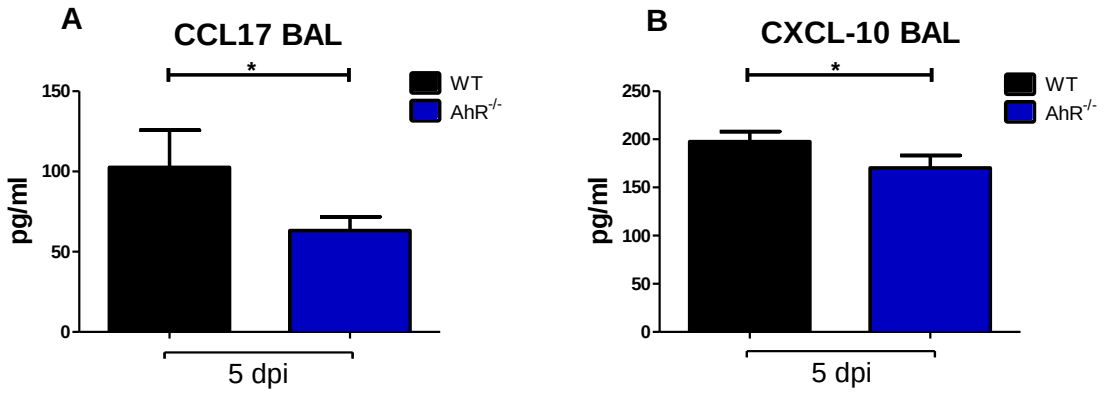

Fig. 26: AhR deficiency decreases CCL17 and CXCL-10 concentrations in the bronchoalveolar lavage. Concentrations of CCL17 (**A**) and CXCL-10 (**B**) in the bronchoalveolar lavage of 5 day-*L. sigmodontis*-infected WT and AhR$^{-/-}$ mice. Results are shown as mean with SEM. Differences were analyzed for statistical significance using the Mann-Whitney U-test *$p<0.05$. Data shown are pooled from two independent experiments with 3-4 mice per group.

With regard to immunological changes within the spleen of naïve animals no differences in frequencies of CD4+ T cells and eosinophils were observed between both mouse strains. However, frequencies of neutrophils and macrophages were significantly increased in naïve AhR$^{-/-}$ animals compared to naïve WT controls (Fig. 27A). *L. sigmodontis* infection led to an increase of total splenocyte number in AhR$^{-/-}$ mice in comparison to WT controls (Fig. 27B). At 5 days post *L. sigmodontis* infection frequencies of CD4+ T cells, eosinophils and macrophages in AhR$^{-/-}$ animals were significantly lower compared to WT mice (Fig. 27C). These observations were further associated with a lower MHCII expression by eosinophils and macrophages in AhR$^{-/-}$ animals (Fig. 27D). These differences vanished at 14dpi and frequencies of macrophages were increased in AhR$^{-/-}$ mice compared to WT mice at 14dpi

(Fig. 27E). Neutrophil frequencies during both time points at 5 and 14dpi did not reveal any statistical differences between immunodeficient and control mice.

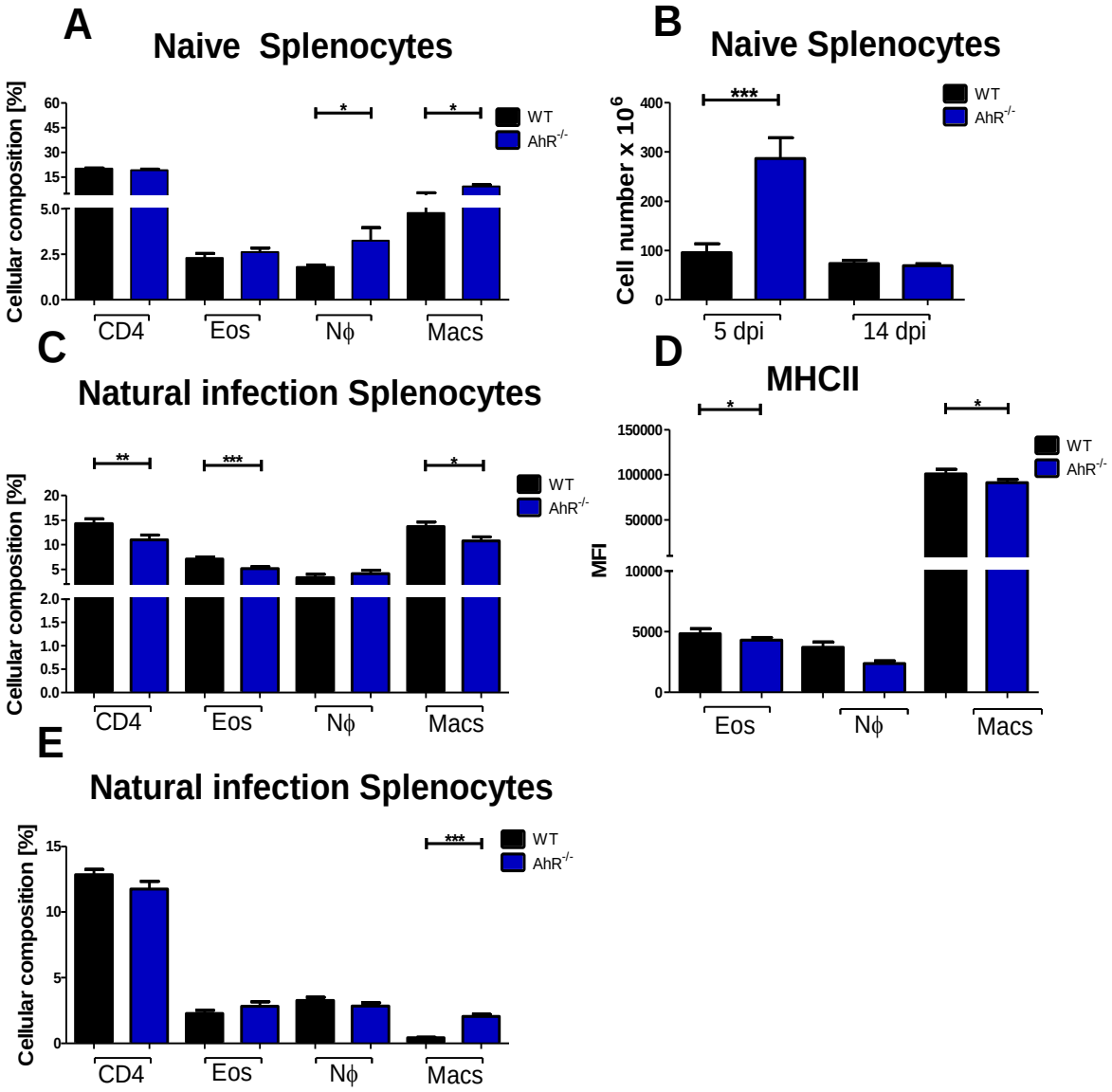

Fig. 27: Reduced macrophage and eosinophil frequencies within the spleen of AhR$^{-/-}$ mice during early *L. sigmodontis* infection. Cellular composition of the spleen in uninfected WT and AhR$^{-/-}$ animals (**A**). Total number of splenocytes (**B**) and cellular composition of the spleen (**C**) 5 days post *L. sigmodontis* infection and MHCII expression of eosinophils, neutrophils and macrophages (**D**) of WT and AhR$^{-/-}$ mice. Cellular composition of the spleen (**E**) 14 days post *L. sigmodontis* infection in WT and AhR$^{-/-}$ mice. Results are shown as mean with SEM. Differences were analyzed for statistical significance using the Mann-Whitney U-test *p<0.05, **p<0.01, ***p<0.001. Data shown in (**A**, **B**) are from one experiment with 5 mice per group. Remaining data (**C**-**E**) are pooled from 2-3 independent experiments with 5-7 mice per group.

3.3.3 Impaired immune responses within the skin of AhR$^{-/-}$ mice

Since AhR is highly expressed on various cell types within the skin including dendritic cells, monocytes and macrophages, the immune responses within the skin in AhR$^{-/-}$ mice after i.d. injection of *L. sigmodontis* crude extract was determined. After 3h post injection the skin tissue was isolated, digested and immune cells were analyzed by flow cytometry. I.d. injections of *L. sigmodontis* L3 larvae increased the influx of cells to the site of infection in WT and AhR$^{-/-}$ mice compared to controls treated with PBS. Cellular influx in the skin of AhR$^{-/-}$ mice after PBS and L3 larvae injection was lower compared to WT controls, indicating an impaired influx of immune cells within the skin of AhR$^{-/-}$ (Fig. 28A). Interestingly, the impaired influx of immune cells in AhR$^{-/-}$ mice was further associated with decreased total cell counts of monocytes (Ly6C+/F4/80-, Fig. 28B), macrophages (F4/80+/SiglecF-, Fig. 28C), neutrophils (Ly6G+/CD11b+, Fig. 28D) and eosinophils (SiglecF+/F4/80-, Fig. 28E) following LsAg injection compared to corresponding WT mice. Furthermore, these decreased cell frequencies in LsAg-injected AhR$^{-/-}$ mice were accompanied by a lower cell activation state, revealing a decreased expression of CD86 on monocytes (Fig. 28F), MHCII on macrophages (Fig. 28G), and CD69 on neutrophils (Fig. 28 H). No differences were observed in the cell activation state of CD54 in the frequency of eosinophils (Fig. 28I).

These results indicate that immune responses within the skin of AhR$^{-/-}$ mice are impaired following L3 injection, resulting in an impaired influx of immune cells as well as less activated monocytes, macrophages, neutrophils and eosinophils.

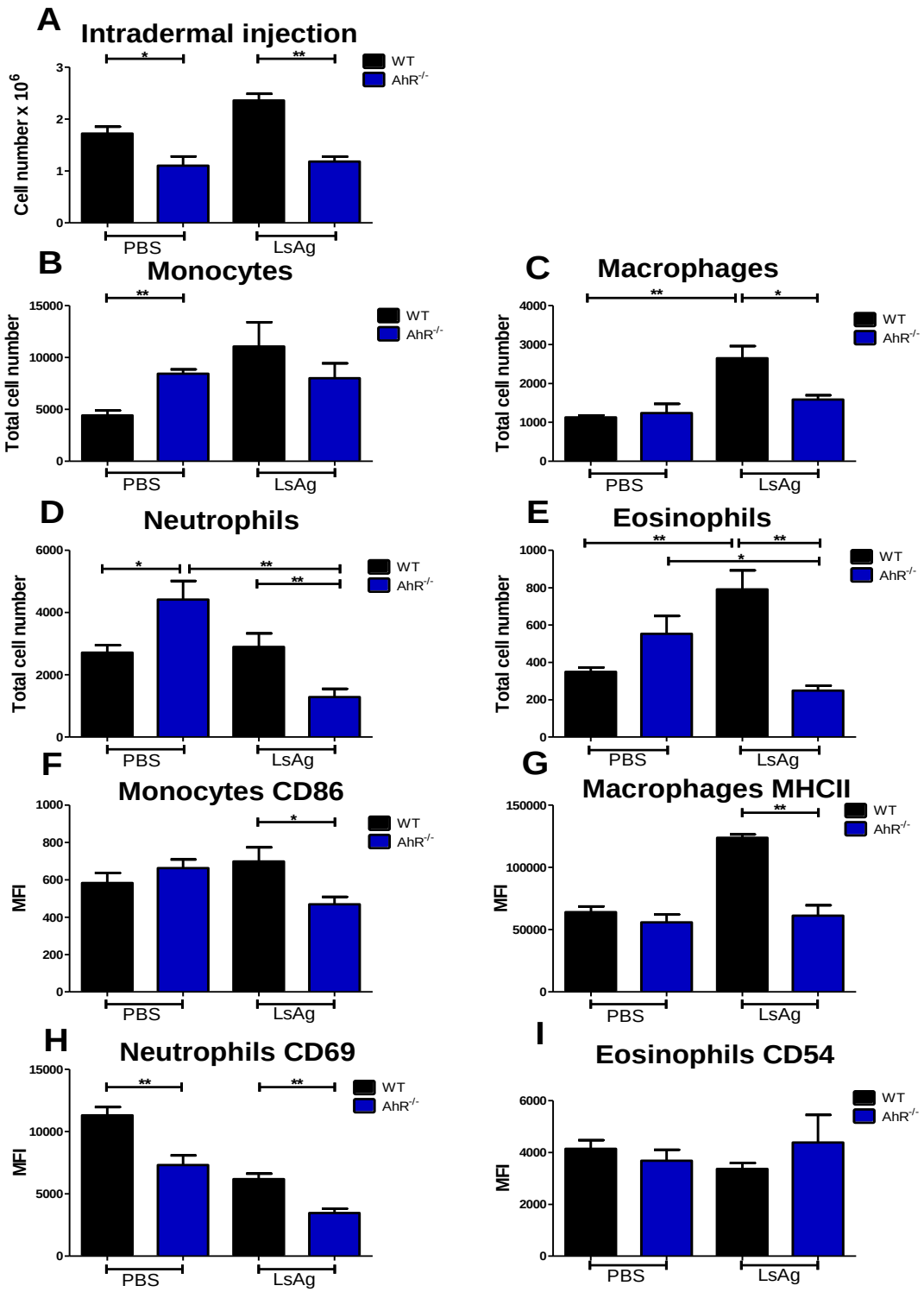

Fig. 28: AhR$^{-/-}$ impairs immune responses within the skin. Total number of skin cells (**A**), monocytes (**B**), macrophages (**C**), neutrophils (**D**) as well as eosinophils (**E**) and their respective CD86 (**F**), MHCII (**G**), CD69 (**H**) and CD54 (**I**) expression in WT and AhR$^{-/-}$ mice 3h post intradermal *L. sigmodontis* infection. Results are shown as mean with SEM. Statistical significance of not normally distributed data (**A**-**I**) was analyzed by Kruskal-Wallis followed by Dunn's multiple comparison test *p<0.05, ** p<0.01. Data shown are from one experiment with 5 mice per group.

3.3.4 AhR deficiency impairs macrophage activation upon LPS and LsAg stimulation

Macrophages belong to the main antigen-presenting cells and expand during *L. sigmodontis* infection as AAMs within the thoracic cavity. Since AhR is highly expressed in myeloid cell types, especially macrophages, and a reduced cell activation of macrophages was observed following i.d. LsAg injection and within the spleen as well as thoracic cavity in $AhR^{-/-}$ mice, cell activation was assessed *in vitro* of bone-marrow-derived macrophages from WT and $AhR^{-/-}$ mice upon LPS and LsAg stimulation. Macrophages of $AhR^{-/-}$ mice exhibited a decreased expression of CD86 (Fig. 29A) and MHCII (Fig. 29B) after 3h of LPS and LsAg stimulation compared to macrophages of WT animals. Although, TNF levels were decreased in $AhR^{-/-}$ mice following LsAg stimulation, the difference was not statistically significant compared to WT animals (Fig. 29C).

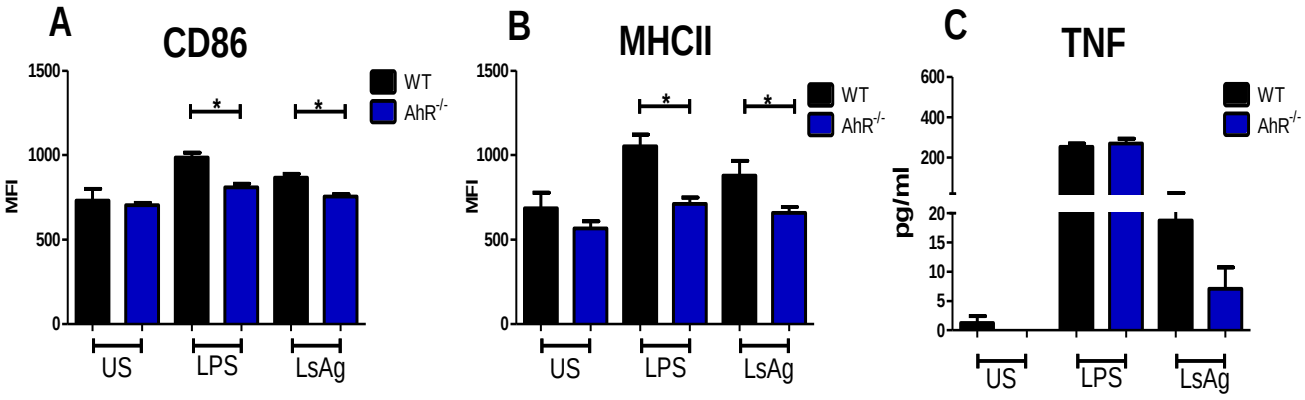

Fig. 29: Absence of AhR impairs macrophage activation. Expression of CD86 (**A**) and MHCII (**B**) on bone-marrow derived macrophages WT and $AhR^{-/-}$ mice and concentration of released TNF (**C**) 3h post *in vitro* culture. Results are shown as mean with SEM. Differences were analyzed for statistical significance using the Mann-Whitney U-test *$p<0.05$. Data shown are from one experiment with 3 mice per group.

Collectively, these data indicate that the absence of AhR impairs cell activation of macrophages and further the release of inflammatory cytokines such as TNF in response to LsAg.

3.3.5 AhR deficiency increases vascular permeability and facilitates larval migration

Next it was set out to investigate if the absence of AhR impact vascular permeability which may facilitate *L. sigmodontis* L3 migration. PBS and LsAg i.d. injected ears of $AhR^{-/-}$ mice and corresponding WT controls were isolated 10min after i.v. injection of Evans blue (30mg/kg). After incubation at 56°C for 24h the optical density was determined in order to analyse *in vivo* vascular permeability. I.d. injections of LsAg increased OD values in WT and $AhR^{-/-}$ mice compared to controls treated with PBS. Interestingly, injection of LsAg revealed a significant increase of vascular permeability in $AhR^{-/-}$ mice compared to WT LsAg treated animals, which may facilitate L3 larval migration (Fig. 30).

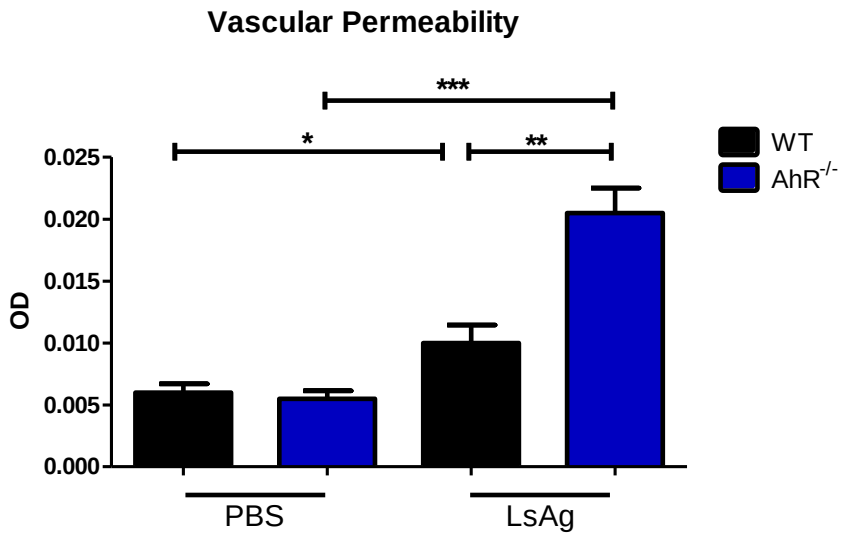

Fig. 30: Increased vascular permeability in $AhR^{-/-}$ animals. Optical density in PBS and LsAg-treated WT and $AhR^{-/-}$ animals. Results are shown as mean with SEM. Differences were analyzed for statistical significance using the Mann-Whitney U-test *p<0.05, ** p<0.01, *** p<0.001. Data shown are pooled from two independent experiments with 4-5 mice per group.

In conclusion, several protective mechanisms related to AhR during *L. sigmodontis* infection have been identified. First of all AhR deficiency led to reduced cell activation as well as limited immune responses within the skin. In addition, this was also associated with an enhanced vascular permeability in $AhR^{-/-}$ compared to WT controls, which facilitated larval migration and resulted in an increased worm burden during early timepoint of *L. sigmodontis* infection.

3.4 LsAg and diet-induced insulin-resistance

3.4.1 LsAg administration improves glucose, but not insulin tolerance

Recent studies have shown that helminth infections and worm-derived products may be beneficial to ameliorate T2D by improving insulin and glucose tolerance. However, further investigations based on the protective mechanism are still rare. Berbudi and colleagues demonstrated that the repeated administration of adult worm extract (LsAg) improved glucose tolerance in diet-induced obese (DIO) mice, which was further associated with an increase of eosinophils and AAMs within the adipose tissue [118]. Therefore, it was investigated whether LsAg may have an impact on other cell frequencies as T cells, which could be associated with the improved glucose tolerance due to LsAg treatment after the onset of obesity. After the repeated administration of LsAg in obese mice a glucose and insulin tolerance test was performed. DIO mice reached highest glucose concentrations 15-30min after glucose challenge. Afterwards, glucose levels in DIO mice treated i.p. with LsAg declined steadily compared to blood glucose levels of DIO mice treated with PBS (Fig. 31A). These results indicated an improved glucose tolerance. The AUC (area under the curve) showed significantly lower values in LsAg-treated DIO mice compared to PBS-treated DIO controls (Fig. 31B).

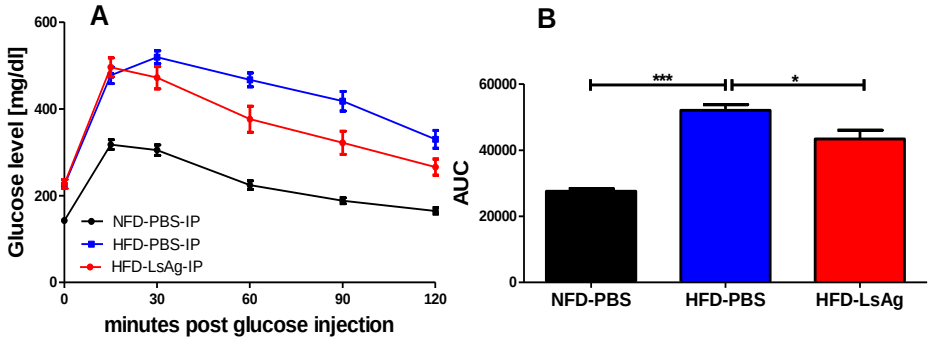

Fig. 31: Intraperitoneal administration of LsAg improves glucose intolerance in HFD mice. Blood glucose levels over the time after intraperitoneal glucose challenge in intraperitoneally PBS- (NFD, HFD) and LsAg-administered HFD mice after 16 weeks of HFD (**A**). Calculated area under curve (AUC) from the course of glucose tolerance test (**B**). Results are shown as mean +/- SEM (**A**) and mean with + SEM (**B**). Differences were analyzed for statistical significance using 1-Way ANOVA followed by Dunnett's test. *p<0.05, ***p<0.001. Data shown are pooled from two independent experiments with 6 mice per group.

In addition, an insulin tolerance test (ITT) similar to the GTT was performed, during which insulin was injected and glucose blood levels were measured at regular intervals. Lowest glucose concentration was observed in DIO mice at 30min after insulin challenge. Subsequently, glucose concentration increased constantly until 120min after insulin challenge. No statistical differences were observed in blood glucose levels at the different time points of LsAg and PBS treated DIO mice (Fig. 32A). The AUC for the ITT showed a significant lower value of NFD-PBS treated mice compared to corresponding PBS-treated DIO mice (Fig. 32B).

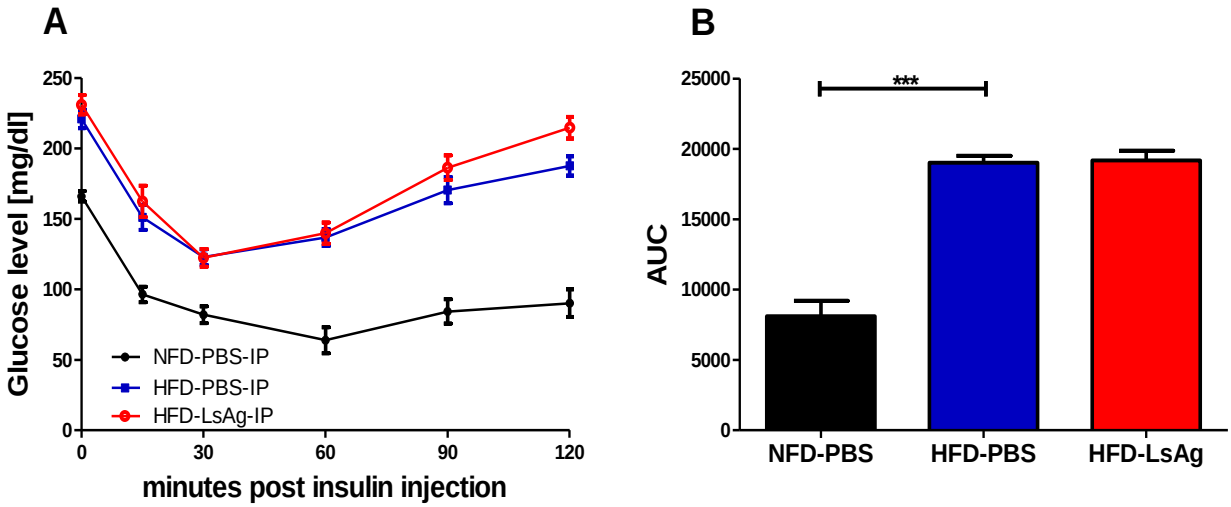

Fig. 32: LsAg does not improve insulin sensitivity in HFD mice. Blood glucose levels over time after intraperitoneal insulin injection in LsAg and PBS intraperitonealy administered HFD mice after 16 weeks of HFD (**A**). Calculated area under curve from the course of the insulin tolerance test (**B**). Results are shown as mean +/- SEM (**A**) and mean + SEM (**B**). Differences were analyzed for statistical significance using 1-Way ANOVA followed by Dunnett's test. ***p<0.001. Data shown are pooled from two experiments with 6 mice per group.

Repeated s.c. treatment of LsAg in DIO treated mice did not improvethe glucose tolerance compared to PBS controls (Fig. 33A, B).

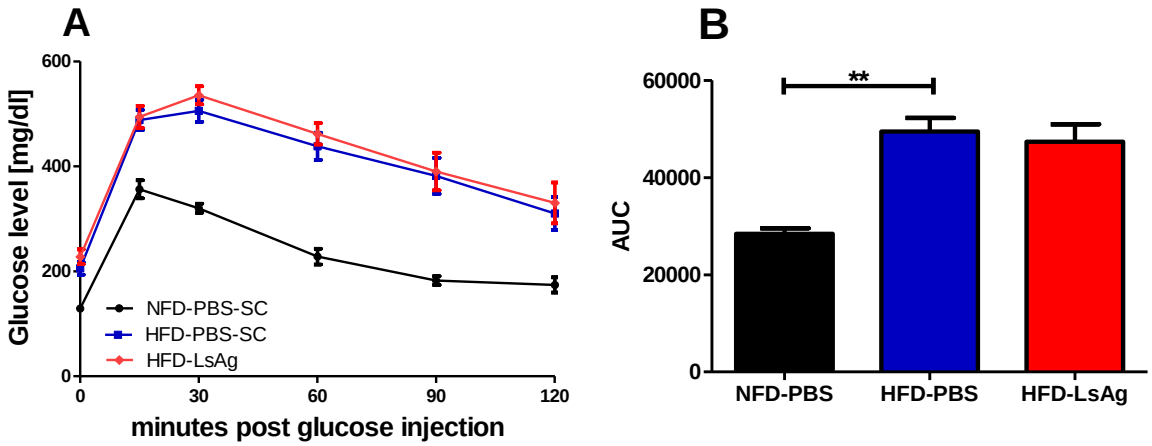

Fig. 33: Subcutaneous administration of LsAg does not impact glucose tolerance in HFD mice. Blood glucose levels over time after intraperitoneal glucose challenge in PBS- and LsAg- subcutaneously administered HFD mice after 16 weeks of HF diet (**A**). Calculated area under the curve (AUC) from the course of glucose tolerance test (**B**). Results are shown as mean +/- SEM (**A**, **B**). Differences were analyzed for statistical significance using 1-Way ANOVA followed by Dunnett's test. **p<0.01. Data shown consist of one experiment with 6 mice per group.

3.4.2 LsAg administration alters adipose tissue T cell frequencies

Obesity leads to chronic inflammation resulting in a pro-inflammatory milieu by altering the cellular composition of the adipose tissue, replacing AAMs by infiltrated classically activated macrophages, increasing CD8+ T cell and Th1 cell frequencies and decreasing regulatory CD4+ T cell frequencies. Recent studies confirmed the essential role of T cells during diet-induced inflammatory responses [110] and showed that depletion of CD8+ T cells decreases adipose tissue inflammation [107]. Therefore, CD4+ and CD8+ T cell frequencies and pro-inflammatory cytokine secretion from CD4+ and CD8+ T cells were determined from adipose tissue. Repeated administration of LsAg increased frequencies of CD4+ T cells (Fig. 34A), whereas CD8+ T cell frequencies declined (Fig. 34B).

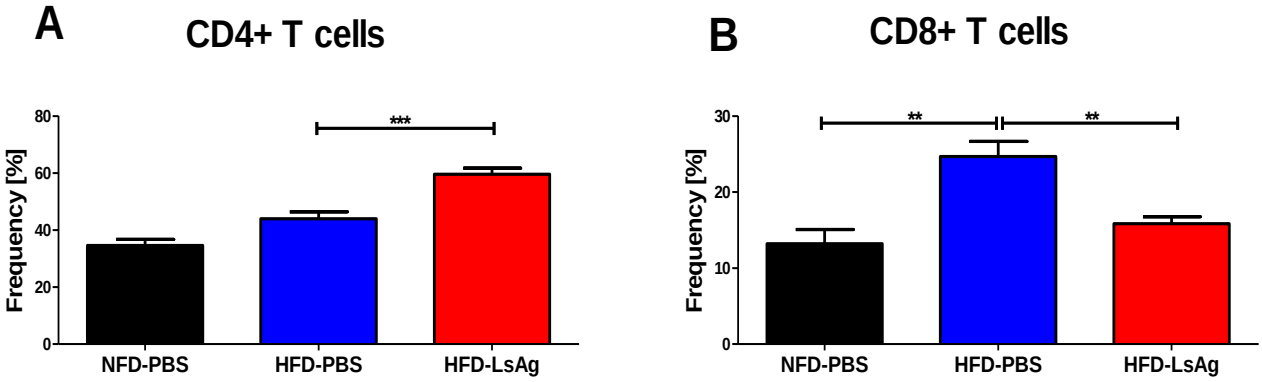

Fig. 34: Repeated administrations of LsAg alters adipose tissue CD4+ and CD8+ T cell frequencies. Frequency of CD4+ T cells (**A**) and CD8+ T cells (**B**) within the visceral adipose tissue of mice fed on a normal chow diet (NFD) or high fat diet (HFD) for 16 weeks and treated with LsAg. Results are shown as mean + SEM. Differences were analyzed for statistical significance using 1-Way ANOVA followed by Dunnett's test. **p<0.01, ***p<0.001. Data shown are pooled from two independent experiments with 6 mice per group.

Repeated LsAg administration increased IL-4+ CD4+ T cells (Fig. 35A) and decreased IL-17+ (Fig. 35B), TNF+ (Fig. 35C) and IFN-γ+ (Fig. 35D) CD4+ T cell frequencies in adipose tissue compared to PBS-treated HFD mice.

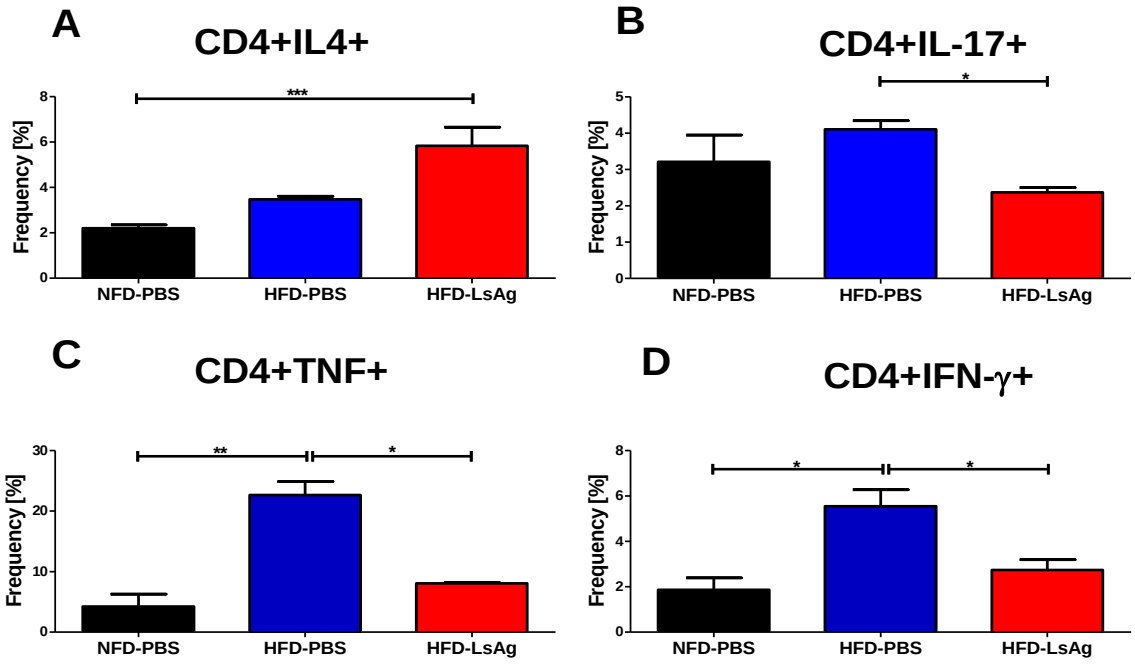

Fig. 35: LsAg treatment reduces pro-inflammatory cytokine production by CD4+ T cells in adipocytes. Frequencies of IL-4+ (**A**), IL-17+ (**B**), TNF+ (**C**) ,and IFN-γ+ (**D**) CD4+ T cells within the adipose tissue of animals receiving a normal food diet (NFD) and treated with PBS and high-fat diet (HFD) fed animals for 16 weeks that were treated daily for 2 weeks intraperitoneal with LsAg or PBS. Results are shown as mean + SEM. Differences were analyzed for statistical significance using 1-Way ANOVA followed by Dunnett's test (**A**, **B**, **D**) and Kruskal-Wallis followed by the Dunn's multiple comparison test (**C**).*p<0.05, **p<0.01, ***p<0.001. Data shown are pooled from two independent experiments with 6 mice per group.

Next the frequencies of IFN-γ+, TNF+ and IL-17+ CD8+ T cells were determined. First of all it was shown that the frequency of IFN-γ+ CD8+ T cells was not influenced by the repeated administration of LsAg compared to PBS-treated HFD mice (Fig. 36A). However, LsAg treatment revealed decreased frequencies of TNF+ (Fig. 36B) and IL-17+ (Fig. 36C) CD8+ T cells compared to HFD-PBS treated animals.

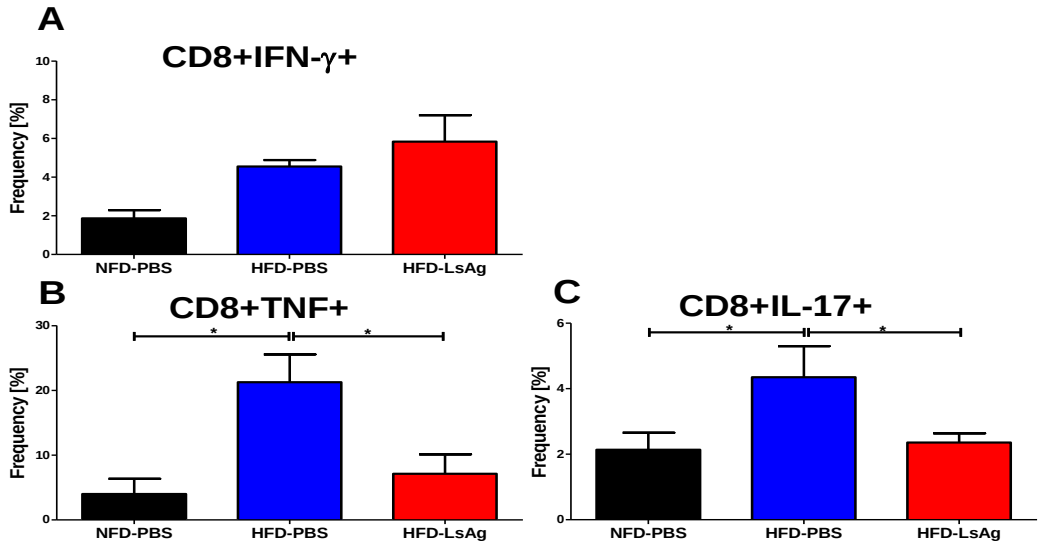

Fig. 36: LsAg treatment reduces pro-inflammatory cytokine production by CD8+ T cells in adipocytes. Frequencies of IFN-γ+ (**A**), TNF+ (**B**) ,and IL-17+ (**C**) CD8+ T cells within the adipose tissue of animals receiving a normal food diet (NFD) and treated with PBS and high-fat diet (HFD) fed animals for 16 weeks that were treated daily for 2 weeks intraperitoneal with LsAg. Results are shown as mean + SEM. Differences were analyzed for statistical significance using 1-Way ANOVA followed by Dunnett's test (**A**, **C**) and Kruskal-Wallis followed by the Dunn's multiple comparison test (**B**). *p<0.05. Data shown are pooled from two independent experiments with 6 mice per group.

Collectively, these results highlight the protective impact of LsAg in DIO mice, improving glucose tolerance as well as alleviating inflammation by decreased pro-inflammatory cytokine producing CD4+ (TNF+, ,IFN-γ+, IL-17+) and CD8+ (TNF+, IL-17+) adipose tissue T cells during the onset of obesity.

3.4.3 LsAg administration does not modulate the lipid profile during diet-induced obesity

Since obesity is associated with changes within the lipid profile, it was assessed if the repeated administrations of LsAg have an impact on the lipid profile during DIO. Therefore, cholesterol, triglycerides and low density lipids (LDL) were measured in the serum. As expected, PBS treated controls that were maintained on a chow diet showed lower levels of cholesterol, triglyceride and LDL compared to the animals receiving 16 weeks of HFD. No statistical differences in total cholesterol (Fig. 37A), triglyceride (Fig. 37B) and LDL (Fig. 37C) levels in DIO mice that were treated with LsAg in comparison to PBS-treated DIO controls were observed, suggesting no impact of LsAg treatment on the lipid profile during the onset of obesity.

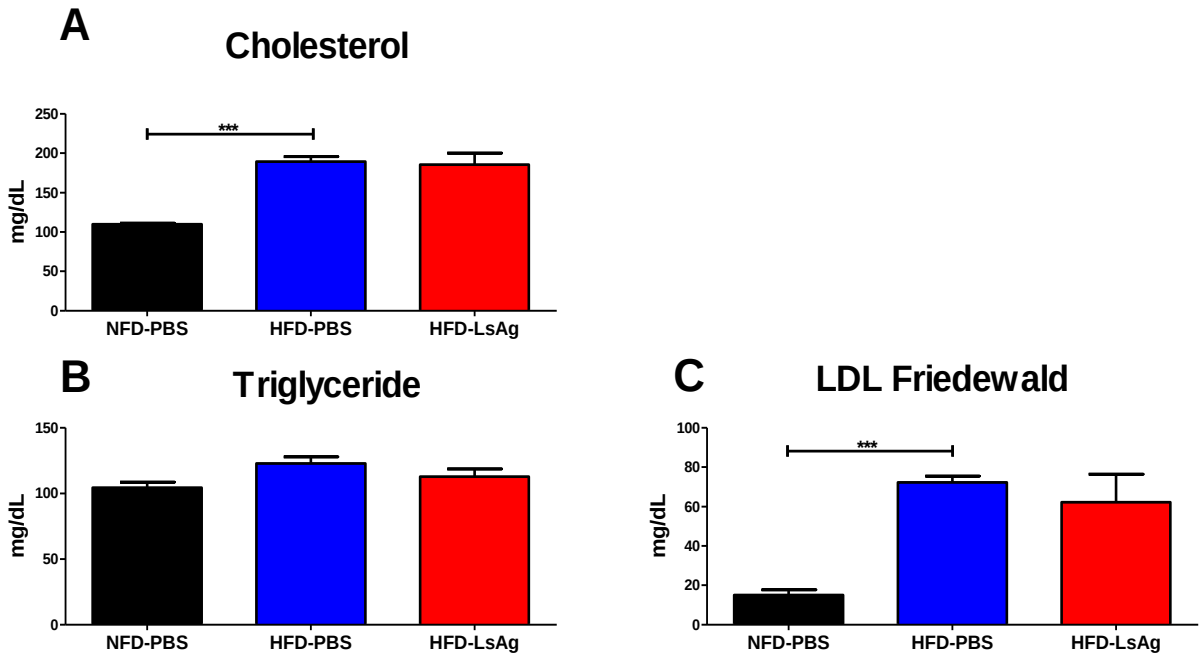

Fig. 37: Repeated LsAg administrations do not modulate the lipid profile in DIO mice. Concentrations of cholesterol (**A**), triglyceride (**B**) and LDL Friedewald (**C**) in peripheral blood of animals receiving a chow diet (NFD) and treated with PBS and high-fat diet (HFD) fed animals for 16 weeks that were treated daily for 2 weeks intraperitoneal with PBS or LsAg. Results are shown as mean + SEM. Differences were analyzed for statistical significance using 1-Way ANOVA followed by Dunnett's test. ***p<0.001. Data shown are pooled from two independent experiments with 6 mice per group.

3.4.4 LsAg increases adiponectin levels and dampen CD4 and CD8 T cell inflammation

In order to investigate potential protective mechanisms induced by LsAg treatment, the impact of the regulatory cytokine IL-10 and the most prominent adipokine (Acrp30) were investigated. Acrp30 levels were measured in the adipose tissue supernatant and serum of LsAg and PBS-treated NFD controls and DIO mice that were fed for 16 weeks with HFD. Adipose tissue Acrp30 levels were increased in the LsAg group in comparison to PBS treated DIO mice; however no statistical significances were observed (Fig. 38A). A similar increase was observed for Acrp30 in the serum of LsAg DIO treated animals compared to PBS-

administered DIO mice (Fig. 38B). Furthermore, LsAg treatment of DIO mice increased adipose tissue supernatant IL-10 levels (Fig. 38C).

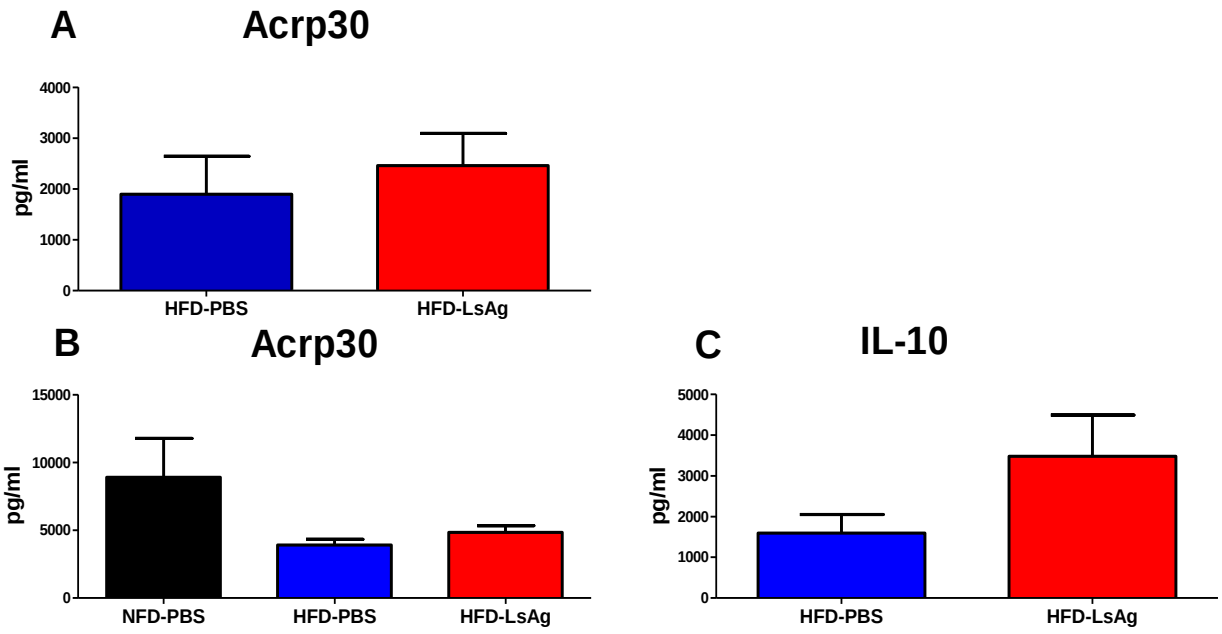

Fig. 38: LsAg treatment increases adiponectin concentration in serum and IL-10 in adipocyte supernatants, respectively. Adiponectin levels in adipose tissue supernatant (**A**) and serum (**B**) as well as IL-10 in adipocyte supernatant (**C**) of animals receiving a chow diet (NFD) and treated with PBS and high-fat diet (HFD) 16 weeks-fed animals that were treated daily for 2 weeks i.p. with LsAg. Results are shown as mean + SEM. Differences were analyzed for statistical significance using by two-tailed non-parametric Mann-Whitney-U-test (**A**, **C**) and Kruskal-Wallis followed by the Dunn's multiple comparison test (**B**). Data shown are pooled from two independent experiments with 6 mice per group.

Therefore, the impact of adipocyte supernatants from LsAg and PBS treated animals on CD4 and CD8 T cell inflammation was further investigated. First splenic CD4+ and CD8+ T cells were stimulated with PMA/ionomycin in the presence of adipocyte conditioned media from PBS-treated HFD mice and LsAg-treated DIO mice to investigate if the conditioned adipocyte media alters T cell cytokine production. Interestingly, adipocyte-conditioned media from LsAg decreased pro-inflammatory CD4+ and CD8+ T cell inflammation based on IFN-γ, TNF- and IL-17-positve CD4+ and CD8+ T cells, reaching statistical differences for CD4+

IFN-γ cultured with LsAg (Fig. 39A), CD4+ TNF+ (Fig. 39B) and CD4+ IL-17+ (Fig. 39C). Frequencies of CD8+ T cells producing IFN-γ (Fig. 39D), TNF (Fig. 39E) and IL-17 (Fig. 39F) were significantly decreased in the presence of LsAg adipocyte-conditioned media compared to HFD PBS-treated adipocyte media.

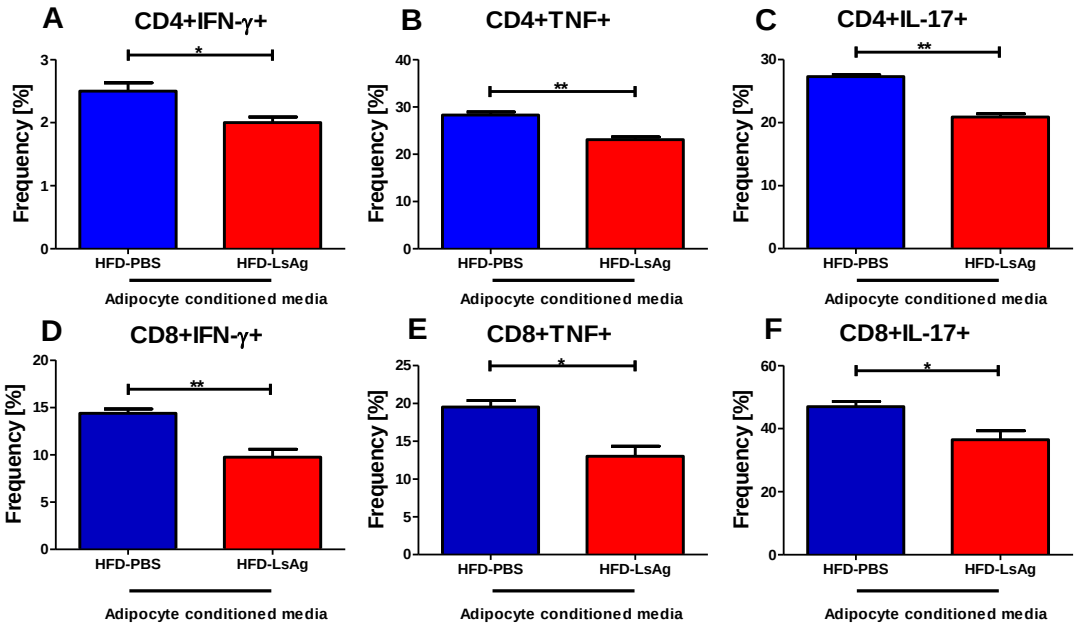

Fig. 39: Adipocyte conditioned media from LsAg treated mice reduces CD4+ and CD8+ T cell inflammation *in vitro*. Splenic CD4+ T cells and CD8+ T cells from HFD mice cultured in the presence of adipocyte conditioned media from mice treated with PBS and high-fat diet (HFD) fed animals for 16 weeks that were treated daily for 2 weeks intraperitoneal with PBS or LsAg. Frequencies of IFN-γ+ (**A**), TNF+ (**B**) and IL-17+ $CD4^+$ T cells (**C**) as well as frequencies of CD8+ T cells IFN-γ+ (**D**), TNF+ (**E**), IL-17+(**F**). Results are shown as median. Differences were analyzed for statistical significance using Kruskal-Wallis followed by the Dunn's multiple comparison test .*$p<0.05$, **$p<0.01$. Data shown are pooled from two independent experiments with 3 mice per group.

Thus, LsAg conditioned adipocyte media showed marked anti-inflammatory properties and elevated levels of Acrp30 in serum and IL-10 in adipocytes, which correlated with decreases in the frequency of CD4+ and CD8+ T cells producing IFN-γ, TNF and IL-17.

Subsequent experiments were performed by Jayagopi Surendar from our group and revealed that induction of IFNγ+ and IL-17+ T cells is inhibited by adiponectin (Surendar, Frohberger et al., manuscript submitted).

4. Discussion

In this thesis protective immune responses against the filarial nematode *L. sigmodontis* and the impact of filariae-derived products on diet-induced insulin resistance were analysed. In the first part of the thesis the type 2 cytokine pathways of IL-4 and IL-5 as well as eosinophils were directly compared for their impact on *L. sigmodontis* infection in susceptible BALB/c mice.

4.1 Role of IL-4R, IL-5, IL-4R/IL-5 and eosinophils during *L. sigmodontis* infection

L. sigmodontis infection was compared in mice deficient for IL-4R, IL-5, IL-4R/IL-5 and eosinophils. Since IL-4R is essential for the development of AAMs and IL-5 for eosinophil differentiation and survival, parasitological results were correlated with those two cell types [182]. Several studies have confirmed a crucial role for IL-4, IL-4R and IL-5 during *L. sigmodontis* infection and that the absence of IL-4 signaling resulted in increased MF levels and extended microfilaremia in BALB/c mice. Furthermore, the lack of IL-5 led to an increased worm burden and an enhanced worm survival [183]. In addition, it has been shown that *L. sigmodontis* infection triggers an eosinophilia, which contributes to adult worm clearance [182, 213]. Results of this study demonstrate that *L. sigmodontis*-infected immune-compromised mice (IL-4R$^{-/-}$, IL-5$^{-/-}$, IL-4R$^{-/-}$/IL-5$^{-/-}$) exhibited increased and extended microfilaremia compared to corresponding WT animals and confirmed previous studies [183, 199, 214]. Our findings further demonstrate that the absence of IL-5 and eosinophils, rather than IL-4R impair essential immune responses, leading to increasing MF levels. Highest MF loads were observed in IL-4R$^{-/-}$/IL-5$^{-/-}$ mice. The MF load in mice lacking eosinophilia (IL-5$^{-/-}$, IL-4R$^{-/-}$/IL-5$^{-/-}$, dblGATA) were increased and sustained for an extended period of time, which was associated with a prolonged adult worm survival and therefore, probably an extended period of MF release. Absence of eosinophils (dblGATA), IL-4R and IL-4R/IL-5 led to an increased microfilaremia in 100% of the tested animals.

Interestingly, IL-5 deficient mice did not exhibit such increased patency compared to WT controls, indicating a divergent phenotype between dblGATA and IL-5$^{-/-}$ mice. Besides, correlation analysis between thoracic cavity eosinophils and adult worm burden at 71dpi revealed a strong negative correlation, confirming previous results for the essential protective role of eosinophils during filariasis [182, 213]. Such an interrelation between extended adult worm survival and prolonged microfilaremia was shown by Volkmann *et al*. for *L. sigmodontis*-infected IL-5 deficient mice [183]. Injected MF led to a comparable clearance in WT, IL-4 and IL-4R deficient mice, whereas survival in IL-5 lacking mice was extended [183]. Previous studies showed that the spleen is essentially involved in the MF clearance and future studies should therefore investigate the impact of the spleen in IL-5 deficient and dblGATA mice in the clearance of MF [174, 215]. On the other hand, all the knockout mouse strains used in this study exhibited enlarged spleens compared to WT controls, which were associated with increased MF levels and extended MF survival in the immune-deficient mice over time. Our results further suggest, that the elevated MF production is due to the enhanced fertility in the female worms residing in knockout mice (dblGATA, IL-5$^{-/-}$, IL-4R$^{-/-}$/IL-5$^{-/-}$), revealing elevated numbers of eggs, morulaes, pretzels and MF. Interestingly, the onset of microfilaremia was observed earlier in IL-4R$^{-/-}$ mice, whereas eosinophil deficient dblGATA and IL-5$^{-/-}$ mice had a comparable onset of microfilaremia compared to WT mice. However, another study demonstrated, that helminth development is dependent on immunological pressure and therefore the absence of essential immunological factors such as IL-5, impairs worm development [216].

Female worm lengths in all immune-deficient mice were significantly increased during chronic *L. sigmodontis* infection at 71dpi, whereas differences in worm length were not observed at 119dpi, demonstrating an accelerated filarial development and embryogenesis by

an increased number of eggs, morulaes, pretzels and MF's in the absence of IL-4R, IL-5 and eosinophils.

Another report has shown contrary results, suggesting that the *L. sigmodontis* larvae development into the L4 stage is delayed in the absence of IL-5. Therefore, co-administration of recombinant IL-5 with L3 inoculation abrogated this impaired larvae development leading again to an earlier onset of microfilaremia and an increased MF load. [216].

The underlying reason behind these diverse results may be the host background, since we used susceptible BALB/c mice, whereas semi-resistant C57BL/6 mice were used in the Babayan study. In addition, different infection time points were analysed. Therefore, future studies should focus on the extent host background and exposure time to eosinophils/IL-5, which may affect *L. sigmodontis* development.

IL-4R is essential for the development and expansion of AAMs in the thoracic cavity of *L. sigmodontis*-infected mice [200] and lack of AAMs in IL-4R$^{-/-}$ and IL-4R$^{-/-}$/IL-5$^{-/-}$ resulted in a reduced total number of thoracic cavity macrophages. A negative correlation was observed between thoracic cavity AAM numbers and the MF load at 71dpi and AAMs were associated with a delayed onset of microfilaremia. Th2 cytokines (IL-4, IL-5, IL-13) within the thoracic cavity did neither correlate with the adult worm burden nor MF counts. Solely IL-6 negatively correlated with the MF counts on 71dpi.

Recently, a protective role of IL-6 against invading L3 larvae was shown, which resulted in an increased adult worm burden at early time points of infection in IL-6 deficient mice [217]**.** However, after the molting into adult worms, the worm burden and MF loads did not differ between IL-6 deficient and corresponding WT mice any longer, indicating no direct impact of IL-6 on MF loads.

Increased IFN-γ levels were observed during the chronic and late phase of *L. sigmodontis* infection in all tested immune-compromised mice, suggesting that either increased MF loads

trigger type 1 immune responses or lack of a part of the type 2 immune responses drives IFN-γ responses. In regard to the induction of IFN-γ responses by MF, Hübner *et al*. showed that IFN-γ responses were increased after the injections of MF into naïve animals [218]. IFN-γ levels may contribute to adult worm clearance, which is supported by a study analysing IFN-γ deficient mice, which exhibited an impaired neutrophil-mediated removal of *L. sigmodontis* adult worms and increased MF levels [219]. Furthermore, neutrophil numbers within the spleen correlated positively with the adult worm burden and MF load.

In summary, findings of this project indicate that the combined lack of eosinophils and AAMs in IL-4R$^{-/-}$/IL-5$^{-/-}$ increased susceptibility for *L. sigmodontis* infection, which led to an earlier onset of microfilaremia, development of microfilaremia in 100% of the tested animals, highest MF loads and an extended adult worm survival.

Considering these data, IL-4R$^{-/-}$/IL-5$^{-/-}$ mice may be used for infections with human pathogenic filariae due to their high susceptibility. Accordingly, Tendongfor *et al*. showed that the human pathogenic filariae *Loa loa* survived up to 70 days after L3 inoculation in IL-4R$^{-/-}$/IL-5$^{-/-}$ mice and completed molting into immature adult worms [220]. Furthermore, IL-4R$^{-/-}$/IL-5$^{-/-}$ mice may represent an interesting animal model for the screening of potential macrofilaricidal and microfilaricidal drug candidates. They possess an extended adult worm survival and increased microfilaremia which allows the identification of slow acting active compounds against adult worms or MF, during the onset of microfilaremia or before the development of microfilaremia as a prophylactic treatment. Furthermore, lack of eosinophils and AAMs allows the investigation of potential interactions between these cell types and drug candidates or the requirement of an intact host immune system.

4.2 Anti-inflammatory properties of S100A8/A9 during *L. sigmodontis* infection

Parasitic filarial nematodes modulate the host immune system to their benefit to evade specific immune responses during early and chronic phases of infection and therefore, enhance parasite maintenance and survival within the host. Several studies confirmed inflammatory [132] and anti-inflammatory properties [149] of S100 calgranulin proteins. However, little is known about their role during filarial infection. S100A8/A9 was shown to be abundant in almost 20% of murine neutrophil granula and 45% of human neutrophil granula [221], exhibiting chemotactic properties on neutrophils [222]. Since an increased expression of S100A8/A9 within the lung was found during *L. sigmodontis* L3 larvae migration [131], the impact of S100A8/A9 on neutrophils and on *L. sigmodontis* infection was investigated.

During the migration of invading infective L3 larvae an increased inflammatory response within the thoracic cavity and BAL was observed in S100A8/A9$^{-/-}$ mice, which was furthermore associated with an increased neutrophil activation in S100A8/A9$^{-/-}$ animals. Karadijan and colleagues revealed a pulmonary phase during *L. sigmodontis* L3 migration in susceptible WT BALB/c mice, which was characterized by increased lung pathology, resulting in inflamed endothelium and parenchyma as well as an elevated number of neutrophils and elevated expression of S100A8/S100A9 [131]. Similar results were observed in C57BL/6 WT mice that were used as control for the S100A8/A9$^{-/-}$ mice in this thesis. Analysis of the worm burden revealed a significantly decreased worm burden in S100A8/A9$^{-/-}$ animals compared to WT controls following natural and subcutaneous infection, which was further associated with a higher chemokine production, granulocyte recruitment and neutrophil activation in the BAL as well as chemokine production in the thoracic cavity lavage.

The previously described data indicate that S100A8/A9 dampens transient pulmonary inflammation, caused by the migration of infective *L. sigmodontis* L3 larvae. Various studies confirmed multifunctional properties of S100A8 and S100A9, which may differ depending on the inflammatory milieu. Calprotectin interacts with TLR4, which represents one of the main receptors for S100A8/S100A9 [135, 136, 223, 224] and is expressed on various innate immune cells. A recent study showed that TLR4$^{-/-}$ animals exhibited no differences in the adult *L. sigmodontis* adult worm and MF burden compared to WT controls [225]. However, the deficiency of TLR4 led to an increased frequency of MF positive animals compared to WT controls. It is possible that S100A8/A9 may interact with RAGE during *L. sigmodontis* infection, leading to a different phenotype as was observed in TLR4$^{-/-}$ animals [225]. Whether RAGE deficient mice have a similar phenotype as S100A8/A9$^{-/-}$ animals should be part of future analysis, since RAGE represents another main receptor for S100A8/A9.

In contrast to previous studies, which demonstrated a S100A8 and S100A9 involvement in the recruitment of murine and human phagocytes to the site of inflammation, S100A8/A9$^{-/-}$ mice revealed increased frequencies of neutrophils within the bronchoalveolar lavage upon *L. sigmodontis* infection. This was associated with increased concentrations of CXCL-1, CXCL-2, CXCL-5, and elastase in the thoracic cavity and bronchoalveolar lavage of S100A8/A9$^{-/-}$ indicating that S100A8/A9 may exhibit anti-inflammatory properties during filarial infection. Therefore, those results are in contrast to previous studies showing a neutrophil-recruiting feature of S100A8 and S100A9 and that the injection of S100A8 into the mouse foot pad leads to an increase of neutrophils within the first 4-6 hours, followed by monocytes over 24 hours [226]. However, potential anti-inflammatory properties of calprotectin are supported by a murine experimental colitis model, where calprotectin given by the intrarectal route led to less tissue damage, decreased MPO activity as well as TNF production [149].

Numerous studies have confirmed protective features of neutrophils during fungal, bacterial and helminth infections by phagocytosis, generation of reactive oxygen species (ROS) [138], degranulation and formation of NETs [150]. Similarly, our group showed that impaired neutrophil recruitment during *L. sigmodontis* infection in NOD2$^{-/-}$ mice results in reduced inflammatory immune responses within the skin and therefore facilitates L3 migration and leads to an increased worm burden [227]. In contrast to these results, the findings described in this thesis demonstrate a novel protective role of S100A8/A9$^{-/-}$ neutrophils during the pulmonary migration of *L. sigmodontis* L3 larvae, since circumventing the skin barrier by s.c. infection of *L. sigmodontis* L3 larvae led to a similar decreased worm burden in S100A8/A9$^{-/-}$ mice. Depletion of pulmonary neutrophils of S100A8/A9$^{-/-}$ animals during the migratory phase of *L. sigmodontis* (2-6 dpi) on the other hand abrogated the observed protective effect and resulted in an increased worm burden compared to isotype-treated S100A8/A9$^{-/-}$ and WT mice.

Bone-marrow-derived neutrophils of S100A8/A9$^{-/-}$ mice exhibited an increased *ex vivo* and *in vitro* activation, which contributed to an inflammatory milieu and may support the elimination of infective L3 larvae in the lung. Furthermore, the increased neutrophil activation observed in S100A8/A9$^{-/-}$ mice was associated with an increased apoptosis, which could explain the elevated levels of S100A8/A9 in the BAL during *L. sigmodontis* infection [131]. L3 larval motility was significantly inhibited in the presence of S100A8/A9$^{-/-}$ neutrophils compared to WT neutrophils in a DNA and NET formation dependent manner. Additional factors such as granula proteins (cathepsin G, proteinase 3) or enzymes like MPO, elastase, may be involved in the parasite motility inhibition as well. Collectively, these results demonstrate a pulmonary role of S100A8/A9 that dampens inflammatory responses within the lung caused by the migration of L3 larvae, decreasing granulocyte recruitment, chemokine production as well as neutrophil activation *ex vivo* and *in vitro* and therefore facilitating larval migration.

In summary, mice deficient for calprotectin exhibited a significantly reduced *L. sigmodontis* worm burden compared to WT controls, which vanished and led to an increased worm burden, during the depletion of neutrophils from S100A8/A9$^{-/-}$ mice within the lung prior to *L. sigmodontis* infection until 5dpi. Considering these findings, S100A8/A9 should be investigated in human pathogenic nematodes such as *Necator americanus*, *Ancylostoma duodenale* [228], *Strongyloides stercoralis* [229], and *Ascaris lumbricoides* [230], which all share a common passage through the pulmonary vasculature and respiratory epithelium [231]. Therefore, infection with *Nippostrongylus brasiliensis*, which represents a model for human hookworm infection in S100A8/A9$^{-/-}$ mice could lead to new insights and understanding of protective immune responses during the lung stage of infection [232-234].

4.3 Role of Aryl hydrocarbon receptor during *L. sigmodontis* infection

AhR, a member of the PRRs, is highly expressed on mature immune cells at barrier sites such as lung, liver, gut [154] and skin [152, 153]. The receptor represents an essential component of the immune system for the recognition of external danger signals and orchestrates specific immune responses against invading pathogens. Ajendra and colleagues showed that the absence of another prominent member of the PRR family, the nucleotide-binding and oligomerization domain-containing protein 2 (NOD2)-like receptors (NLRs), led to an impaired neutrophil recruitment within the skin and to an increased worm burden during the early phase of *L. sigmodontis* infection [227]. However, still less is known about the role of AhR during filarial infections. Therefore, the impact of AhR which is highly expressed within the skin, a barrier traversed by infective L3 larvae, on *L. sigmodontis* infection was investigated.

Immune responses within the skin in dependence of AhR were analyzed by i.d. injections of crude adult worm extract (LsAg) in $AhR^{-/-}$ and WT animals. Three hours post LsAg injection total cell counts as well as total numbers of macrophages, neutrophils and eosinophils within the skin of $AhR^{-/-}$ mice were significantly lower and less activated (CD86 ↓ on monocytes, MHCII ↓ on macrophages, CD69 ↓ on neutrophils) compared to WT LsAg treated animals. As described by Ajendra *et al*. [227] the decreased frequencies of macrophages and eosinophils may be due to the impaired recruitment of neutrophils, since neutrophils represent the first cell type to encounter invading pathogens and play a major key role during the recruitment of other effector cells to the site of infection [227]. Several studies confirmed such an essential key role of neutrophils as the first line of defense against invading larval stages from several helminth species, revealing a crucial role in the parasite's elimination against *Strongyloides stercoarlis* [235] or *Trichinella spiralis* [236] as well as against *Schistosoma mansoni* [237]. Neutrophils have been further shown to contribute to the

formation of inflammatory nodules around adult filariae and therefore accelerate parasite elimination [238].

The AhR has also been shown to be expressed in Langerhans [239, 240] and dendritic cells [241], which may additionally have a crucial impact on the cell recruitment, especially on neutrophils. Nevertheless, these assumptions are contrary to a study performed by Cotton *et al.* where no essential involvement of Langerhans and DCs during the migration of *B. malayi* L3 larvae was observed [242]. They failed to be activated by the invading larvae, indicating that DCs and Langerhans cells may also not be essential or crucial for the elimination of infective *L. sigmodontis* L3 larvae.

Interestingly, our results further indicate that deficiency of AhR also impairs immune responses at the site of infection, the pleural cavity. Frequencies of CD4+ T cells and neutrophils were significantly decreased in the pleural cavity at 5 and 14 days post *L. sigmodontis* infection. Al-Quaoud and colleagues demonstrated a role of CD4+ T cells in the controlling of larval *L. sigmodontis* development, whereupon depletion of CD4+ T cells from infected BALB/c mice led to an increased worm and microfilarial burden compared to infected controls [181].

In addition, eosinophilia was diminished in the absence of CD4+ T cells-depleted animals. Eosinophils, which have been shown in several helminth studies to contribute to worm clearance during chronic infections, were decreased at 14dpi within the pleural cavity lavage. Results from this thesis and previous studies demonstrated that the absence of eosinophils for instance in dblGATA or IL-5 deficient mice [216] resulted in an increased *L. sigmodontis* worm burden, indicating that adult worms have an survival benefit in $AhR^{-/-}$ mice.

Another prominent chemokine and prominent indicator for inflammation and autoimmune diseases (rheumatoid arthritis, systemic lupus rythematosus, sjogren syndrome, systemic sclerosis) is CXCL-10 [243]. CXCL-10, also known as IP-10, was present at increased

concentrations within the thoracic cavity lavage at 5 and 14 days post *L. sigmodontis* infection in AhR$^{-/-}$ mice. CXCL-10 has been described to play an important role during the chemoattraction of other effector cells such as macrophages [244-247], which may explain the increased frequency of macrophages within the thoracic cavity during both time points in AhR$^{-/-}$ animals compared to WT controls.

AhR deficiency and the increased worm burden in AhR$^{-/-}$ mice may also be associated with an increased vascular permeability, as such an increased vascular permeability was previously shown to lead to an increased worm recovery in CCL17 deficient mice [248].

Next to the impaired immune response in the skin and the thoracic cavity, AhR deficiency was indeed associated with an increased vascular permeability, which may facilitate L3 migration and therefore, leading to an increased worm recovery in AhR$^{-/-}$ mice [248]. Accordingly, decreased levels of CCL17 at 14dpi within the thoracic cavity and at 5dpi within the bronchoalveolar lavage were observed in AhR$^{-/-}$ mice. To confirm that changes in the vascular permeability are responsible for the increased worm burden in AhR$^{-/-}$ mice, additional analysis of mast cells should be included in future experiments. Mast cell degranulation and release of histamine may be the responsible mediators for the enhanced vascular permeability, which facilitates *L. sigmodontis* larval migration within the host. Inhibition experiments for mast cell degranulation for instance with cromolyn or histamine blockade could be performed to address the impact of mast cell degranulation and histamine release as it is the responsible factor for the increased vascular permeability and worm recovery in CCL17 deficient mice [248].

Taken together, these findings demonstrate that the absence of AhR impairs several potential protective immune responses against *L. sigmodontis*. It impairs immune responses within the skin, enhances vascular permeabilization which possibly facilites the migration of infective L3 *L. sigmodontis* larvae and finally reduces protective immune responses in the thoracic

cavity, resulting overall in a significantly increased worm burden in $AhR^{-/-}$ mice compared to WT animals.

While several studies confirmed an essential antimicrobial role of AhR [165-169], results shown in this thesis demonstrate a novel role of AhR-mediated protective immune responses against the filarial nematode *L. sigmodontis*. Considering the fact that AhR is highly expressed in several tissues such as skin [152, 153], lung, liver, and gut [154] and $AhR^{-/-}$ mice lack intraepithelial lymphocytes as well as intestinal innate lymphoid cells within several barrier organs [170], next approaches may include the investigations of AhR during infections with intestinal helminths or species characterized by a lung passage during their migration phase. Therefore, the role of AhR in the gut may be investigated via murine infection with the gastrointestinal nematode *Heligosomoides polygyrus*, since this helminth does not pass the lung in its migration phase [249]. Findings may improve our understanding and the potential involvement of AhR in the initiation of protective immune responses against diverse helminths species with different routes of infection. New insights could lead to new therapeutic approaches against human helminth parasites, such as *Ascaris lumbricoides* (roundworm), *Trichiuris trichiuria* (whipworm), *Ancylostoma duodenale*, and *Necator americanicus* (hookworms) [250].

4.4 LsAg dampens T cell inflammation and improves glucose tolerance in diet-induced obese mice

Due to the immunomodulatory capacity of helminths, recent studies showed that helminth infections or the repeated administration of crude adult worm extracts (LsAg) improve obesity-induced insulin resistance [117, 118]. Berbudi and colleagues revealed that LsAg treatment in 14 weeks HFD fed mice alleviated obesity-associated inflammatory immune responses and improved glucose tolerance [118]. Despite these findings less is known about the protective mechanisms of helminth-derived immunomodulatory molecules on DIO.

In this thesis, repeated administrations of LsAg were tested for their potential to lessen DIO induced pro-inflammatory T cell responses and their impact to improve glucose tolerance. As expected, the body weight of mice, which received HFD for 12-16 weeks were increased compared to corresponding NFD mice. HFD impaired glucose tolerance and insulin sensitivity compared to lean controls and repeated i.p. administrations of LsAg improved glucose tolerance, confirming previous results with LsAg [118]. No improvement of insulin sensitivity in DIO mice was observed after LsAg treatment. Interestingly, DIO mice which were treated s.c. either with LsAg did not show any improvement on glucose tolerance, indicating that a potential depot effect in the s.c. tissue, in which LsAg may be slowly released and elicit a prolonged efficacy, has no beneficial effect. Similar results were observed in another study using non-obese diabetic (NOD) mice, which spontaneously develop T1D. Similarly, s.c. administrations of ES-62-derived SMAs had no beneficial impact in reducing the incidence of T1D onset in NOD mice [251].

In contrast, DBA/1 mice treated s.c. with ES-62 were protected from arthritis in the collagen-induced arthritis model, which were characterized by a reduced articular score as well as inflammatory cell infriltration, cartilage and bone destruction [125].

These studies demonstrate the complexity of filarial extracts such as ES-62 and SMAs targeting multiple potential targets within the immune system [26, 252, 253] and that these multifunctional roles of helminth-derived products and SMAs may differ depending on the inflammatory milieu.

Furthermore, elevated levels of cholesterol, triglycerides and LDLs were observed in HFD mice in comparison to lean individuals, confirming that obesity is associated with an increased lipid accumulation. Repeated administration of LsAg had no statistically significant impact on the lipid profile, indicating that LsAg treatments improve glucose tolerance without altering lipogenesis and adiposity.

Previous studies have shown that obesity is characterized by T cell inflammation [107-109] and that helminth infections or helminth-derived products alleviate adipose tissue inflammation by inducing type 2 immune responses [118]. Nevertheless, not much is known about their impact on DIO T cell inflammation. As expected, obesity increased the frequencies of IFN-γ+ and IL-17+ T cells in adipose tissue from DIO mice compared to NFD mice, which is in accordance with the study of Winer *et al*., revealing elevated frequencies of IFN-γ+ CD4+ T cells in adipose tissue and IL-17+ CD4+T cells in spleen during obesity [110]. Observed elevated frequencies of adipose tissue TNF+ CD4+ T cells, IFN-γ+ CD8+ T cells, TNF+ CD8+ T cells and IL-17+ CD8+ T cells in our study are in contrast to the results from Winer *et al.* [110]. Divergences may be due to differences in the duration of the administered HFD treatment, as in our project animals received a prolonged HFD (16 weeks) compared to the study performed by Winer and colleagues (8 weeks).

Repeated LsAg administration in DIO mice decreased the frequency of TNF+, IFN-γ+ and IL-17+ adipose tissue CD4+ T cells and TNF+ as well as IL-17+ CD8+ T cells compared to HFD PBS-treated mice. Thus, repeated administrations of LsAg reduced obesity-associated T cell inflammation within the adipose tisse during the onset of obesity. However, whether pro-

inflammatory CD8+ T cells are indeed contributing to local adipose tissue inflammation during obesity is still controversally discussed. Nishimura *et al*. demonstrated that adipose tissue inflammation and insulin resistance is improved in CD8+ T cell deficient mice and following CD8 antibody depletion [107]. However, another report showed that the transfer of CD8+ T cells into T cell deficient RAG1, which received HFD, do not contribute or worsen adipose tissue inflammation [110]. Thus, additional studies are required to investigate, whether CD8+ T cells contribute to adipose tissue inflammamtion and insulin resistance and whether the reduction of those pro-inflammatory CD8 T cells by helminth product treatment is mediating the observed improvement in glucose tolerance.

In regard to the mechanisms by which obesity-induced CD4 and CD8 T cell inflammation is inhibited by helminth products, the impact of Acrp30, an essential mediator of metabolic homeostasis in adipose tissue was investigated. Acrp30 represents a protein hormone, which is produced by adipocytes and circulates in the bloodstream. It has been shown to be involved in numerous pathways and modulates metabolic processes, such as glucose regulation and fatty acid oxidation [126, 127].

A recent report demonstrated that Acrp30 in combination with leptin reverses insulin resistance in mice [128]. Further studies have also shown an inverse correlation between obesity and Acrp30 concentrations [127, 129, 130]. Acrp30 levels within the serum of LsAg-treated HFD animals were increased compared to PBS-treated HFD controls. Although the difference did not reach statisctical significance in this thesis, subsequent experiments that were performed by Dr. Surendar confirmed an increased adiponectin concentration in serum and adipocyte supernatant of LsAg treated animals and demonstrated that the inhibition of Th1 and Th17 cells is mediated via adiponectin (Surendar, Frohberger et al., manuscript submitted). Furthermore, results from this thesis indicate that repeated administration of LsAg increased IL-10 concentrations within the adipocyte supernatant, which may contribute to the

counter regulation of adipose tissue inflammation. For that reason future experiments should include neutralisation experiments to investigate and to verifiy, if the observed protective effect caused by LsAg may be also dependent on IL-10.

Data shown in this thesis indicate that LsAg improve glucose tolerance and counterregulate DIO adipocyte T cell inflammation highlighting that LsAg or filarial extracts contain new promising candidates that should be further persued to target obesity induced glucose intolerance and adipose tissue inflammation. Various human studies indicate that helminth infections may improve insulin sensitivity in humans. Nevertheless, the investigations of the underlying beneficial mechanisms of helminth infections using animal models are still rare [115, 116, 254, 255] and the contribution of helminth-derived molecules is not completely understood. Next experiments should further concentrate on the impact on metabolic changes in the liver and energy metabolism including pancreatic β-cell function, glucose uptake into muscle cells, insulin resistance of target organs, glucose formation in the liver, release of fatty acids in adipose tissue as well as detection of insulin in the brain.

Complimentary projects

Identification of macrofilaricidal substances

The elimination of onchocerciasis (river blindness) [44] and lymphatic filariasis (elephantiasis) [8] is hampered by the lack of macrofilaricidal drugs. Current programs rely on the microfilaricidal drugs DEC, IVM and ALB, which require an annual to bi-annual treatment for the reproductive life span of the female adult worms and harbour the risk to cause severe adverse events in *Loa loa* patients [8, 35]. *Wolbachia,* an essential bacterial endosymbiont of nematodes have been successful validated as new promising target for anti-filarial therapy [60, 78, 79, 82].

Within a collaboration of industry, non-profit organizations (Drugs for Neglected Disease initiative and Bill & Melinda Gates Foundation) as well as partners from Universities, new macrofilaricidal drug candidates were identified. As part of my PhD thesis I was involved in the efficacy testing of the clinical candidates AWZ1066 (LSTM, EISAI), ABBV-4083 (Abbvie), AN11251 (Anacor), CBR417 and CBR490 (Calibr) in the *L. sigmodontis* rodent model.

Complimentary project A- AWZ1066S, a highly specific anti-*Wolbachia* drug candidate for a short-course treatment of filariasis

W. David Hong, Farid Benayoud, Gemma L. Nixon, Louise Ford, Kelly L. Johnston, Rachel H. Clare, Andrew Cassidy, Darren A. N. Cook, Amy Siu, Motohiro Shiotani, Peter J. H. Webborn, Stefan Kavanagh, Ghaith Aljayyoussi, Emma Murphy, Andrew Steven, John Archer, Dominique Struever, **Stefan J. Frohberger**, Alexandra Ehrens, Marc P. Hübner, Achim Hoerauf, Adam P. Roberts, Alasdair T. M. Hubbard, Edward W. Tate, Remigiusz A. Serwa, Suet C. Leung, Li Qie, Neil G. Berry, Fabian Gusovsky, Janet Hemingway, Joseph D. Turner,Mark J. Taylorb, Stephen A. Wardb, Paul M. O'Neill. AWZ1066S, a highly specific anti-*Wolbachia* drug candidate for a short-course treatment of filariasis. **Proc Natl Acad Sci U S A. 2019** Jan 22;116(4):1414-1419. doi: 10.1073/pnas.1816585116. Epub 2019 Jan 7.

New screenings identified AWZ1066S as a novel anti-*Wolbachia* candidate against onchocerciasis and lymphatic filariasis. In two independent filarial infection models the efficacy of AWZ1066S was tested with a seven-day oral dosing regimen (100mg/kg), which resulted in a >90% *Wolbachia* depletion in female *B. malayi* infected SCID mice as well as in female *L. sigmodontis* infected gerbils. Similar results were observed *in vitro* for *B. malayi* MF. Longitudinal effects of AWZ1066S on circulating *L. sigmodontis* microfilaremia after 1-18 weeks post treatment further revealed a gradual depletion of MF, suggesting adult inhibition of the filarial embryogenesis and potential sterilization. Results of this study highlight AWZ1066S as promising pre-clinical drug candidate. Therefore, further clinical studies (phase 1-3) are required to confirm its non-toxicity and compatibility in humans.

Complimentary project B- Discovery of ABBV-4083, a novel analog of Tylosin A that has potent anti-*Wolbachia* and anti-filarial activity

Thomas W. von Geldern, Howard Morton, Rick F. Clark, Brian Brown, Kelly L. Johnston, Louise Ford, Sabine Specht, Marc P. Hübner, Robert Carr, Deanne Stolarik, Junli Ma, Matt Rieser, Dominique Struever, **Stefan J. Frohberger**, Marianne Koschel, Alexandra Ehrens, Joseph D. Turner, Achim Hoerauf, Mark J. Taylor, Stephen A. Ward, Kennan Marsh and Dale J. Kempf. Discovery of ABBV-4083, a novel analog of Tylosin A that has potent anti-*Wolbachia* and anti-filarial activity. **PLoS Negl Trop Dis. 2019.** Feb 28;13(2):e0007159. doi: 10.1371/journal.pntd.0007159. eCollection 2019 Feb.

In another separate study chemical modifications that led to an improved metabolic stability of the veterinary antibiotic Tylosin A (TylA) revealed an optimized analogue (ABBV-4083) with improved anti-*Wolbachia* efficacy and oral pharmacokinetic properties. TylA has been shown to elicit similar *in vitro* and *in vivo* activity as doxycycline against *Wolbachia*. However, the poor oral bioavailability posed a big challenge. The efficacy of TylA and the analogue ABBV-4083 was compared and investigated in the *L. sigmodontis* murine animal model. Although, *L. sigmodontis* infected mice treated i.p. with TylA (twice daily 200mg/kg) revealed an impaired worm development, oral treatment of TylA had only minimal efficacy. These results were related to differences in the bioavailability of TylA administered i.p. (>30-fold higher) compared to oral regimens. Promising results were achieved in an *in vivo* experiment with gerbils (*Meriones unguiculatus*) infected with *L. sigmodontis*, which were treated with ABBV-4083 orally (150mg/kg daily for 14 days). *Wolbachia* levels were reduced by >99.9% until 16 weeks post treatment in the recovered female adult worms, which was further accompanied a decline of circulating MF as well as impaired embryogenesis of the remaining female worms (decreased numbers of eggs, pretzels, morulae, MF).Collectively, the modified analog ABBV-4083, which undergoes currently phase 1 clinical evaluation in healthy human volunteers, represents a promising drug candidate for oral regimens for onchocerciasis and/or lymphatic filariasis-infected patients.

Complimentary project C- Boron-Pleuromutilins as anti-*Wolbachia* agents with potential for treatment of onchocerciasis and lymphatic filariasis

Robert T. Jacobs, Christopher S. Lunde, Yvonne R. Freund, Vincent Hernandez, Xianfeng Li, Yi Xia, David S. Carter, Pamela W. Berry, Jason Halladay, Fernando Rock, Rianna Stefanakis, Eric Easom, Jacob J. Plattner, Louise Ford, Kelly L. Johnston, Darren A.N. Cook, Rachel Clare, Andrew Cassidy, Laura Myhill, Hayley Tyrer, Joanne Gamble, Ana F. Guimaraes, Andrew Steven, Franziska Lenz, Alexandra Ehrens, **Stefan J. Frohberger**, Marianne Koschel, Achim Hoerauf, Marc P. Hübner, Case W. McNamara, Malina A. Bakowski, Joseph D. Turner, Mark J. Taylor, Stephen A. Ward. Boron-Pleuromutilins as Anti-*Wolbachia* Agents with Potential for Treatment of Onchocerciasis and Lymphatic Filariasis. **J Med Chem. 2019** Feb 7. doi: 10.1021/acs.jmedchem.8b01854.

Pleuromutilins are natural-product antibiotics (discovered in 1950) which elicit antibacterial efficacy against various pathogens involved in skin and respiratory tract infections. Numerous pleuromutilins were screened, chemically modified and tested for its potency as anti-*Wolbachia* drugs. *In vitro* and *in vivo* experiments in this study demonstrated AN11251 as a potential lead candidate due to its high activity against *Wolbachia* as well as physiochemical and pharmacokinetic characteristics. Performed experiments demonstrated that the treatment with AN11251 (orally 25mg/kg, BID) in *B. malayi* L3-infected SCID mice led to a >99% *Wolbachia* clearance in worms after 14 days of treatment compared to 75.4% in 7 day-treated animals. However, efficacy of AN11251 against adult *B. malayi* worms dosed orally at 25 mg/kg (BID for 7, 14, 28 days) was moderate and not satisfying, as only 45.5% of the *Wolbachia* load was reduced after 28 days of treatment. In contrast, an excellent efficacy of AN11251 was observed in the *L. sigmodontis* BALB/c mouse model (<99% *Wolbachia* depletion) using a higher concentration of 50mg/kg, BID for 14 or 28 days.

In summary, AN11251 fulfills all requirements to proceed into the clinical safety evaluation studies.

Complimentary project D- A single-dose cure for the treatment of lymphatic filariasis and river blindness

Malina A. Bakowski, Reza Kazem-Shiroodi, Renhe Liu, Jason Olejniczak, Baiyuan Yang, Kerstin Gagaring, Pamela M. White, Hui Guo, Laura Chappell, Alain Debec, Frédéric Landmann, Ashley K. Woods, Nicolas Pionnier, Sean B. Joseph, Mitchell Hull, Wen Xiong, Kelli L. Kuhen, Joseph D Turner, Bettina Dubben, Franziska Lenz, Dominique Struever, Alexandra Ehrens, **Stefan J. Frohberger**, Marc P. Hübner, Achim Hoerauf, Jason Roland, Matt S. Tremblay, Peter G. Schultz, William Sullivan, Xin-Jie Chu, H. Michael Petrassi, Case W. McNamara. A single-dose cure for the treatment of lymphatic filariasis and river blindness. **Science Translational Medicine 2019. In Press..**

There is an urgent need for novel screening systems characterized by a high-throughput to identify potent active ingredients for instance against *Wolbachia* in order to accelerate the drug discovery and finally elimination of lymphatic filariasis and onchocerciasis. The goal of the study performed by Bakowski and colleagues was to identify drugs with high anti-*Wolbachia* efficacy and shortened treatment duration (<7 days). New potential compounds would help to overcome general challenges such as impaired infrastructures, which hinder equal and consistent drug distribution. Two quinazoline compounds (CBR417, CBR490) were discovered by novel *ex vivo* (high content imaging screening- Quantification of *Wolbachia* in *Brugia pahangi* filarial ovaries) and *in vivo* screening systems. As expected for anti-*Wolbachia* candidates, CBR417 and CBR490 have been shown to elicit no effect against *Loa loa*. During the study a total number of 300,368 small molecules were screened for potential anti-*Wolbachia* efficacy, which finally led to the identification of various antibiotics (46%), antifungals, antivirals, signal transduction modulators and antineoplastics. CBR417 and CBR490 efficacy was assessed *in vivo* in the murine *L. sigmodontis* model. Animals were treated once a day for a total of 4 days with 60mg/kg. Analysis revealed a *Wolbachia* clearance in adult female worms by 99.96% for CBR417 and 99.80% for CBR490.

Interestingly, even 2 single doses of 100mg/kg of CBR417 and CBR490 (weekly once) and one regimen of 200mg/kg resulted in an excellent *Wolbachia* clearance of >99% in *L. sigmodontis* adult female worms.

Results with CBR417 and CBR490 highlight that it is possible to achieve sufficient *Wolbachia* clearance with a single administration.

Complimentary project E- Macrofilaricidal efficacy of single and repeated oral and subcutaneous doses of flubendazole in *Litomosoides sigmodontis* infected jirds

Marc P. Hübner, Alexandra Ehrens, Marianne Koschel, Bettina Dubben, Franziska Lenz, **Stefan J. Frohberger**, Sabine Specht, Ludo Quirynen, Sophie Lachau-Durand, Fetene Tekle, Benny Baeten, Marc Engelen, Charles D. Mackenzie Achim Hoerauf. Macrofilaricidal efficacy of single and repeated oral and subcutaneous doses of flubendazole in *Litomosoides sigmodontis* infected jirds. **PLoS Negl Trop Dis. 2019** Jan 16;13(1):e0006320. doi: 10.1371/journal.pntd.0006320. eCollection 2019 Jan.

Flubendazole (FBZ), a member of the family benzimidazole, is known as a very potent and broad-spectrum antihelmintic to treat worm infections in domestic and farm animals. Due to its high efficacy against filarial nematodes after s.c. regimen, FBZ represents another promising macrofilaricidal drug candidate for onchocerciasis and lymphatic filariasis. However, if possible drug candidates should be administered as an oral formulation or a single parenteral administration to facilitate therapy implementation in the required communities.

In order to study and improve the efficacy of FBZ, a novel developed bioavailable amorphous solid dispersion (ASD) as oral formulation of FBZ was investigated in the *L. sigmodontis* jird model. Chronically infected MF positive animals were treated by different oral and s.c. FBZ regimens (Oral: single 40mg/kg, repeated 2, 6 or 15mg/kg for 5 or 10 days) (S.c. single injection 2 or 10mg/kg) compared to infected untreated controls. The study demonstrated that s.c. administered FBZ was slowly released from the injection site and remained longer within the host compared to oral doses, which was characterized by a rapidly absorption and clearance of FBZ. S.c. FBZ-treated animals (1x or 5x10mg/kg) resulted in a complete adult worm clearance, whereas 10x15mg/kg oral FBZ reduced the adult worm burden by 95% and 1x40mg/kg and 5x15mg/kg by 85% and 84%, respectively. Interestingly, microfilaremia was completely cleared in all s.c. FBZ administered animals (100%) compared to oral FBZ treated

(10x15mg/kg, 1x40mg/kg, 5x15mg/kg) jirds (90%) in a dose and duration dependent manner, suggesting an excellent macrofilaricidal efficacy of FBZ. Oral treatment was furthermore associated with the inhibition of embryogenesis of remaining female adult worms, which was also confirmed by histopathological analysis illustrating irreversible damage of the female uteri and uterine components.

Taken together, these results indicate oral and s.c. administered FBZ as a potent macrofilaricidal candidate, which impairs filarial embryogenesis and therefore, the release of MF.

Complimentary project F- Filarial extract of *Litomosoides sigmodontis* induces a type 2 immune response and attenuates plaque development in hyperlipidemic ApoE-knockout mice

Constanze Kuehn, Miyuki Tauchi, Roman Furtmair, Katharina Urschel, Dorette Raaz-Schrauder, Anna-Lena Neumann, **Stefan J. Frohberger**, Achim Hoerauf, Susanne Regus, Werner Lang, Atilla Sagban Tolga, Stephan Achenbach, Marc P Hübner, Barbara· Dietel. Filarial extract of *Litomosoides sigmodontis* modulates the Th1/Th2 ratio and attenuates plaque development in hyperlipidemic ApoE-knockout mice. **The FASEB Journal. 2019**. Feb 26:fj201800947RR. doi: 10.1096/fj.201800947RR.

Atherosclerosis represents a predominant metabolic progressive disease in which arteries narrow due to the build-up of plaque. Plaques are formed by the accumulation of cholesterol, further lipids and inflammatory cells (Th1 cells, macrophages). Severe course of disease may results in stroke, peripheral or coronary artery disease and kidney problems. The aim of the study was to investigate the immunomodulatory capacity of *L. sigmodontis* adult worm extract (LsAg) in a mouse model of atherosclerosis with focus on plaque progression and vascular inflammation. Such a beneficial effect by helminth infections and helminth-derived products has been shown in various autoimmune diseases and inflammatory conditions.

For the preventive model of initital atherosclerosis, six week-old male ApoE$^{-/-}$ mice were fed a high-fat Western-type diet for 12 weeks and from week 5 to 12 animals were i.p. treated at weekly intervals with PBS or LsAg (50µg per injection). A second batch of mice (therapeutic model) received high-fat diet for 12 weeks followed by additional 12 weeks on a regular chow diet as well as weekly LsAg administration (50µg). Repeated LsAg administration delayed plaque progression (size ↓) in ApoE$^{-/-}$ mice (therapeutic + preventive approach), which was associated with a shift towards a type 2 immune response. LsAg treatment further reduced the number of inflammatory cells (classically activated macrophages) and cytokines (IL-18 ↓, IL-2 ↓, IFN-γ ↓). This was further accompanied with an increased number of regulatory AAMs,

Foxp3-expressing regulatory T cells, and elevated levels of TGF-β within the plaque deposits as well as eosinophils and AAMs within the peritoneum.

With respect to immunological changes within the spleen, repeated LsAg administration reduced the expression of CTLA-4, IL-12 and TNF and decreased levels of Eotaxin, MCP-1 and MCP-3 within the serum in ApoE$^{-/-}$ mice, which confirmed the immunomodulatory properties of LsAg. Moreover, it was shown that LsAg reduced *in vitro* monocyte adhesion to a human endothelial cell monolayer due to the inhibition of JNK1/2 pathway, which represents an essential inflammatory signaling during atherosclerosis.

Results of this study indicate that LsAg represents an effective experimental therapy against atherosclerosis due to its immunomodulatory capacities.

References

1. Zelmer DA: An evolutionary definition of parasitism. International journal for parasitology 1998, 28(3):531-533.
2. Dobson A, Lafferty KD, Kuris AM, Hechinger RF, Jetz W: Colloquium paper: homage to Linnaeus: how many parasites? How many hosts? Proceedings of the National Academy of Sciences of the United States of America 2008, 105 Suppl 1:11482-11489.
3. Reed TE, Daunt F, Hall ME, Phillips RA, Wanless S, Cunningham EJ: Parasite treatment affects maternal investment in sons. Science 2008, 321(5896):1681-1682.
4. Martin LB, 2nd, Scheuerlein A, Wikelski M: Immune activity elevates energy expenditure of house sparrows: a link between direct and indirect costs? Proc Biol Sci 2003, 270(1511):153-158.
5. Smyth KN, Greene LK, Clutton-Brock T, Drea CM: Androgens predict parasitism in female meerkats: a new perspective on a classic trade-off. Biol Lett 2016, 12(10).
6. McElroy EJ, de Buron I: Host performance as a target of manipulation by parasites: a meta-analysis. J Parasitol 2014, 100(4):399-410.
7. Binning SA, Shaw AK, Roche DG: Parasites and Host Performance: Incorporating Infection into Our Understanding of Animal Movement. Integr Comp Biol 2017, 57(2):267-280.
8. Taylor MJ, Hoerauf A, Bockarie M: Lymphatic filariasis and onchocerciasis. Lancet (London, England) 2010, 376(9747):1175-1185.
9. Hoerauf A, Fleischer B, Walter RD: Of filariasis, mice and men. Trends Parasitol 2001, 17(1):4-5.

10. HM P: Foreword. In Lorenzen,S. (ed.), The Phylogenetic Systematics of Free-Living Nematodes. . 1994, The Ray Society, London.: pp. i–ii.

11. Schar F, Inpankaew T, Traub RJ, Khieu V, Dalsgaard A, Chimnoi W, Chhoun C, Sok D, Marti H, Muth S et al: The prevalence and diversity of intestinal parasitic infections in humans and domestic animals in a rural Cambodian village. Parasitol Int 2014, 63(4):597-603.

12. Savioli L, Stansfield S, Bundy DA, Mitchell A, Bhatia R, Engels D, Montresor A, Neira M, Shein AM: Schistosomiasis and soil-transmitted helminth infections: forging control efforts. Trans R Soc Trop Med Hyg 2002, 96(6):577-579.

13. Lefoulon E, Bain O, Bourret J, Junker K, Guerrero R, Canizales I, Kuzmin Y, Satoto TB, Cardenas-Callirgos JM, de Souza Lima S et al: Shaking the Tree: Multi-locus Sequence Typing Usurps Current Onchocercid (Filarial Nematode) Phylogeny. PLoS neglected tropical diseases 2015, 9(11):e0004233.

14. Bain O, Babayan S, Gomes J, Rojas G, Guerrero R: First account on the larval biology of a Litomosoides filaria, from a bat. Parassitologia 2002, 44(1-2):89-92.

15. Rujeni N, Nausch N, Bourke CD, Midzi N, Mduluza T, Taylor DW, Mutapi F: Atopy is inversely related to schistosome infection intensity: a comparative study in Zimbabwean villages with distinct levels of Schistosoma haematobium infection. Int Arch Allergy Immunol 2012, 158(3):288-298.

16. van den Biggelaar AH, van Ree R, Rodrigues LC, Lell B, Deelder AM, Kremsner PG, Yazdanbakhsh M: Decreased atopy in children infected with Schistosoma haematobium: a role for parasite-induced interleukin-10. Lancet (London, England) 2000, 356(9243):1723-1727.

17. Flohr C, Tuyen LN, Lewis S, Quinnell R, Minh TT, Liem HT, Campbell J, Pritchard D, Hien TT, Farrar J et al: Poor sanitation and helminth infection protect against skin

sensitization in Vietnamese children: A cross-sectional study. J Allergy Clin Immunol 2006, 118(6):1305-1311.

18. Fleming JO, Cook TD: Multiple sclerosis and the hygiene hypothesis. Neurology 2006, 67(11):2085-2086.

19. Correale J, Farez M: Association between parasite infection and immune responses in multiple sclerosis. Ann Neurol 2007, 61(2):97-108.

20. Allen JE, Maizels RM: Diversity and dialogue in immunity to helminths. Nat Rev Immunol 2011, 11(6):375-388.

21. Nutman TB: Lymphatic filariasis: new insights and prospects for control. Curr Opin Infect Dis 2001, 14(5):539-546.

22. Grencis RK: Immunity to helminths: resistance, regulation, and susceptibility to gastrointestinal nematodes. Annu Rev Immunol 2015, 33:201-225.

23. Stoll NR: This wormy world. 1947. J Parasitol 1999, 85(3):392-396.

24. Gale EA: A missing link in the hygiene hypothesis? Diabetologia 2002, 45(4):588-594.

25. Elliott DE, Summers RW, Weinstock JV: Helminths as governors of immune-mediated inflammation. International journal for parasitology 2007, 37(5):457-464.

26. Rzepecka J, Pineda MA, Al-Riyami L, Rodgers DT, Huggan JK, Lumb FE, Khalaf AI, Meakin PJ, Corbet M, Ashford ML et al: Prophylactic and therapeutic treatment with a synthetic analogue of a parasitic worm product prevents experimental arthritis and inhibits IL-1beta production via NRF2-mediated counter-regulation of the inflammasome. J Autoimmun 2015, 60:59-73.

27. Rodgers DT, Pineda MA, Suckling CJ, Harnett W, Harnett MM: Drug-like analogues of the parasitic worm-derived immunomodulator ES-62 are therapeutic in the MRL/Lpr model of systemic lupus erythematosus. Lupus 2015, 24(13):1437-1442.

28. Suckling CJ, Mukherjee S, Khalaf AI, Narayan A, Scott FJ, Khare S, Dhakshinamoorthy S, Harnett MM, Harnett W: Synthetic analogues of the parasitic worm product ES-62 reduce disease development in in vivo models of lung fibrosis. Acta Trop 2018, 185:212-218.

29. Hubner MP, Shi Y, Torrero MN, Mueller E, Larson D, Soloviova K, Gondorf F, Hoerauf A, Killoran KE, Stocker JT et al: Helminth protection against autoimmune diabetes in nonobese diabetic mice is independent of a type 2 immune shift and requires TGF-beta. Journal of immunology (Baltimore, Md : 1950) 2012, 188(2):559-568.

30. Surendar J, Indulekha K, Hoerauf A, Hubner MP: Immunomodulation by helminths: Similar impact on type 1 and type 2 diabetes? Parasite immunology 2017, 39(5).

31. Hubner MP, Stocker JT, Mitre E: Inhibition of type 1 diabetes in filaria-infected non-obese diabetic mice is associated with a T helper type 2 shift and induction of FoxP3+ regulatory T cells. Immunology 2009, 127(4):512-522.

32. Hubner MP, Larson D, Torrero MN, Mueller E, Shi Y, Killoran KE, Mitre E: Anti-FcepsilonR1 antibody injections activate basophils and mast cells and delay Type 1 diabetes onset in NOD mice. Clin Immunol 2011, 141(2):205-217.

33. Morimoto M, Azuma N, Kadowaki H, Abe T, Suto Y: Regulation of type 2 diabetes by helminth-induced Th2 immune response. J Vet Med Sci 2017, 78(12):1855-1864.

34. de Ruiter K, Tahapary DL, Sartono E, Soewondo P, Supali T, Smit JWA, Yazdanbakhsh M: Helminths, hygiene hypothesis and type 2 diabetes. Parasite immunology 2017, 39(5).

35. Hoerauf A, Pfarr K, Mand S, Debrah AY, Specht S: Filariasis in Africa--treatment challenges and prospects. Clin Microbiol Infect 2011, 17(7):977-985.

36. Hoerauf A, Specht S, Marfo-Debrekyei Y, Buttner M, Debrah AY, Mand S, Batsa L, Brattig N, Konadu P, Bandi C et al: Efficacy of 5-week doxycycline treatment on adult Onchocerca volvulus. Parasitol Res 2009, 104(2):437-447.

37. Hoerauf A: Control of filarial infections: not the beginning of the end, but more research is needed. Curr Opin Infect Dis 2003, 16(5):403-410.

38. Hoerauf A: New strategies to combat filariasis. Expert Rev Anti Infect Ther 2006, 4(2):211-222.

39. Layland LE, Specht S: Helpful or a hindrance: co-infections with helminths during malaria. Adv Exp Med Biol 2014, 828:99-129.

40. Kroidl I, Saathoff E, Maganga L, Makunde WH, Hoerauf A, Geldmacher C, Clowes P, Maboko L, Hoelscher M: Effect of Wuchereria bancrofti infection on HIV incidence in southwest Tanzania: a prospective cohort study. Lancet (London, England) 2016, 388(10054):1912-1920.

41. Babu S, Nutman TB: Helminth-Tuberculosis Co-infection: An Immunologic Perspective. Trends Immunol 2016, 37(9):597-607.

42. Cooper PJ, Chico ME, Losonsky G, Sandoval C, Espinel I, Sridhara R, Aguilar M, Guevara A, Guderian RH, Levine MM et al: Albendazole treatment of children with ascariasis enhances the vibriocidal antibody response to the live attenuated oral cholera vaccine CVD 103-HgR. J Infect Dis 2000, 182(4):1199-1206.

43. Cooper PJ, Espinel I, Paredes W, Guderian RH, Nutman TB: Impaired tetanus-specific cellular and humoral responses following tetanus vaccination in human onchocerciasis: a possible role for interleukin-10. J Infect Dis 1998, 178(4):1133-1138.

44. Tamarozzi F, Halliday A, Gentil K, Hoerauf A, Pearlman E, Taylor MJ: Onchocerciasis: the role of Wolbachia bacterial endosymbionts in parasite biology,

disease pathogenesis, and treatment. Clinical microbiology reviews 2011, 24(3):459-468.

45. WHO: Weekly report eliminating lymphatic filariasis. Wkly Epidemiol Rec 2017, 92(40).

46. WHO: WHO: Progress report on the elimination of human onchocerciasis 2017. Wkly Epidemiol Rec 2017, 92(45):681-700.

47. Hoerauf A: Filariasis: new drugs and new opportunities for lymphatic filariasis and onchocerciasis. Curr Opin Infect Dis 2008, 21(6):673-681.

48. King CL, Suamani J, Sanuku N, Cheng YC, Satofan S, Mancuso B, Goss CW, Robinson LJ, Siba PM, Weil GJ et al: A Trial of a Triple-Drug Treatment for Lymphatic Filariasis. N Engl J Med 2018, 379(19):1801-1810.

49. Irvine MA, Stolk WA, Smith ME, Subramanian S, Singh BK, Weil GJ, Michael E, Hollingsworth TD: Effectiveness of a triple-drug regimen for global elimination of lymphatic filariasis: a modelling study. The Lancet Infectious diseases 2017, 17(4):451-458.

50. Thomsen EK, Sanuku N, Baea M, Satofan S, Maki E, Lombore B, Schmidt MS, Siba PM, Weil GJ, Kazura JW et al: Efficacy, Safety, and Pharmacokinetics of Coadministered Diethylcarbamazine, Albendazole, and Ivermectin for Treatment of Bancroftian Filariasis. Clin Infect Dis 2016, 62(3):334-341.

51. Dunn C, Callahan K, Katabarwa M, Richards F, Hopkins D, Withers PC, Jr., Buyon LE, McFarland D: The Contributions of Onchocerciasis Control and Elimination Programs toward the Achievement of the Millennium Development Goals. PLoS neglected tropical diseases 2015, 9(5):e0003703.

52. Vercruysse J, Levecke B, Prichard R: Human soil-transmitted helminths: implications of mass drug administration. Curr Opin Infect Dis 2012, 25(6):703-708.

53. Molyneux DH, Hopkins A, Bradley MH, Kelly-Hope LA: Multidimensional complexities of filariasis control in an era of large-scale mass drug administration programmes: a can of worms. Parasites & vectors 2014, 7:363.

54. Johnston KL, Ford L, Umareddy I, Townson S, Specht S, Pfarr K, Hoerauf A, Altmeyer R, Taylor MJ: Repurposing of approved drugs from the human pharmacopoeia to target Wolbachia endosymbionts of onchocerciasis and lymphatic filariasis. Int J Parasitol Drugs Drug Resist 2014, 4(3):278-286.

55. Liu LX, Weller PF: Antiparasitic drugs. N Engl J Med 1996, 334(18):1178-1184.

56. Gardon J, Gardon-Wendel N, Demanga N, Kamgno J, Chippaux JP, Boussinesq M: Serious reactions after mass treatment of onchocerciasis with ivermectin in an area endemic for Loa loa infection. Lancet (London, England) 1997, 350(9070):18-22.

57. Geary TG, Mackenzie CD: Progress and challenges in the discovery of macrofilaricidal drugs. Expert Rev Anti Infect Ther 2011, 9(8):681-695.

58. McNulty SN, Foster JM, Mitreva M, Dunning Hotopp JC, Martin J, Fischer K, Wu B, Davis PJ, Kumar S, Brattig NW et al: Endosymbiont DNA in endobacteria-free filarial nematodes indicates ancient horizontal genetic transfer. PloS one 2010, 5(6):e11029.

59. Taylor MJ, Hoerauf A: Wolbachia bacteria of filarial nematodes. Parasitol Today 1999, 15(11):437-442.

60. Taylor MJ, Bandi C, Hoerauf AM, Lazdins J: Wolbachia bacteria of filarial nematodes: a target for control? Parasitol Today 2000, 16(5):179-180.

61. Desjardins CA, Cerqueira GC, Goldberg JM, Dunning Hotopp JC, Haas BJ, Zucker J, Ribeiro JM, Saif S, Levin JZ, Fan L et al: Genomics of Loa loa, a Wolbachia-free filarial parasite of humans. Nat Genet 2013, 45(5):495-500.

62. Bouchery T, Lefoulon E, Karadjian G, Nieguitsila A, Martin C: The symbiotic role of Wolbachia in Onchocercidae and its impact on filariasis. Clin Microbiol Infect 2013, 19(2):131-140.

63. Hoerauf A, Nissen-Pahle K, Schmetz C, Henkle-Duhrsen K, Blaxter ML, Buttner DW, Gallin MY, Al-Qaoud KM, Lucius R, Fleischer B: Tetracycline therapy targets intracellular bacteria in the filarial nematode Litomosoides sigmodontis and results in filarial infertility. J Clin Invest 1999, 103(1):11-18.

64. Landmann F, Voronin D, Sullivan W, Taylor MJ: Anti-filarial activity of antibiotic therapy is due to extensive apoptosis after Wolbachia depletion from filarial nematodes. PLoS Pathog 2011, 7(11):e1002351.

65. Debrah AY, Mand S, Marfo-Debrekyei Y, Batsa L, Pfarr K, Buttner M, Adjei O, Buttner D, Hoerauf A: Macrofilaricidal effect of 4 weeks of treatment with doxycycline on Wuchereria bancrofti. Trop Med Int Health 2007, 12(12):1433-1441.

66. Lefoulon E, Bain O, Makepeace BL, d'Haese C, Uni S, Martin C, Gavotte L: Breakdown of coevolution between symbiotic bacteria Wolbachia and their filarial hosts. PeerJ 2016, 4:e1840.

67. Lo N, Casiraghi M, Salati E, Bazzocchi C, Bandi C: How many wolbachia supergroups exist? Mol Biol Evol 2002, 19(3):341-346.

68. McLaren DJ, Worms MJ, Laurence BR, Simpson MG: Micro-organisms in filarial larvae (Nematoda). Trans R Soc Trop Med Hyg 1975, 69(5-6):509-514.

69. Landmann F, Foster JM, Slatko B, Sullivan W: Asymmetric Wolbachia segregation during early Brugia malayi embryogenesis determines its distribution in adult host tissues. PLoS neglected tropical diseases 2010, 4(7):e758.

70. Fischer K, Beatty WL, Jiang D, Weil GJ, Fischer PU: Tissue and stage-specific distribution of Wolbachia in Brugia malayi. PLoS neglected tropical diseases 2011, 5(5):e1174.

71. Kozek WJ: Transovarially-transmitted intracellular microorganisms in adult and larval stages of Brugia malayi. J Parasitol 1977, 63(6):992-1000.

72. Landmann F, Bain O, Martin C, Uni S, Taylor MJ, Sullivan W: Both asymmetric mitotic segregation and cell-to-cell invasion are required for stable germline transmission of Wolbachia in filarial nematodes. Biol Open 2012, 1(6):536-547.

73. Brattig NW, Buttner DW, Hoerauf A: Neutrophil accumulation around Onchocerca worms and chemotaxis of neutrophils are dependent on Wolbachia endobacteria. Microbes Infect 2001, 3(6):439-446.

74. Pfarr KM, Hoerauf AM: Antibiotics which target the Wolbachia endosymbionts of filarial parasites: a new strategy for control of filariasis and amelioration of pathology. Mini Rev Med Chem 2006, 6(2):203-210.

75. Turner JD, Langley RS, Johnston KL, Gentil K, Ford L, Wu B, Graham M, Sharpley F, Slatko B, Pearlman E et al: Wolbachia lipoprotein stimulates innate and adaptive immunity through Toll-like receptors 2 and 6 to induce disease manifestations of filariasis. The Journal of biological chemistry 2009, 284(33):22364-22378.

76. Pathak M, Verma M, Srivastava M, Misra-Bhattacharya S: Wolbachia endosymbiont of Brugia malayi elicits a T helper type 17-mediated pro-inflammatory immune response through Wolbachia surface protein. Immunology 2015, 144(2):231-244.

77. Taylor MJ, Cross HF, Ford L, Makunde WH, Prasad GB, Bilo K: Wolbachia bacteria in filarial immunity and disease. Parasite immunology 2001, 23(7):401-409.

78. Hoerauf A, Mand S, Adjei O, Fleischer B, Buttner DW: Depletion of wolbachia endobacteria in Onchocerca volvulus by doxycycline and microfilaridermia after ivermectin treatment. Lancet (London, England) 2001, 357(9266):1415-1416.

79. Hoerauf A, Volkmann L, Hamelmann C, Adjei O, Autenrieth IB, Fleischer B, Buttner DW: Endosymbiotic bacteria in worms as targets for a novel chemotherapy in filariasis. Lancet (London, England) 2000, 355(9211):1242-1243.

80. Hoerauf A, Adjei O, Buttner DW: Antibiotics for the treatment of onchocerciasis and other filarial infections. Curr Opin Investig Drugs 2002, 3(4):533-537.

81. Schaberle TF, Schiefer A, Schmitz A, Konig GM, Hoerauf A, Pfarr K: Corallopyronin A - a promising antibiotic for treatment of filariasis. Int J Med Microbiol 2014, 304(1):72-78.

82. Hoerauf A, Mand S, Volkmann L, Buttner M, Marfo-Debrekyei Y, Taylor M, Adjei O, Buttner DW: Doxycycline in the treatment of human onchocerciasis: Kinetics of Wolbachia endobacteria reduction and of inhibition of embryogenesis in female Onchocerca worms. Microbes Infect 2003, 5(4):261-273.

83. Hoerauf A, Mand S, Fischer K, Kruppa T, Marfo-Debrekyei Y, Debrah AY, Pfarr KM, Adjei O, Buttner DW: Doxycycline as a novel strategy against bancroftian filariasis-depletion of Wolbachia endosymbionts from Wuchereria bancrofti and stop of microfilaria production. Med Microbiol Immunol 2003, 192(4):211-216.

84. Foster J, Ganatra M, Kamal I, Ware J, Makarova K, Ivanova N, Bhattacharyya A, Kapatral V, Kumar S, Posfai J et al: The Wolbachia genome of Brugia malayi: endosymbiont evolution within a human pathogenic nematode. PLoS Biol 2005, 3(4):e121.

85. Cooper PJ: Interactions between helminth parasites and allergy. Curr Opin Allergy Clin Immunol 2009, 9(1):29-37.

86. Zaccone P, Fehervari Z, Phillips JM, Dunne DW, Cooke A: Parasitic worms and inflammatory diseases. Parasite Immunol 2006, 28(10):515-523.

87. Correale J, Farez M: Helminth antigens modulate immune responses in cells from multiple sclerosis patients through TLR2-dependent mechanisms. Journal of immunology (Baltimore, Md : 1950) 2009, 183(9):5999-6012.

88. Stoll NR: This wormy world. J Parasitol 1947, 33(1):1-18.

89. Araujo MI, de Carvalho EM: Human schistosomiasis decreases immune responses to allergens and clinical manifestations of asthma. Chem Immunol Allergy 2006, 90:29-44.

90. Araujo MI, Lopes AA, Medeiros M, Cruz AA, Sousa-Atta L, Sole D, Carvalho EM: Inverse association between skin response to aeroallergens and Schistosoma mansoni infection. Int Arch Allergy Immunol 2000, 123(2):145-148.

91. Medeiros M, Jr., Figueiredo JP, Almeida MC, Matos MA, Araujo MI, Cruz AA, Atta AM, Rego MA, de Jesus AR, Taketomi EA et al: Schistosoma mansoni infection is associated with a reduced course of asthma. J Allergy Clin Immunol 2003, 111(5):947-951.

92. Flohr C, Tuyen LN, Quinnell RJ, Lewis S, Minh TT, Campbell J, Simmons C, Telford G, Brown A, Hien TT et al: Reduced helminth burden increases allergen skin sensitization but not clinical allergy: a randomized, double-blind, placebo-controlled trial in Vietnam. Clin Exp Allergy 2010, 40(1):131-142.

93. van den Biggelaar AH, Rodrigues LC, van Ree R, van der Zee JS, Hoeksma-Kruize YC, Souverijn JH, Missinou MA, Borrmann S, Kremsner PG, Yazdanbakhsh M: Long-term treatment of intestinal helminths increases mite skin-test reactivity in Gabonese schoolchildren. J Infect Dis 2004, 189(5):892-900.

94. Endara P, Vaca M, Chico ME, Erazo S, Oviedo G, Quinzo I, Rodriguez A, Lovato R, Moncayo AL, Barreto ML et al: Long-term periodic anthelmintic treatments are associated with increased allergen skin reactivity. Clin Exp Allergy 2010, 40(11):1669-1677.

95. Elliott AM, Ndibazza J, Mpairwe H, Muhangi L, Webb EL, Kizito D, Mawa P, Tweyongyere R, Muwanga M: Treatment with anthelminthics during pregnancy: what gains and what risks for the mother and child? Parasitology 2011, 138(12):1499-1507.

96. Mpairwe H, Webb EL, Muhangi L, Ndibazza J, Akishule D, Nampijja M, Ngom-wegi S, Tumusime J, Jones FM, Fitzsimmons C et al: Anthelminthic treatment during pregnancy is associated with increased risk of infantile eczema: randomised-controlled trial results. Pediatr Allergy Immunol 2011, 22(3):305-312.

97. Wammes LJ, Mpairwe H, Elliott AM, Yazdanbakhsh M: Helminth therapy or elimination: epidemiological, immunological, and clinical considerations. The Lancet Infectious diseases 2014, 14(11):1150-1162.

98. Alberti KG, Zimmet PZ: Definition, diagnosis and classification of diabetes mellitus and its complications. Part 1: diagnosis and classification of diabetes mellitus provisional report of a WHO consultation. Diabet Med 1998, 15(7):539-553.

99. Orasanu G, Plutzky J: The pathologic continuum of diabetic vascular disease. J Am Coll Cardiol 2009, 53(5 Suppl):S35-42.

100. Nazimek-Siewniak B, Moczulski D, Grzeszczak W: Risk of macrovascular and microvascular complications in Type 2 diabetes: results of longitudinal study design. J Diabetes Complications 2002, 16(4):271-276.

101. Rewers M, Gottlieb P: Immunotherapy for the prevention and treatment of type 1 diabetes: human trials and a look into the future. Diabetes Care 2009, 32(10):1769-1782.

102. Lumeng CN: Innate immune activation in obesity. Mol Aspects Med 2013, 34(1):12-29.

103. Alkhouri N, Gornicka A, Berk MP, Thapaliya S, Dixon LJ, Kashyap S, Schauer PR, Feldstein AE: Adipocyte apoptosis, a link between obesity, insulin resistance, and hepatic steatosis. The Journal of biological chemistry 2010, 285(5):3428-3438.

104. Zhang Y, Huang C: Targeting adipocyte apoptosis: a novel strategy for obesity therapy. Biochem Biophys Res Commun 2012, 417(1):1-4.

105. Trayhurn P: Hypoxia and adipocyte physiology: implications for adipose tissue dysfunction in obesity. Annu Rev Nutr 2014, 34:207-236.

106. Hosogai N, Fukuhara A, Oshima K, Miyata Y, Tanaka S, Segawa K, Furukawa S, Tochino Y, Komuro R, Matsuda M et al: Adipose tissue hypoxia in obesity and its impact on adipocytokine dysregulation. Diabetes 2007, 56(4):901-911.

107. Nishimura S, Manabe I, Nagasaki M, Eto K, Yamashita H, Ohsugi M, Otsu M, Hara K, Ueki K, Sugiura S et al: CD8+ effector T cells contribute to macrophage recruitment and adipose tissue inflammation in obesity. Nature medicine 2009, 15(8):914-920.

108. Kintscher U, Hartge M, Hess K, Foryst-Ludwig A, Clemenz M, Wabitsch M, Fischer-Posovszky P, Barth TF, Dragun D, Skurk T et al: T-lymphocyte infiltration in visceral adipose tissue: a primary event in adipose tissue inflammation and the development of obesity-mediated insulin resistance. Arterioscler Thromb Vasc Biol 2008, 28(7):1304-1310.

109. Yang H, Youm YH, Vandanmagsar B, Ravussin A, Gimble JM, Greenway F, Stephens JM, Mynatt RL, Dixit VD: Obesity increases the production of proinflammatory mediators from adipose tissue T cells and compromises TCR

repertoire diversity: implications for systemic inflammation and insulin resistance. J Immunol 2010, 185(3):1836-1845.

110. Winer S, Chan Y, Paltser G, Truong D, Tsui H, Bahrami J, Dorfman R, Wang Y, Zielenski J, Mastronardi F et al: Normalization of obesity-associated insulin resistance through immunotherapy. Nature medicine 2009, 15(8):921-929.

111. Brook CG, Lloyd JK, Wolf OH: Relation between age of onset of obesity and size and number of adipose cells. Br Med J 1972, 2(5804):25-27.

112. Chawla A, Nguyen KD, Goh YP: Macrophage-mediated inflammation in metabolic disease. Nat Rev Immunol 2011, 11(11):738-749.

113. Hotamisligil GS: Inflammatory pathways and insulin action. Int J Obes Relat Metab Disord 2003, 27 Suppl 3:S53-55.

114. Hotamisligil GS, Shargill NS, Spiegelman BM: Adipose expression of tumor necrosis factor-alpha: direct role in obesity-linked insulin resistance. Science 1993, 259(5091):87-91.

115. Aravindhan V, Mohan V, Surendar J, Muralidhara Rao M, Pavankumar N, Deepa M, Rajagopalan R, Kumaraswami V, Nutman TB, Babu S: Decreased prevalence of lymphatic filariasis among diabetic subjects associated with a diminished pro-inflammatory cytokine response (CURES 83). PLoS neglected tropical diseases 2010, 4(6):e707.

116. Chen Y, Lu J, Huang Y, Wang T, Xu Y, Xu M, Li M, Wang W, Li D, Bi Y et al: Association of previous schistosome infection with diabetes and metabolic syndrome: a cross-sectional study in rural China. The Journal of clinical endocrinology and metabolism 2013, 98(2):E283-287.

117. Hussaarts L, Garcia-Tardon N, van Beek L, Heemskerk MM, Haeberlein S, van der Zon GC, Ozir-Fazalalikhan A, Berbee JF, Willems van Dijk K, van Harmelen V et al:

Chronic helminth infection and helminth-derived egg antigens promote adipose tissue M2 macrophages and improve insulin sensitivity in obese mice. Faseb j 2015, 29(7):3027-3039.

118. Berbudi A, Surendar J, Ajendra J, Gondorf F, Schmidt D, Neumann AL, Wardani AP, Layland LE, Hoffmann LS, Pfeifer A et al: Filarial Infection or Antigen Administration Improves Glucose Tolerance in Diet-Induced Obese Mice. J Innate Immun 2016, 8(6):601-616.

119. Berbudi A, Ajendra J, Wardani AP, Hoerauf A, Hübner MP: Parasitic helminths and their beneficial impact on type 1 and type 2 diabetes. Diabetes Metab Res Rev 2016, 32(3):238-250.

120. Zaccone P, Fehervari Z, Jones FM, Sidobre S, Kronenberg M, Dunne DW, Cooke A: Schistosoma mansoni antigens modulate the activity of the innate immune response and prevent onset of type 1 diabetes. European journal of immunology 2003, 33(5):1439-1449.

121. Lund ME, O'Brien BA, Hutchinson AT, Robinson MW, Simpson AM, Dalton JP, Donnelly S: Secreted proteins from the helminth Fasciola hepatica inhibit the initiation of autoreactive T cell responses and prevent diabetes in the NOD mouse. PloS one 2014, 9(1):e86289.

122. Rodgers DT, McGrath MA, Pineda MA, Al-Riyami L, Rzepecka J, Lumb F, Harnett W, Harnett MM: The parasitic worm product ES-62 targets myeloid differentiation factor 88-dependent effector mechanisms to suppress antinuclear antibody production and proteinuria in MRL/lpr mice. Arthritis & rheumatology (Hoboken, NJ) 2015, 67(4):1023-1035.

123. Rzepecka J, Siebeke I, Coltherd JC, Kean DE, Steiger CN, Al-Riyami L, McSharry C, Harnett MM, Harnett W: The helminth product, ES-62, protects against airway

inflammation by resetting the Th cell phenotype. International journal for parasitology 2013, 43(3-4):211-223.

124. Coltherd JC, Rodgers DT, Lawrie RE, Al-Riyami L, Suckling CJ, Harnett W, Harnett MM: The parasitic worm-derived immunomodulator, ES-62 and its drug-like small molecule analogues exhibit therapeutic potential in a model of chronic asthma. Scientific reports 2016, 6:19224.

125. Doonan J, Lumb FE, Pineda MA, Tarafdar A, Crowe J, Khan AM, Suckling CJ, Harnett MM, Harnett W: Protection Against Arthritis by the Parasitic Worm Product ES-62, and Its Drug-Like Small Molecule Analogues, Is Associated With Inhibition of Osteoclastogenesis. Frontiers in immunology 2018, 9:1016.

126. Yamauchi T, Kamon J, Ito Y, Tsuchida A, Yokomizo T, Kita S, Sugiyama T, Miyagishi M, Hara K, Tsunoda M et al: Cloning of adiponectin receptors that mediate antidiabetic metabolic effects. Nature 2003, 423(6941):762-769.

127. Diez JJ, Iglesias P: The role of the novel adipocyte-derived protein adiponectin in human disease: an update. Mini Rev Med Chem 2010, 10(9):856-869.

128. Lopez-Jaramillo P, Gomez-Arbelaez D, Lopez-Lopez J, Lopez-Lopez C, Martinez-Ortega J, Gomez-Rodriguez A, Triana-Cubillos S: The role of leptin/adiponectin ratio in metabolic syndrome and diabetes. Horm Mol Biol Clin Investig 2014, 18(1):37-45.

129. Ukkola O, Santaniemi M: Adiponectin: a link between excess adiposity and associated comorbidities? J Mol Med (Berl) 2002, 80(11):696-702.

130. Nedvidkova J, Smitka K, Kopsky V, Hainer V: Adiponectin, an adipocyte-derived protein. Physiol Res 2005, 54(2):133-140.

131. Karadjian G, Fercoq F, Pionnier N, Vallarino-Lhermitte N, Lefoulon E, Nieguitsila A, Specht S, Carlin LM, Martin C: Migratory phase of Litomosoides sigmodontis filarial infective larvae is associated with pathology and transient increase of S100A9

expressing neutrophils in the lung. PLoS neglected tropical diseases 2017, 11(5):e0005596.

132. Vogl T, Gharibyan AL, Morozova-Roche LA: Pro-inflammatory S100A8 and S100A9 proteins: self-assembly into multifunctional native and amyloid complexes. Int J Mol Sci 2012, 13(3):2893-2917.

133. Goyette J, Geczy CL: Inflammation-associated S100 proteins: new mechanisms that regulate function. Amino Acids 2011, 41(4):821-842.

134. Hsu K, Champaiboon C, Guenther BD, Sorenson BS, Khammanivong A, Ross KF, Geczy CL, Herzberg MC: ANTI-INFECTIVE PROTECTIVE PROPERTIES OF S100 CALGRANULINS. Antiinflamm Antiallergy Agents Med Chem 2009, 8(4):290-305.

135. Srikrishna G, Freeze HH: Endogenous damage-associated molecular pattern molecules at the crossroads of inflammation and cancer. Neoplasia 2009, 11(7):615-628.

136. Ehrchen JM, Sunderkotter C, Foell D, Vogl T, Roth J: The endogenous Toll-like receptor 4 agonist S100A8/S100A9 (calprotectin) as innate amplifier of infection, autoimmunity, and cancer. J Leukoc Biol 2009, 86(3):557-566.

137. Srikrishna G, Nayak J, Weigle B, Temme A, Foell D, Hazelwood L, Olsson A, Volkmann N, Hanein D, Freeze HH: Carboxylated N-glycans on RAGE promote S100A12 binding and signaling. J Cell Biochem 2010, 110(3):645-659.

138. Yan WX, Armishaw C, Goyette J, Yang Z, Cai H, Alewood P, Geczy CL: Mast cell and monocyte recruitment by S100A12 and its hinge domain. The Journal of biological chemistry 2008, 283(19):13035-13043.

139. Pietzsch J, Hoppmann S: Human S100A12: a novel key player in inflammation? Amino Acids 2009, 36(3):381-389.

140. Sakaguchi M, Sonegawa H, Murata H, Kitazoe M, Futami J, Kataoka K, Yamada H, Huh NH: S100A11, an dual mediator for growth regulation of human keratinocytes. Mol Biol Cell 2008, 19(1):78-85.

141. Kiryushko D, Novitskaya V, Soroka V, Klingelhofer J, Lukanidin E, Berezin V, Bock E: Molecular mechanisms of Ca(2+) signaling in neurons induced by the S100A4 protein. Molecular and cellular biology 2006, 26(9):3625-3638.

142. Klingelhofer J, Moller HD, Sumer EU, Berg CH, Poulsen M, Kiryushko D, Soroka V, Ambartsumian N, Grigorian M, Lukanidin EM: Epidermal growth factor receptor ligands as new extracellular targets for the metastasis-promoting S100A4 protein. The FEBS journal 2009, 276(20):5936-5948.

143. Riuzzi F, Sorci G, Donato R: S100B protein regulates myoblast proliferation and differentiation by activating FGFR1 in a bFGF-dependent manner. J Cell Sci 2011, 124(Pt 14):2389-2400.

144. Foell D, Frosch M, Sorg C, Roth J: Phagocyte-specific calcium-binding S100 proteins as clinical laboratory markers of inflammation. Clin Chim Acta 2004, 344(1-2):37-51.

145. Shabani F, Farasat A, Mahdavi M, Gheibi N: Calprotectin (S100A8/S100A9): a key protein between inflammation and cancer. Inflamm Res 2018, 67(10):801-812.

146. Salama I, Malone PS, Mihaimeed F, Jones JL: A review of the S100 proteins in cancer. Eur J Surg Oncol 2008, 34(4):357-364.

147. Chan JK, Roth J, Oppenheim JJ, Tracey KJ, Vogl T, Feldmann M, Horwood N, Nanchahal J: Alarmins: awaiting a clinical response. J Clin Invest 2012, 122(8):2711-2719.

148. Pruenster M, Vogl T, Roth J, Sperandio M: S100A8/A9: From basic science to clinical application. Pharmacol Ther 2016, 167:120-131.

149. Aranda CJ, Ocon B, Arredondo-Amador M, Suarez MD, Zarzuelo A, Chazin WJ, Martinez-Augustin O, Sanchez de Medina F: Calprotectin protects against experimental colonic inflammation in mice. Br J Pharmacol 2018, 175(19):3797-3812.

150. Urban CF, Ermert D, Schmid M, Abu-Abed U, Goosmann C, Nacken W, Brinkmann V, Jungblut PR, Zychlinsky A: Neutrophil extracellular traps contain calprotectin, a cytosolic protein complex involved in host defense against Candida albicans. PLoS Pathog 2009, 5(10):e1000639.

151. Frosch M, Strey A, Vogl T, Wulffraat NM, Kuis W, Sunderkotter C, Harms E, Sorg C, Roth J: Myeloid-related proteins 8 and 14 are specifically secreted during interaction of phagocytes and activated endothelium and are useful markers for monitoring disease activity in pauciarticular-onset juvenile rheumatoid arthritis. Arthritis and rheumatism 2000, 43(3):628-637.

152. Carlstedt-Duke JM: Tissue distribution of the receptor for 2,3,7,8-tetrachlorodibenzo-p-dioxin in the rat. Cancer Res 1979, 39(8):3172-3176.

153. Di Meglio P, Perera GK, Nestle FO: The multitasking organ: recent insights into skin immune function. Immunity 2011, 35(6):857-869.

154. Johansson G, Gillner M, Hogberg B, Gustafsson JA: The TCDD receptor in rat intestinal mucosa and its possible dietary ligands. Nutr Cancer 1982, 3(3):134-144.

155. Meyer BK, Perdew GH: Characterization of the AhR-hsp90-XAP2 core complex and the role of the immunophilin-related protein XAP2 in AhR stabilization. Biochemistry 1999, 38(28):8907-8917.

156. Carver LA, Bradfield CA: Ligand-dependent interaction of the aryl hydrocarbon receptor with a novel immunophilin homolog in vivo. The Journal of biological chemistry 1997, 272(17):11452-11456.

157. Meyer BK, Pray-Grant MG, Vanden Heuvel JP, Perdew GH: Hepatitis B virus X-associated protein 2 is a subunit of the unliganded aryl hydrocarbon receptor core complex and exhibits transcriptional enhancer activity. Molecular and cellular biology 1998, 18(2):978-988.

158. Grenert JP, Sullivan WP, Fadden P, Haystead TA, Clark J, Mimnaugh E, Krutzsch H, Ochel HJ, Schulte TW, Sausville E et al: The amino-terminal domain of heat shock protein 90 (hsp90) that binds geldanamycin is an ATP/ADP switch domain that regulates hsp90 conformation. The Journal of biological chemistry 1997, 272(38):23843-23850.

159. Furue M, Takahara M, Nakahara T, Uchi H: Role of AhR/ARNT system in skin homeostasis. Arch Dermatol Res 2014, 306(9):769-779.

160. McGuire J, Whitelaw ML, Pongratz I, Gustafsson JA, Poellinger L: A cellular factor stimulates ligand-dependent release of hsp90 from the basic helix-loop-helix dioxin receptor. Molecular and cellular biology 1994, 14(4):2438-2446.

161. Fukunaga BN, Probst MR, Reisz-Porszasz S, Hankinson O: Identification of functional domains of the aryl hydrocarbon receptor. The Journal of biological chemistry 1995, 270(49):29270-29278.

162. Furman DP, Oshchepkova EA, Oshchepkov DY, Shamanina MY, Mordvinov VA: Promoters of the genes encoding the transcription factors regulating the cytokine gene expression in macrophages contain putative binding sites for aryl hydrocarbon receptor. Comput Biol Chem 2009, 33(6):465-468.

163. Stockinger B, Di Meglio P, Gialitakis M, Duarte JH: The aryl hydrocarbon receptor: multitasking in the immune system. Annu Rev Immunol 2014, 32:403-432.

164. Bessede A, Gargaro M, Pallotta MT, Matino D, Servillo G, Brunacci C, Bicciato S, Mazza EM, Macchiarulo A, Vacca C et al: Aryl hydrocarbon receptor control of a disease tolerance defence pathway. Nature 2014, 511(7508):184-190.

165. Basu R, O'Quinn DB, Silberger DJ, Schoeb TR, Fouser L, Ouyang W, Hatton RD, Weaver CT: Th22 cells are an important source of IL-22 for host protection against enteropathogenic bacteria. Immunity 2012, 37(6):1061-1075.

166. Yeste A, Mascanfroni ID, Nadeau M, Burns EJ, Tukpah AM, Santiago A, Wu C, Patel B, Kumar D, Quintana FJ: IL-21 induces IL-22 production in CD4+ T cells. Nature communications 2014, 5:3753.

167. Vorderstrasse BA, Lawrence BP: Protection against lethal challenge with Streptococcus pneumoniae is conferred by aryl hydrocarbon receptor activation but is not associated with an enhanced inflammatory response. Infection and immunity 2006, 74(10):5679-5686.

168. Shi LZ, Faith NG, Nakayama Y, Suresh M, Steinberg H, Czuprynski CJ: The aryl hydrocarbon receptor is required for optimal resistance to Listeria monocytogenes infection in mice. Journal of immunology (Baltimore, Md : 1950) 2007, 179(10):6952-6962.

169. Moura-Alves P, Fae K, Houthuys E, Dorhoi A, Kreuchwig A, Furkert J, Barison N, Diehl A, Munder A, Constant P et al: AhR sensing of bacterial pigments regulates antibacterial defence. Nature 2014, 512(7515):387-392.

170. Li Y, Innocentin S, Withers DR, Roberts NA, Gallagher AR, Grigorieva EF, Wilhelm C, Veldhoen M: Exogenous stimuli maintain intraepithelial lymphocytes via aryl hydrocarbon receptor activation. Cell 2011, 147(3):629-640.

171. Kiss EA, Vonarbourg C, Kopfmann S, Hobeika E, Finke D, Esser C, Diefenbach A: Natural aryl hydrocarbon receptor ligands control organogenesis of intestinal lymphoid follicles. Science 2011, 334(6062):1561-1565.

172. Qiu J, Heller JJ, Guo X, Chen ZM, Fish K, Fu YX, Zhou L: The aryl hydrocarbon receptor regulates gut immunity through modulation of innate lymphoid cells. Immunity 2012, 36(1):92-104.

173. Hoffmann W, Petit G, Schulz-Key H, Taylor D, Bain O, Le Goff L: Litomosoides sigmodontis in mice: reappraisal of an old model for filarial research. Parasitol Today 2000, 16(9):387-389.

174. Ajendra J, Specht S, Neumann AL, Gondorf F, Schmidt D, Gentil K, Hoffmann WH, Taylor MJ, Hoerauf A, Hubner MP: ST2 deficiency does not impair type 2 immune responses during chronic filarial infection but leads to an increased microfilaremia due to an impaired splenic microfilarial clearance. PloS one 2014, 9(3):e93072.

175. Fox EM, Morris CP, Hubner MP, Mitre E: Histamine 1 Receptor Blockade Enhances Eosinophil-Mediated Clearance of Adult Filarial Worms. PLoS neglected tropical diseases 2015, 9(7):e0003932.

176. Torrero MN, Hubner MP, Larson D, Karasuyama H, Mitre E: Basophils amplify type 2 immune responses, but do not serve a protective role, during chronic infection of mice with the filarial nematode Litomosoides sigmodontis. Journal of immunology (Baltimore, Md : 1950) 2010, 185(12):7426-7434.

177. Le Goff L, Martin C, Oswald IP, Vuong PN, Petit G, Ungeheuer MN, Bain O: Parasitology and immunology of mice vaccinated with irradiated Litomosoides sigmodontis larvae. Parasitology 2000, 120 (Pt 3):271-280.

178. Allen JE, Adjei O, Bain O, Hoerauf A, Hoffmann WH, Makepeace BL, Schulz-Key H, Tanya VN, Trees AJ, Wanji S et al: Of mice, cattle, and humans: the immunology and treatment of river blindness. PLoS neglected tropical diseases 2008, 2(4):e217.

179. Maizels RM, Balic A, Gomez-Escobar N, Nair M, Taylor MD, Allen JE: Helminth parasites--masters of regulation. Immunol Rev 2004, 201:89-116.

180. Hoerauf A, Satoguina J, Saeftel M, Specht S: Immunomodulation by filarial nematodes. Parasite immunology 2005, 27(10-11):417-429.

181. Al-Qaoud KM, Taubert A, Zahner H, Fleischer B, Hoerauf A: Infection of BALB/c mice with the filarial nematode Litomosoides sigmodontis: role of CD4+ T cells in controlling larval development. Infect Immun 1997, 65(6):2457-2461.

182. Specht S, Saeftel M, Arndt M, Endl E, Dubben B, Lee NA, Lee JJ, Hoerauf A: Lack of eosinophil peroxidase or major basic protein impairs defense against murine filarial infection. Infection and immunity 2006, 74(9):5236-5243.

183. Volkmann L, Bain O, Saeftel M, Specht S, Fischer K, Brombacher F, Matthaei KI, Hoerauf A: Murine filariasis: interleukin 4 and interleukin 5 lead to containment of different worm developmental stages. Med Microbiol Immunol 2003, 192(1):23-31.

184. Hubner MP, Torrero MN, Mitre E: Type 2 immune-inducing helminth vaccination maintains protective efficacy in the setting of repeated parasite exposures. Vaccine 2010, 28(7):1746-1757.

185. Ziewer S, Hubner MP, Dubben B, Hoffmann WH, Bain O, Martin C, Hoerauf A, Specht S: Immunization with *L. sigmodontis* microfilariae reduces peripheral microfilaraemia after challenge infection by inhibition of filarial embryogenesis. PLoS neglected tropical diseases 2012, 6(3):e1558.

186. King CL, Nutman TB: Regulation of the immune response in lymphatic filariasis and onchocerciasis. Immunol Today 1991, 12(3):A54-58.

187. Boyd A, Ribeiro JM, Nutman TB: Human CD117 (cKit)+ innate lymphoid cells have a discrete transcriptional profile at homeostasis and are expanded during filarial infection. PloS one 2014, 9(9):e108649.

188. Babu S, Kumaraswami V, Nutman TB: Alternatively activated and immunoregulatory monocytes in human filarial infections. J Infect Dis 2009, 199(12):1827-1837.

189. Taylor MD, LeGoff L, Harris A, Malone E, Allen JE, Maizels RM: Removal of regulatory T cell activity reverses hyporesponsiveness and leads to filarial parasite clearance in vivo. Journal of immunology (Baltimore, Md : 1950) 2005, 174(8):4924-4933.

190. Babu S, Blauvelt CP, Kumaraswami V, Nutman TB: Regulatory networks induced by live parasites impair both Th1 and Th2 pathways in patent lymphatic filariasis: implications for parasite persistence. Journal of immunology (Baltimore, Md : 1950) 2006, 176(5):3248-3256.

191. Babu S, Blauvelt CP, Kumaraswami V, Nutman TB: Diminished expression and function of TLR in lymphatic filariasis: a novel mechanism of immune dysregulation. Journal of immunology (Baltimore, Md : 1950) 2005, 175(2):1170-1176.

192. Adjobimey T, Hoerauf A: Induction of immunoglobulin G4 in human filariasis: an indicator of immunoregulation. Ann Trop Med Parasitol 2010, 104(6):455-464.

193. Prodjinotho UF, von Horn C, Debrah AY, Batsa Debrah L, Albers A, Layland LE, Hoerauf A, Adjobimey T: Pathological manifestations in lymphatic filariasis correlate with lack of inhibitory properties of IgG4 antibodies on IgE-activated granulocytes. PLoS neglected tropical diseases 2017, 11(7):e0005777.

194. Katawa G, Layland LE, Debrah AY, von Horn C, Batsa L, Kwarteng A, Arriens S, D WT, Specht S, Hoerauf A et al: Hyperreactive onchocerciasis is characterized by a

combination of Th17-Th2 immune responses and reduced regulatory T cells. PLoS neglected tropical diseases 2015, 9(1):e3414.

195. Arndts K, Deininger S, Specht S, Klarmann U, Mand S, Adjobimey T, Debrah AY, Batsa L, Kwarteng A, Epp C et al: Elevated adaptive immune responses are associated with latent infections of Wuchereria bancrofti. PLoS neglected tropical diseases 2012, 6(4):e1611.

196. Babu S, Bhat SQ, Pavan Kumar N, Lipira AB, Kumar S, Karthik C, Kumaraswami V, Nutman TB: Filarial lymphedema is characterized by antigen-specific Th1 and th17 proinflammatory responses and a lack of regulatory T cells. PLoS neglected tropical diseases 2009, 3(4):e420.

197. Gentil K, Lentz CS, Rai R, Muhsin M, Kamath AD, Mutluer O, Specht S, Hubner MP, Hoerauf A: Eotaxin-1 is involved in parasite clearance during chronic filarial infection. Parasite immunology 2014, 36(2):60-77.

198. Le Goff L, Lamb TJ, Graham AL, Harcus Y, Allen JE: IL-4 is required to prevent filarial nematode development in resistant but not susceptible strains of mice. International journal for parasitology 2002, 32(10):1277-1284.

199. Volkmann L, Saeftel M, Bain O, Fischer K, Fleischer B, Hoerauf A: Interleukin-4 is essential for the control of microfilariae in murine infection with the filaria Litomosoides sigmodontis. Infection and immunity 2001, 69(5):2950-2956.

200. Jenkins SJ, Ruckerl D, Cook PC, Jones LH, Finkelman FD, van Rooijen N, MacDonald AS, Allen JE: Local macrophage proliferation, rather than recruitment from the blood, is a signature of TH2 inflammation. Science 2011, 332(6035):1284-1288.

201. Dittrich AM, Erbacher A, Specht S, Diesner F, Krokowski M, Avagyan A, Stock P, Ahrens B, Hoffmann WH, Hoerauf A et al: Helminth Infection with Litomosoides

sigmodontis Induces Regulatory T Cells and Inhibits Allergic Sensitization, Airway Inflammation, and Hyperreactivity in a Murine Asthma Model. J Immunol 2008, 180(3):1792-1799.

202. Evans H, Killoran KE, Mitre BK, Morris CP, Kim SY, Mitre E: Ten Weeks of Infection with a Tissue-Invasive Helminth Protects against Local Immune Complex-Mediated Inflammation, but Not Cutaneous Type I Hypersensitivity, in Previously Sensitized Mice. J Immunol 2015.

203. Haben I, Hartmann W, Breloer M: Nematode-induced interference with vaccination efficacy targets follicular T helper cell induction and is preserved after termination of infection. PLoS Negl Trop Dis 2014, 8(9):e3170.

204. Kolbaum J, Tartz S, Hartmann W, Helm S, Nagel A, Heussler V, Sebo P, Fleischer B, Jacobs T, Breloer M: Nematode-induced interference with the anti-Plasmodium CD8+ T-cell response can be overcome by optimizing antigen administration. Eur J Immunol 2012, 42(4):890-900.

205. Hartmann W, Schramm C, Breloer M: Litomosoides sigmodontis induces TGF-beta receptor responsive, IL-10-producing T cells that suppress bystander T-cell proliferation in mice. Eur J Immunol 2015, 45(9):2568-2581.

206. Haben I, Hartmann W, Specht S, Hoerauf A, Roers A, Muller W, Breloer M: T-cell-derived, but not B-cell-derived, IL-10 suppresses antigen-specific T-cell responses in Litomosoides sigmodontis-infected mice. Eur J Immunol 2013, 43(7):1799-1805.

207. Taylor MD, Harris A, Nair MG, Maizels RM, Allen JE: F4/80+ alternatively activated macrophages control CD4+ T cell hyporesponsiveness at sites peripheral to filarial infection. J Immunol 2006, 176(11):6918-6927.

208. Ajendra J, Berbudi A, Hoerauf A, Hubner MP: Combination of worm antigen and proinsulin prevents type 1 diabetes in NOD mice after the onset of insulitis. Clin Immunol 2016, 164:119-122.

209. Gondorf F, Berbudi A, Buerfent BC, Ajendra J, Bloemker D, Specht S, Schmidt D, Neumann AL, Layland LE, Hoerauf A et al: Chronic filarial infection provides protection against bacterial sepsis by functionally reprogramming macrophages. PLoS Pathog 2015, 11(1):e1004616.

210. Specht S, Ruiz DF, Dubben B, Deininger S, Hoerauf A: Filaria-induced IL-10 suppresses murine cerebral malaria. Microbes Infect 2010, 12(8-9):635-642.

211. Hubner MP, Killoran KE, Rajnik M, Wilson S, Yim KC, Torrero MN, Morris CP, Nikonenko B, Blanco JC, Hemming VG et al: Chronic helminth infection does not exacerbate Mycobacterium tuberculosis infection. PLoS neglected tropical diseases 2012, 6(12):e1970.

212. Hubner MP, Torrero MN, McCall JW, Mitre E: Litomosoides sigmodontis: a simple method to infect mice with L3 larvae obtained from the pleural space of recently infected jirds (Meriones unguiculatus). Exp Parasitol 2009, 123(1):95-98.

213. Martin C, Al-Qaoud KM, Ungeheuer MN, Paehle K, Vuong PN, Bain O, Fleischer B, Hoerauf A: IL-5 is essential for vaccine-induced protection and for resolution of primary infection in murine filariasis. Med Microbiol Immunol 2000, 189(2):67-74.

214. Ritter M, Tamadaho RS, Feid J, Vogel W, Wiszniewsky K, Perner S, Hoerauf A, Layland LE: IL-4/5 signalling plays an important role during Litomosoides sigmodontis infection, influencing both immune system regulation and tissue pathology in the thoracic cavity. International journal for parasitology 2017, 47(14):951-960.

215. Hawking F: The role of the spleen in controlling the number of microfilariae (Dirofilaria immitis, D. repens, Litomosoides carinii and Dipetalonema witei) in the blood. Ann Trop Med Parasitol 1962, 56:168-172.

216. Babayan SA, Read AF, Lawrence RA, Bain O, Allen JE: Filarial parasites develop faster and reproduce earlier in response to host immune effectors that determine filarial life expectancy. PLoS Biol 2010, 8(10):e1000525.

217. Muhsin M, Ajendra J, Gentil K, Berbudi A, Neumann AL, Klaas L, Schmidt KE, Hoerauf A, Hubner MP: IL-6 is required for protective immune responses against early filarial infection. International journal for parasitology 2018, 48(12):925-935.

218. Hubner MP, Pasche B, Kalaydjiev S, Soboslay PT, Lengeling A, Schulz-Key H, Mitre E, Hoffmann WH: Microfilariae of the filarial nematode Litomosoides sigmodontis exacerbate the course of lipopolysaccharide-induced sepsis in mice. Infection and immunity 2008, 76(4):1668-1677.

219. Saeftel M, Volkmann L, Korten S, Brattig N, Al-Qaoud K, Fleischer B, Hoerauf A: Lack of interferon-gamma confers impaired neutrophil granulocyte function and imparts prolonged survival of adult filarial worms in murine filariasis. Microbes Infect 2001, 3(3):203-213.

220. Tendongfor N, Wanji S, Ngwa JC, Esum ME, Specht S, Enyong P, Matthaei KI, Hoerauf A: The human parasite Loa loa in cytokine and cytokine receptor gene knock out BALB/c mice: survival, development and localization. Parasites & vectors 2012, 5:43.

221. Edgeworth J, Gorman M, Bennett R, Freemont P, Hogg N: Identification of p8,14 as a highly abundant heterodimeric calcium binding protein complex of myeloid cells. The Journal of biological chemistry 1991, 266(12):7706-7713.

222. Ryckman C, McColl SR, Vandal K, de Medicis R, Lussier A, Poubelle PE, Tessier PA: Role of S100A8 and S100A9 in neutrophil recruitment in response to monosodium urate monohydrate crystals in the air-pouch model of acute gouty arthritis. Arthritis and rheumatism 2003, 48(8):2310-2320.

223. Vogl T, Tenbrock K, Ludwig S, Leukert N, Ehrhardt C, van Zoelen MA, Nacken W, Foell D, van der Poll T, Sorg C et al: Mrp8 and Mrp14 are endogenous activators of Toll-like receptor 4, promoting lethal, endotoxin-induced shock. Nature medicine 2007, 13(9):1042-1049.

224. Vogl T, Stratis A, Wixler V, Voller T, Thurainayagam S, Jorch SK, Zenker S, Dreiling A, Chakraborty D, Frohling M et al: Autoinhibitory regulation of S100A8/S100A9 alarmin activity locally restricts sterile inflammation. J Clin Invest 2018, 128(5):1852-1866.

225. Rodrigo MB, Schulz S, Krupp V, Ritter M, Wiszniewsky K, Arndts K, Tamadaho RS, Endl E, Hoerauf A, Layland LE: Patency of Litomosoides sigmodontis infection depends on Toll-like receptor 4 whereas Toll-like receptor 2 signalling influences filarial-specific CD4(+) T-cell responses. Immunology 2016, 147(4):429-442.

226. Lackmann M, Cornish CJ, Simpson RJ, Moritz RL, Geczy CL: Purification and structural analysis of a murine chemotactic cytokine (CP-10) with sequence homology to S100 proteins. The Journal of biological chemistry 1992, 267(11):7499-7504.

227. Ajendra J, Specht S, Ziewer S, Schiefer A, Pfarr K, Parcina M, Kufer TA, Hoerauf A, Hubner MP: NOD2 dependent neutrophil recruitment is required for early protective immune responses against infectious Litomosoides sigmodontis L3 larvae. Scientific reports 2016, 6:39648.

228. Loukas A, Prociv P: Immune responses in hookworm infections. Clinical microbiology reviews 2001, 14(4):689-703, table of contents.

229. Bisoffi Z, Buonfrate D, Montresor A, Requena-Mendez A, Munoz J, Krolewiecki AJ, Gotuzzo E, Mena MA, Chiodini PL, Anselmi M et al: Strongyloides stercoralis: a plea for action. PLoS neglected tropical diseases 2013, 7(5):e2214.

230. Crompton DW: Ascaris and ascariasis. Advances in parasitology 2001, 48:285-375.

231. Craig JM, Scott AL: Helminths in the lungs. Parasite immunology 2014, 36(9):463-474.

232. Bouchery T, Kyle R, Camberis M, Shepherd A, Filbey K, Smith A, Harvie M, Painter G, Johnston K, Ferguson P et al: ILC2s and T cells cooperate to ensure maintenance of M2 macrophages for lung immunity against hookworms. Nature communications 2015, 6:6970.

233. Marsland BJ, Kurrer M, Reissmann R, Harris NL, Kopf M: Nippostrongylus brasiliensis infection leads to the development of emphysema associated with the induction of alternatively activated macrophages. European journal of immunology 2008, 38(2):479-488.

234. Reece JJ, Siracusa MC, Southard TL, Brayton CF, Urban JF, Jr., Scott AL: Hookworm-induced persistent changes to the immunological environment of the lung. Infection and immunity 2008, 76(8):3511-3524.

235. O'Connell AE, Hess JA, Santiago GA, Nolan TJ, Lok JB, Lee JJ, Abraham D: Major basic protein from eosinophils and myeloperoxidase from neutrophils are required for protective immunity to Strongyloides stercoralis in mice. Infection and immunity 2011, 79(7):2770-2778.

236. Buys J, Wever R, Ruitenberg EJ: Myeloperoxidase is more efficient than eosinophil peroxidase in the in vitro killing of newborn larvae of Trichinella spiralis. Immunology 1984, 51(3):601-607.

237. Jong EC, Mahmoud AA, Klebanoff SJ: Peroxidase-mediated toxicity to schistosomula of Schistosoma mansoni. Journal of immunology (Baltimore, Md : 1950) 1981, 126(2):468-471.

238. Al-Qaoud KM, Pearlman E, Hartung T, Klukowski J, Fleischer B, Hoerauf A: A new mechanism for IL-5-dependent helminth control: neutrophil accumulation and neutrophil-mediated worm encapsulation in murine filariasis are abolished in the absence of IL-5. Int Immunol 2000, 12(6):899-908.

239. Jux B, Kadow S, Esser C: Langerhans cell maturation and contact hypersensitivity are impaired in aryl hydrocarbon receptor-null mice. Journal of immunology (Baltimore, Md : 1950) 2009, 182(11):6709-6717.

240. Platzer B, Richter S, Kneidinger D, Waltenberger D, Woisetschlager M, Strobl H: Aryl hydrocarbon receptor activation inhibits in vitro differentiation of human monocytes and Langerhans dendritic cells. Journal of immunology (Baltimore, Md : 1950) 2009, 183(1):66-74.

241. Frericks M, Meissner M, Esser C: Microarray analysis of the AHR system: tissue-specific flexibility in signal and target genes. Toxicology and applied pharmacology 2007, 220(3):320-332.

242. Cotton RN, McDonald-Fleming R, Boyd A, Spates K, Nutman TB, Tolouei Semnani R: Brugia malayi infective larvae fail to activate Langerhans cells and dermal dendritic cells in human skin. Parasite immunology 2015, 37(2):79-91.

243. Lee EY, Lee ZH, Song YW: CXCL10 and autoimmune diseases. Autoimmunity reviews 2009, 8(5):379-383.

244. Dufour JH, Dziejman M, Liu MT, Leung JH, Lane TE, Luster AD: IFN-gamma-inducible protein 10 (IP-10; CXCL10)-deficient mice reveal a role for IP-10 in

effector T cell generation and trafficking. Journal of immunology (Baltimore, Md : 1950) 2002, 168(7):3195-3204.

245. Tomita K, Freeman BL, Bronk SF, LeBrasseur NK, White TA, Hirsova P, Ibrahim SH: CXCL10-Mediates Macrophage, but not Other Innate Immune Cells-Associated Inflammation in Murine Nonalcoholic Steatohepatitis. Scientific reports 2016, 6:28786.

246. Kwak HB, Ha H, Kim HN, Lee JH, Kim HS, Lee S, Kim HM, Kim JY, Kim HH, Song YW et al: Reciprocal cross-talk between RANKL and interferon-gamma-inducible protein 10 is responsible for bone-erosive experimental arthritis. Arthritis and rheumatism 2008, 58(5):1332-1342.

247. Mohan K, Issekutz TB: Blockade of chemokine receptor CXCR3 inhibits T cell recruitment to inflamed joints and decreases the severity of adjuvant arthritis. Journal of immunology (Baltimore, Md : 1950) 2007, 179(12):8463-8469.

248. Specht S, Frank JK, Alferink J, Dubben B, Layland LE, Denece G, Bain O, Forster I, Kirschning CJ, Martin C et al: CCL17 controls mast cells for the defense against filarial larval entry. Journal of immunology (Baltimore, Md : 1950) 2011, 186(8):4845-4852.

249. Kitagaki K, Businga TR, Racila D, Elliott DE, Weinstock JV, Kline JN: Intestinal helminths protect in a murine model of asthma. Journal of immunology (Baltimore, Md : 1950) 2006, 177(3):1628-1635.

250. Haque R: Human intestinal parasites. Journal of health, population, and nutrition 2007, 25(4):387-391.

251. Doonan J, Thomas D, Wong MH, Ramage HJ, Al-Riyami L, Lumb FE, Bell KS, Fairlie-Clarke KJ, Suckling CJ, Michelsen KS et al: Failure of the Anti-Inflammatory Parasitic Worm Product ES-62 to Provide Protection in Mouse Models of Type I

Diabetes, Multiple Sclerosis, and Inflammatory Bowel Disease. Molecules (Basel, Switzerland) 2018, 23(10).

252. Al-Riyami L, Pineda MA, Rzepecka J, Huggan JK, Khalaf AI, Suckling CJ, Scott FJ, Rodgers DT, Harnett MM, Harnett W: Designing anti-inflammatory drugs from parasitic worms: a synthetic small molecule analogue of the Acanthocheilonema viteae product ES-62 prevents development of collagen-induced arthritis. Journal of medicinal chemistry 2013, 56(24):9982-10002.

253. Pineda MA, McGrath MA, Smith PC, Al-Riyami L, Rzepecka J, Gracie JA, Harnett W, Harnett MM: The parasitic helminth product ES-62 suppresses pathogenesis in collagen-induced arthritis by targeting the interleukin-17-producing cellular network at multiple sites. Arthritis and rheumatism 2012, 64(10):3168-3178.

254. Hays R, Esterman A, Giacomin P, Loukas A, McDermott R: Does Strongyloides stercoralis infection protect against type 2 diabetes in humans? Evidence from Australian Aboriginal adults. Diabetes research and clinical practice 2015, 107(3):355-361.

255. Wiria AE, Hamid F, Wammes LJ, Prasetyani MA, Dekkers OM, May L, Kaisar MM, Verweij JJ, Guigas B, Partono F et al: Correction: Infection with Soil-Transmitted Helminths Is Associated with Increased Insulin Sensitivity. PloS one 2015, 10(8):e0136002.

List of abbreviations

AAM	-	Alternatively activated macrophages
AhR	-	Aryl Hydrocarbon receptor
AhRR	-	Aryl Hydrocarbon receptor Repressor
AIP	-	AhR-interacting protein
ALB	-	Albendazole
APC	-	Allophycocyanine
AUC	-	Area under curve
ASD	-	Amorphous solid dispersion
ARNT	-	Aryl Hydrocarbon receptor nuclear translocator
BSA	-	Bovine serum albumin
bHLH PAS	-	Basic helix-loop-helix/PAS
°C	-	Degree Celsius
CCL / CCR	-	Chemokine (c-c motif) ligand / receptor
CXCL	-	C-X-C motif ligand
CD	-	Cluster of differentiation
cm	-	Centimeter
ConA	-	Concanavalin A
CXCL	-	Chemokine C-X-C motif ligand
DAMP	-	Damage-associated molecular pattern
DEC	-	Diethylcarbamazine
DIO	-	Diet induced obesity
DMSO	-	Dimethyl sulfoxide
DNA	-	Deoxyribonucleic acid

DOX	-	Doxycycline
DRE	-	Dioxin response element
dpi	-	Days post infection
E.coli	-	*Escherichia coli*
EDTA	-	Ethylenediaminetetraacetic acid
EGF	-	Epidermal growth factor
E/S	-	Excretory/secretory
ELISA	-	Enzyme-linked immunosorbent assay
EPO	-	Eosinophil peroxidase
FACS	-	Fluorescence activated cell sorting
FGFR1	-	Fibroblast growth factor receptor 1
FITC	-	Fluorescein isothiocyanate
FLU	-	Flubendazole
FMO	-	Fluorescence minus one
FSC	-	Forward scatter
g	-	Gravity
GTT	-	Glucose Tolerance Test
H&E	-	Haematoxylin-eosin
HER2	-	Human epidermal growth factor receptor 2
HFD	-	High fat diet
hi	-	High expressing
HIV	-	Human immunodeficiency virus
HER2	-	Human epidermal growth factor receptor 2
HSP	-	Heat shock protein
HSPG	-	Heoaran sulphate proteoglycans

IBD	-	Inflammatory bowel disease
IDF	-	International diabetes federation
IFN-γ	-	Interferon gamma
Ig	-	Immunoglobulin
IL	-	Interleukin
ILC	-	Innate lymphoid cells
IL-R	-	Interleukin receptor
IL-1b	-	Interleukin 1-beta
IMMIP	-	Institute for Medical Microbiology and Immunology
i.d.	-	Intra-dermal
i.p.	-	Intra-peritoneal
IR	-	Insulin resistance
ITT	-	Insulin Tolerance Test
i.v.	-	Intra-venous
IVM	-	Ivermectin
ko	-	Knock-out
L1	-	First larval stage
L2	-	Second larval stage
L3	-	Third larval stage
L4	-	Fourth larval stage
LDL	-	Low density lipids
LF	-	Lymphatic filariasis
Lo	-	Low expressing
LPS	-	Lipopolysaccharide
LsAg	-	*Litomosoides sigmodontis* antigen

L. sigmodontis	-	Adult worms
MACS	-	Magnet activated cell sorting
MCP	-	Monocyte chemotactic protein
MBP	-	Major basic protein
MDA	-	Mass drug administration
M	-	Molarity (mol/L)
Med.	-	Medium (RPMI1640)
Min	-	Minute(s)
MF	-	Microfilariae
MFI	-	Mean fluorescence intensity
MHC	-	Mayor histocompatibility complex
ml	-	Millilitre
MS	-	Multiple sclerosis
M. tuberculosis	-	*Mycobacterium tuberculosis*
Nat	-	Natural
NETs	-	Neutrophil extracellular traps
NFD	-	Normal food diet
NLRs	-	(NOD)-like receptors
NOD	-	Non-obese diabetic
NOD	-	Nucleotide-binding and oligomerization domain
NOS	-	Nitrit oxidative species
OD	-	Optical density
o/n	-	Over night
Pam3Cys	-	P3C Pam3Cys-Ser-(Lys)4, Trihydrochloride 132
PAMP	-	Pathogen-associated molecular pattern

PBS	-	Phosphate buffered saline
PCR	-	Polymerase chain reaction
PE	-	Phycoerythrin
PFA	-	Para-formaldehyde
PI	-	Propidium iodide
PMA	-	Phorbol-12-myristat-13-acetat
PRR	-	Pattern recognition receptor
PVS	-	Perivascular space
RAGE	-	Receptor for advanced glycation endproducts
RBC	-	Red blood cell
RIF	-	Rifampicin
RIG	-	Retinoid acid-inducible gene I
RLR	-	RIG-I like receptors
rpm	-	Rounds per minute
RPMI	-	Roswell Park Memorial Institute
RT	-	Room temperature
RT-PCR	-	Realtime PCR
ROS	-	Reactive oxygen species
SAE	-	Severe adverse events
s.c.	-	Subcutaneous
SEM	-	Standard error of mean
SLE	-	Systemic lupus erythematosus
SMA	-	Small molecule analog
SSC	-	Side scatter
SVF	-	Stromal vascular fraction

Th	-	T helper cell
T1D	-	Type 1 diabetes
T2D	-	Type 2 diabetes
TLR	-	Toll-like receptor
TMB	-	Tetramethylbenzidine
Treg	-	Regulatory T cells
TNF	-	Tumor necrosis factor
U	-	Unit
WHO	-	World Health Organization
WT	-	Wild type
VAT	-	Visceral adipose tissue
+/-	-	Positive/negative

Publications in peer-reviewed journals

Published:

1) Marc P. Hübner, Alexandra Ehrens, Marianne Koschel, Bettina Dubben, Franziska Lenz, **Stefan J. Frohberger**, Sabine Specht, Ludo Quirynen, Sophie Lachau-Durand, Fetene Tekle, Benny Baeten, Marc Engelen, Charles D. Mackenzie Achim Hoerauf. Macrofilaricidal efficacy of single and repeated oral and subcutaneous doses of flubendazole in *Litomosoides sigmodontis* infected jirds. **PLoS Negl Trop Dis**. 2019 Jan 16;13(1):e0006320. doi: 10.1371/journal.pntd.0006320. eCollection 2019 Jan.
2) W. David Hong, Farid Benayoud, Gemma L. Nixon, Louise Ford, Kelly L. Johnston, Rachel H. Clare, Andrew Cassidy, Darren A. N. Cook, Amy Siu, Motohiro Shiotani, Peter J. H. Webborn, Stefan Kavanagh, Ghaith Aljayyoussi, Emma Murphy, Andrew Steven, John Archer, Dominique Struever, **Stefan J. Frohberger**, Alexandra Ehrens, Marc P. Hübner, Achim Hoerauf, Adam P. Roberts, Alasdair T. M. Hubbard, Edward W. Tate, Remigiusz A. Serwa, Suet C. Leung, Li Qie, Neil G. Berry, Fabian Gusovsky, Janet Hemingway, Joseph D. Turner,Mark J. Taylorb, Stephen A. Wardb, Paul M. O'Neill.. AWZ1066S, a highly specific anti-*Wolbachia* drug candidate for a short-course treatment of filariasis. **Proc Natl Acad Sci U S A**. 2019 Jan 22;116(4):1414-1419. doi: 10.1073/pnas.1816585116. Epub 2019 Jan 7.
3) Malina A. Bakowski, Reza Kazem-Shiroodi, Renhe Liu, Jason Olejniczak, Baiyuan Yang, Kerstin Gagaring, Pamela M. White, Hui Guo, Laura Chappell, Alain Debec, Frédéric Landmann, Ashley K. Woods, Nicolas Pionnier, Sean B. Joseph, Mitchell Hull, Wen Xiong, Kelli L. Kuhen, Joseph D Turner, Bettina Dubben, Franziska Lenz, Dominique Struever, Alexandra Ehrens**, Stefan J. Frohberger**, Marc P. Hübner, Achim Hoerauf, Jason Roland, Matt S. Tremblay, Peter G. Schultz, William Sullivan, Xin-Jie Chu, H. Michael Petrassi, Case W. McNamara (2019). TA single-dose cure for the treatment of lymphatic filariasis and river blindness. **Science Translational Medicine**.**In press**.

4) Robert T. Jacobs, Christopher S. Lunde, Yvonne R. Freund, Vincent Hernandez, Xianfeng Li, Yi Xia, David S. Carter, Pamela W. Berry, Jason Halladay, Fernando Rock, Rianna Stefanakis, Eric Easom, Jacob J. Plattner, Louise Ford, Kelly L. Johnston, Darren A.N. Cook, Rachel Clare, Andrew Cassidy, Laura Myhill, Hayley Tyrer, Joanne Gamble, Ana F. Guimaraes, Andrew Steven, Franziska Lenz,Alexandra Ehrens, **Stefan J. Frohberger**, Marianne Koschel, Achim Hoerauf, Marc P. Hübner, Case W. McNamara, Malina A. Bakowski, Joseph D. Turner, Mark J. Taylor, Stephen A. Ward. Boron-Pleuromutilins as Anti-*Wolbachia* Agents with Potential for Treatment of Onchocerciasis and Lymphatic Filariasis. **J Med Chem**. 2019 Feb 7. doi: 10.1021/acs.jmedchem.8b01854.

5) Constanze Kuehn, Miyuki Tauchi, Roman Furtmair, Katharina Urschel, Dorette Raaz-Schrauder, Anna-Lena Neumann, **Stefan J. Frohberger**, Achim Hoerauf, Susanne Regus, Werner Lang, Atilla Sagban Tolga, Stephan Achenbach, Marc P Hübner, Barbara· Dietel. Filarial extract of *Litomosoides sigmodontis* modulates the Th1/Th2 ratio and attenuates plaque development in hyperlipidemic ApoE-knockout mice. **The FASEB Journal**. 2019. Feb 26:fj201800947RR. doi: 10.1096/fj.201800947RR.

6) Thomas W. von Geldern, Howard Morton, Rick F. Clark, Brian Brown, Kelly L. Johnston, Louise Ford, Sabine Specht, Marc P. Hübner, Robert Carr, Deanne Stolarik, Junli Ma, Matt Rieser, Dominique Struever, **Stefan J. Frohberger**, Marianne Koschel, Alexandra Ehrens, Joseph D. Turner, Achim Hoerauf, Mark J. Taylor, Stephen A. Ward, Kennan Marsh and Dale J. Kempf. Discovery of ABBV-4083, a novel analog of Tylosin A that has potent anti-*Wolbachia* and anti-filarial activity. **PLoS Negl Trop Dis.** 2019. Feb 28;13(2):e0007159. doi: 10.1371/journal.pntd.0007159. eCollection 2019 Feb.

Accepted:

7) **Stefan J. Frohberger**, Jesuthas Ajendra, Surendar Jayagopi, Wiebke Stamminger, Alexandra, Ehrens, Benedikt C. Buerfent, Katrin Gentil, Achim Hoerauf, Marc P. Hübner (2019).

Susceptibility to *L. sigmodontis* infection is highest in animals lacking IL-4R/IL-5 compared to single knockouts of IL-4R, IL-5 or eosinophils. **Parasit Vectors**. 2019.

Submitted:

8) **Stefan J. Frohberger**, Frederic Fercoq, Anna-Lena Neumann, Jayagopi Surendar, Wiebke Stamminger, Estelle Rémion, Alexandra Ehrens, Thomas Vogl, Achim Hoerauf, Coralie Martin, Marc P. Hübner. S100A8/A9 deficiency increases neutrophil activation and protective immune responses within the lung against invading infective L3 larvae of the filarial nematode *Litomosoides sigmodontis*.
9) Jayagopi Surendar, **Stefan J. Frohberger**, Karunakaran Indulekha, Vanessa Schmitt, Wiebke Stamminger, Anna-Lena Neumann, Christoph Wilhelm, Achim Hoerauf, Marc P. Hübner. Adiponectin limits IFN-γ and IL-17 producing CD4 T cells in obesity by restraining cell intrinsic glycolysis.
10) Indulekha Karunakaran, Surendar Jayagopi, **Stefan J. Frohberger**, Shah Alam, Janina Kuepper, Jan N. Hansen, Daniel Mitroi, Beatrix Schumak, Marc P. Hübner, Annett Halle, Gerhild van Echten-Deckert. S1P/S1PR2 mediated microglial inflammation and autophagy defects during brain specific SGPL1 ablation.
11) Frédéric Fercoq, Estelle Rémion, **Stefan J. Frohberger**, Nathaly Vallarino-Lhermitte, Achim Hoerauf, John Le Quesne, Frédéric Landmann, Marc P Hübner, Leo M. Carlin, Coralie Martin. IL-4 receptor dependent expansion of lung $CD169^{+}$ macrophages in microfilaria-driven inflammation.
12) Marc P. Hübner, Thomas W. von Geldern, Marianne Koschel, Dominique Struever, Venelin Nikolov, **Stefan J. Frohberger**, Alexandra Ehrens, Martina Fendler, Iliana Johannes, Kenneth Pfarr, Kennan Marsh, Joseph D. Turner, Mark J. Taylor, Stephen A. Ward, Dale J. Kempf, Achim Hoerauf. *In vivo* kinetics of *Wolbachia* depletion by ABBV-4083 in *L. sigmodontis* adult worms and microfilariae.

Under preparation:

13) **Stefan J. Frohberger**, Fabian Gondorf, Surendar Jayagopi, Anna-Lena Neumann, Wiebke Stamminger, Achim Hoerauf, Irmgard Förster, Marc P. Hübner. Absence of Aryl hydrocarbon receptor impairs protective immune responses within the skin and enhances vascular permeability leading to an increased worm recovery of the filarial nematode *Litomosoides sigmodontis*.

14) Marc P. Hübner, Coralie Martin, Sabine Specht, Marianne Koschel, Bettina Dubben, **Stefan J. Frohberger**, Alexandra Ehrens, Martina Fendler, Dominique Struever, Edward Mitre, Nathaly Vallarino-Lhermitte, Suzanne Gokool, Sara Lustigman, Manfred Schneider, Simon Townson, Achim Hoerauf, Ivan Scandale. Macrofilaricidal efficacy of oxfendazole against filarial nematodes *in vitro* and *in vivo.*

15) Marc P. Hübner, Simon Townson, Mary J. Maclean, Dominique Struever, Guilherme Verocai, Adrian J. Wolstenholme, **Stefan J. Frohberger**, Achim Hoerauf, Sabine Specht, Ivan Scandale, Achim Harder, Martin Glenschek-Sieberth, ‚Daniel Kulke . Evaluation of the *in vitro* susceptibility of microfilariae, third stage larvae and adult worms of related filarial nematodes to emodepside.

16) Alexandra Ehrens, Christopher S. Lunde, Robert T. Jacobs, Dominique Struever, Marianne Koschel, **Stefan J. Frohberger**, Franziska Lenz, Martina Fendler, Yvonne R. Freund, Rianna Stefanakis, Eric Easom, Achim Hoerauf, Marc P. Hübner. *In Vivo* efficacy of the boron-pleuromutilin AN11251 against *Wolbachia* of the rodent filarial nematode *Litomosoides sigmodontis.*

17) Alexandra Ehrens, Benjamin Lenz, Anna-Lena Neumann, Samuela Giarrizzo, **Stefan J. Frohberger**, Wiebke Stamminger, Benedikt C. Bürfent, Frederic Fercoq, Coralie Martin, Daniel Kulke, Achim Hoerauf, Marc P. Hübner**,** Microfilariae trigger eosinophil extracellular traps in a Dectin-1 dependent manner**.**

18) Jayagopi Surendar, **Stefan J. Frohberger**, Indulekha Karunakharan, Achim Hörauf, Marc P. Hübner. Macrophages mediate increased CD8 T cell inflammation during weight loss.

Conferences and schools

Oral presentation at the 27th Annual Meeting of the German Society for Parasitology (DGP), Göttingen, 9th-12th March 2016; (title of the talk: Comparison of *Litomosoides sigmodontis* infection in immune deficient mice – implications for the screening of macrofilaricidal drug candidates"

Oral presentation at the 27th Annual Meeting of the German Society for Parasitology (DGP), Berlin, 21th-24th March 2018; (title of the talk: Absence of S100A9 improves protective immune responses against *L. sigmodontis* L3 larvae and increases inflammatory responses and neutrophil activation)

Poster presentation at the “Science Day 2018” of the “Immunosensation Excellence Cluster”, Bonn, 4th-5th November 2018; (title of the poster: S100A9 deficiency increases neutrophil activation and protective immune responses within the lung against invading infective L3 larvae of the filarial nematode *Litomosoides sigmodontis*)

Acknowledgements

First of all I would like to thank Prof. Dr. Achim Hörauf, the director of the Institute for Medical Microbiology, Immunology and Parasitology (IMMIP) for giving me the opportunity to fullfill my PhD thesis in the field of parasitology and immunology. Furthermore I would also like to thank Prof. Dr. Irmgard Förster (co-supervisor) and the members of the examination committee including PD Dr. Gerhild van Echten-Deckert and Prof Dr. Ian Brock.

My deepest gratidude goes to my group leader PD Dr. Marc Hübner for his excellent supervision and his full commitment during my PhD. He was always available to me as an intensive consultant, personal mentor and scientific guidance. His personal engagement and passion for research has motivated me a lot.

I am also grateful to the recent and former group members of AG Hübner for their support, collegiality and in particular for the endless precious memories (in chronologic order): Dr. Afiat Berbudi, David Schmidt, Dr. Jesuthas Ajendra, Dr. Dominique Strüver, Dr. Benedikt Christian Bürfent, Dr. Fabian Gondorf, Dr. Jayagopi Surendar, Dr. Indulekha Karunakaran, Anna-Lena Neumann, Alexandra Ehrens, Wiebke Stamminger, Benjamin Lenz, as well as Bettina Dubben, Martina Fendler, Marianne Koschel, Franziska Lenz, Ilianna Johannes, and Venilin Nikolov. I would also like to share my appreciation with my colleagues of the other research groups at the IMMIP (AG Schumak, AG Layland, AG Pfarr, and AG Adjobimey).

Most credits are going to my family and friends, for their endless support and encouragement during this unique and exciting phase of my life.